



Ribbed moraines in the Vopnafjörður region, Iceland

Erla Guðný Helgadóttir



Faculty of Earth Sciences
University of Iceland

Ribbed moraines in the Vopnafjörður region, Iceland

Erla Guðný Helgadóttir

60 ECTS thesis submitted in partial fulfillment of a
Magister Scientiarum degree in geology

MS Committee
Ívar Örn Benediktsson
Faculty of Earth Sciences, University of Iceland

Ólafur Ingólfsson
Faculty of Earth Sciences, University of Iceland

Master's Examiner
Þorsteinn Sæmundsson, University of Iceland

Faculty of Earth Sciences
School of Engineering and Natural Sciences
University of Iceland
Reykjavík, May 2020

Ribbed moraines in the Vopnafjörður region, Iceland
60 ECTS thesis submitted in partial fulfillment of a *Magister Scientiarum* degree in
Geology.

Copyright © 2020 Erla Guðný Helgadóttir
All rights reserved

Faculty of Earth Sciences
School of Engineering and Natural Sciences
University of Iceland
Sturlugata 7
101, Reykjavík
Iceland

Telephone: 525 4000

Bibliographic information:

Erla Guðný Helgadóttir, 2020, *Ribbed moraines in the Vopnafjörður region, Iceland*,
Master's thesis, Faculty of Earth Sciences, University of Iceland.

Printing: Háskólaprent, Fálkagata 2, 107 Reykjavík
Reykjavík, Iceland, May 2020

Abstract

Ice streams provide a primary drainage pathway for ice sheet mass loss. Studying palaeo-ice stream beds improves understanding of current ice streams' dynamics in modern ice sheets. This study sheds light on palaeo-ice streaming and deglaciation of the eastern part of the Iceland ice sheet (IIS). Palaeo-ice stream features are well preserved in the area, including streamlined bedforms and transverse bedforms known as ribbed moraines, which are the focus of this study. Ribbed moraines have not previously been described in Iceland and their origin and formation are highly debated. Ribbed moraines are often thought to indicate the transition zone between cold and warm based ice flow or fast and slow ice flow. Ribbed moraines located between estimated ice streaming and an ice divide west of Vopnafjörður are the subject of this study. They can potentially be linked to the onset of palaeo-ice streaming at the start of the highland plateau. This study reveals the sedimentology and architecture of ribbed moraines near Vopnafjörður and their morphological characteristics, distribution and spatial relationships. A model of formation was constructed for ribbed moraines in Hauksstaðaheiði. They are proposed to form as a result of extensional ice flow between the ice divide and ice streaming which pulls on ice in the transition zone. This would lead to the formation of extensional surface crevasses. Basal water saturated in sediments seeks lowest pressure underneath the transverse crevasses facilitating the stacking of blocks of subglacial material into transverse ridges. The ice stream shut down and became subject to passive retreat which was key to preservation of the ridges. This study has implications for improving the understanding and insight into the behavior of ice streaming in the northeast part of the IIS and sheds light on the role of ribbed moraines in palaeo- and modern ice sheets.

Ágrip

Hraðskreiðir farvegir meginlandsjökla kallast ísstraumar. Þeir flytja mikið magn af ís og seti sem frá jöklunum kemur. Algengt er að rannsaka fornjökulumhverfi til þess að varpa ljósi á eðli og virkni ísstrauma. Þessi rannsókn lýtur að fornum ísstraumum sem runnu um Norðausturland við lok síðasta jökulskeiðs og skildu eftir sig sérstök landform. Ein tegund þessara landforma eru svokallaðir rifjagarðar, sem eru hryggir sem myndast undir ísstraumum þvert á flæðistefnu. Uppruni rifjagarða er óljós enda erfitt að rannsaka þá í virku jökulumhverfi þar sem botn nútímaísstrauma eru óaðgengilegur. Sunnan Vopnafjarðar eru að finna svokallaða rifjagarða sem talið er að hafi myndast undir ísstraumi sem náði frá ísaskilum út á landgrunn. Rifjagörðum hefur ekki verið áður lýst á Íslandi en eru lykill að því að auka þekkingu okkar á íslenska ísaldarjöklunum og mikilvægi ísstrauma í honum. Innri og ytri gerð hryggjanna er rannsökuð ásamt tengslum við landslag og umhverfi. Afurð rannsóknarinnar er líkan að myndun rifjagarða sunnan Vopnafjarðar. Garðarnir tengjast líklega breytingum á botnaðstæðum og hraða flæðis nærri ísaskilum. Teygt flæði milli ísaskila og ísstraums olli myndun þversprungna á yfirborði jökuls. Vatn í setlögum við botn leitaði lægsta þrýstings undir þversprungum sem gerði það að verkum að set gat staflast upp undir sprungunum og myndað þverhryggi. Ísstraumurinn varð óvirkur við hörfun og bráðnun jökulsins sem varð til þess að rifjagarðarnir varðveittust í nokkuð upprunalegri mynd. Verkefnið varpar og ljósi á afjöklun á Norðausturlandi, sem hingað til hefur verið illa þekkt, og getur gagnast við að auka skilning á hegðun nútímaísstrauma á Grænlandi og Suðurskautslandinu.

Table of contents

<i>List of Figures</i>	<i>viii</i>
<i>List of Tables</i>	<i>xiv</i>
<i>Abbreviations</i>	<i>xv</i>
<i>Acknowledgements</i>	<i>xvi</i>
1 Introduction	17
1.1 Objective and motivation of this study	20
2 Ice streams	21
2.1 Geomorphology of ice streams	22
3 Ribbed moraines	24
3.1 Importance of studying ribbed moraines	26
3.2 Previous research on ribbed moraines	26
3.3 Internal characteristics of ribbed moraines	32
3.4 Spatial relationships of ribbed moraines	34
3.5 Ribbed moraines in a modern context	36
4 Study area	38
4.1 Regional setting	38
4.2 Previous research/ Glacial history of Vopnafjörður	41
5 Methods	44
5.1 Geomorphological mapping.....	44
5.2 Field work.....	45
5.3 Laboratory analyses.....	47
5.3.1 Clast morphology	47
5.3.2 Sections and logs	49
6 Geomorphology and sedimentology of ribbed moraines	50
6.1 Geomorphology.....	50
6.1.1 Ridge geometry	54
6.1.2 Ridge spacing.....	56
6.1.3 Ridge shape	58
6.1.4 Ridge trend.....	58
6.1.5 Interpretation and discussion.....	59
6.2 Sedimentology.....	61
6.2.1 Section 1	61
6.2.2 Section 2	66
6.2.3 Section 3	72
6.2.4 Section 4	77
6.2.5 Ridge surface clast measurements	83
7 Discussion	86
7.1 Ridge characteristics	86

7.2	Comparison with previous studies	88
7.3	Model of ribbed moraine formation	90
8	<i>Conclusion</i>	94
	<i>References</i>	95

List of Figures

- Fig. 1-1. A) Surface ice velocities between LGM (22.9 cal. ka BP) and 11.7 cal. ka BP estimated by Patton et al. (2017), compared with the Hubbard (2006) reconstruction of the IIS. Time slices show the IIS extent from the LGM, 14.5 cal. ka BP, Bølling retreat at 13.2 cal. ka BP and the YD stadial (11.7 cal. ka BP). The Fig. also shows ice divides and their evolution over this time period. The Dimmifjallgarður and Smjörfjöll mountain ranges isolate Vopnafjörður at the LGM according to this model. B) Geomorphology map of the Icelandic continental shelf by Spagnolo and Clark (2009) and edited by Patton et al. (2017). The map shows the main flow sets within the IIS, indicating fast ice flow or ice streaming. 19
- Fig. 2-1. A conceptual model for palaeo-ice stream geomorphology on the west-Antarctic continental shelf, from Graham et al. (2009). This Fig. highlights the time-transgressive landform evolution. 23
- Fig. 3-1. Classification scheme of ribbed moraine geomorphology from Dunlop and Clark (2006). 25
- Fig. 3-2. The fracturing model of ribbed moraine formation model taken from Hättestrand (1997) proposes that they result from the rise of a pressure melting isotherm (PCS) through a glacier bed. (a) Ice flow velocity (u) for stages 1-3 which is shown in (b). (b) Time slice boxes (1-3), showing how pre-existing drift sheet develops into ribbed moraines with different stages of underlying drift sheet. The frozen drift ribs detach as soon as the pressure melting isotherm reaches the bedrock surface. (c) The fracture zone where the drift sheet has experienced detachment and extension as ice velocity increased. 29
- Fig. 3-3. The shear and stack model of ribbed moraine formation model from Lindén et al. (2008). T_0 : pre-existing sequences of laminated, undisturbed sediments deposited in valley areas. T_{1A} : ridge starts forming due to bed compression where pre-existing sediments fold and thrust (T_{1B}) in ice-flow direction causing a transverse thickening of the bed, forming an obstacle to the ice-flow and causing a lee-side cavity to form parallel to the ridge developed. Ridge forms in stages T_2 - T_3 with folding followed by erosion and thrust sheet stacking of sediment (T_{2A}). T_{2B} shows a brittle deformation case where ridge forms only through thrust-fault stacking. Distal cavity infilling starts, with a variable deposition of glaciofluvial sediments including suspension of fine-grained sediment to high flow velocity gravels of traction load interbedded with stratified and massive diamicts. The diamicts are interpreted to be deposited from sediment gravity flows into the lee-side cavity from the deforming bed. Larger clasts are interpreted as drop stones. Lee-side cavity sediments include small-scale normal faulting and reverse faulting due to extensional and compressional faulting. T_4 is the draping stage where the ridge is

smoothed with erosion, creating an unconformity in the sediments and then draped over by a diamict with a high clast orientation.....	31
Fig. 3-4. A schematic diagram showing the spatial relationships between ribbed moraines and other glacial landforms. The direction of ice flow is indicated with an arrow. Taken from Dunlop and Clark (2006).	35
Fig. 3-5. Comparison from Stokes et al. (2016) between types of ribbed features observed in palaeo-settings (a., b., d.) and 'traction ribs' (c.). They split ribbed palaeo-features into three subcategories; ribbed moraines, mega ribs and the more irregularly patterned rib-like features. Blue arrows show the estimated ice flow direction. In the paper, d. and c. were compared and authors suggested a continuum of subglacial rib formations.	37
Fig. 4-1. The study area of Vopnafjörður and its location in Iceland. The large map shows the focus area of Hauksstaðaheiði inside the red box but Tunguheiði and Selárdalur were also mapped. Map base is from the ArcticDEM (Porter, 2018) and the National Land Survey of Iceland (Landmælingar Íslands)(LMÍ, 2016).....	39
Fig. 4-2. <i>The Hauksstaðaheiði and Leirvatnsvos area with place names taken from www.maps.google.com (Airbus, Landsat/Copernicus, Maxar Technologies, U.S. Geological Survey). The ridges are situated in a vegetated depression in Leirvatnsvos where the Skeljungsa river runs from lake Leirvatn to lake Arnarvatn. The Fig. shows the road, Norðausturvegur, which leads to Vopnafjörður.</i>	40
Fig. 4-3. A view of the Leirvatnsvos basin (looking towards the west). The Skeljungsa river runs from Leirvatn on the left and into Arnarvatn which is not seen on this figure, creating useful sections in the ridges for investigations of internal composition. Section 4 can be seen on the figure.	41
Fig. 5-1. Sketching Section 1, with a string grid for reference.	46
Fig. 5-2. Lithofacies codes for field description of glacial diamicts and associated sediments, modified from Krüger and Kjær (1999). The data chart from Krüger and Kjær (1999) was used as a guide for the logs and facies description.	Error! Bookmark not defined.
Fig. 5-3. Roundness diagram used for determining morphology for each clast (Powers, 1953).	48
Fig. 5-4. Sneed and Folk shape continuum diagram modified from Benn and Evans (2004). The C40 0.4 line indicates that sediments shaped below have undergone significant erosion.....	48
Fig. 5-5 Legend for logs and section drawings (Figs. 6-9; 6-10; 6-12; 6-13; 6-16; 6-17; 6-19; 6-20).	49

- Fig. 6-1. An overview map showing glaciogenic landforms in the interior of Vopnafjörður and geomorphology at the highland margin. The transverse ridges (to estimated ice flow (Sæmundsson, 1995) in Tunguheiði, Hauksstaðaheiði and Selárdalur are shown here along with streamlined landforms. Arrows signify general ice flow directions. The streamlined landforms are densely packed on Bustarfell, in Fossheiði and Hraunfellsheiði. It is notable that the areas with highest density of transverse ridges are situated at higher altitudes or inland of the most densely spaced streamlined landforms, forming a belt at the highland margin. 51
- Fig. 6-2. Transverse ridges on Hauksstaðaheiði shown in relation to streamlined bedforms in the area. In the upstream part of the Leirvatnsvos depression, the ridges are most densely distributed. It is notable that the most densely situated ridges also have a distinct transverse alignment. 52
- Fig. 6-3. Skeljungsá river runs between the Leirvatnsvos ridges. People (approx. 1.7 m) indicate the scale of the ridges which range up to 19.3 m. The ridge crests have a gravelly and rocky appearance compared to the surrounding, vegetated lowlands. A) A perpendicular view of the ridges in Leirvatnsvos along the ridge crests towards the southeast. B) An upstream view of the ridges in Leirvatnsvos towards the southwest with Leirvatnshnjúkur in the background. 54
- Fig. 6-4. A map showing the relief of individual ridges. Most of the tallest ridges are located in the Leirvatnsvos basin and ridges with lower relief occur on the basin flanks and further down-stream. 55
- Fig. 6-5. Normal frequency distribution of ridge morphometrics on Hauksstaðaheiði showing their length (A), width (B), elongation ratio (C) and relief (D). Elongation ratio graph (E) shows a strong correlation between length and width of the ridges. The line in (E) graph shows the trendline of the graph. 56
- Fig. 6-6. A) Map showing terrain cross-profiles across the main segments of the ridge system in Hauksstaðaheiði. B) Graph showing Profile 1 seen in A above. C) Graph showing Profile 2 seen in A above. The profiles have vertical indicator lines showing the distance between ridge crests. The numbers between the indicator lines show a roughly estimated spacing between ridge crests. The profiles show the downslope evolution of ridge relief and spacing. Grey horizontal lines on graphs indicate 10 m in elevation. 57
- Fig. 6-7. Ridge trend map. The rose diagram (B) shows directional trends for 251 ridge crest lines and has a general trend between 135° and 180°. The pink line in the rose diagram shows the direction mean for the transverse ridges. 58

- Fig. 6-8. A map showing a clearer direction trend for selected ridge crests in Leirvatnsvos that have a particularly clear transverse orientation. B is a rose diagram for the selected ridge crests and the pink line in the rose diagram shows the direction mean for the transverse ridges. The red lines in A represent ridges that were not included in the selection. 61
- Fig. 6-9. A) Photograph of Section 1 showing the location of log in Fig. 6.10 in white box. B) Drawing of Section 1 showing the measurements for dip and dip direction of stratigraphic beds. The measurements are plotted on a stereograph to the right where red dots are from unit 1 and black dots are from unit 2. Samples from both units are marked with S1-CS-U1 and S1-CS-U2. 63
- Fig. 6-10. Stratigraphic log of Section 1. Clast shape data with C40 and frequency for striae, bullet-shaped clasts and facets on clasts . RA index shows the percentage of angular and very angular clasts in the sample (Benn and Ballantyne, 1993). 64
- Fig. 6-11 A) Shows Section 1 with white boxes indicating the location of figures B-E. B) Fissile diamict in unit 2 draping over unit 1. C) White line showing the approximate layer dip in the section. D) Gravel and sand lenses within unit 1. E) Layers in unit 1 dipping towards the proximal end of the ridge. 65
- Fig. 6-12 A) Photograph of Section 2 showing the location of log in Figs. 6.13; 6.14 in white boxes. B) Drawing of Section 2 showing the measurements for dip and dip direction of stratigraphic beds in white boxes. The measurements from the diamictic Unit 3 are plotted on a stereograph to the right as black dots. Samples from all units are marked with S2-CS-U1, S2-CS-U2 and S2-CS-U3. Topmost diamict has stratification but no other structures. A sand layer can be traced across from the proximal side of section and its upper boundary is truncated by the lower diamict. A large part of the center of the diamict Unit 3 is scree but continues towards the distal side. The lower diamict and gravel/sand boundaries are unclear but can be traced into the Unit 3 where they are discontinued, indicating that the surface (marked with a bold line in Fig.) is eroded. 68
- Fig. 6-13. Stratigraphic log of Section 2, proximal log. Clast shape data with C40 diagrams and frequency for striae, bullet-shaped clasts and facets on clasts. RA index shows the percentage of angular and very angular clasts in the sample (Benn and Ballantyne, 1993). 69
- Fig. 6-14. Stratigraphic log of Section 2, central log. Clast shape data with C40 diagrams and frequency for striae, bullet-shaped clasts and facets on clasts. RA index shows the percentage of angular and very angular clasts in the sample (Benn and Ballantyne, 1993). 70

Fig. 6-15 A) Shows Section 2 with white boxes indicating the location of figures B-F. B) Unit 3 is fissile but clast rich. C) A close-up of the unconformity between Unit 3, where overlying diamict unit 2, truncates the underlying sand layers that are discontinued into the diamict unit. D) The unconformity seen for more layers. E) Boundary between Unit 3 and Unit 2. F) Boundary between Unit 2 and Unit 1 towards the distal (down-stream) side of the section.....	71
Fig. 6-16 A) Photograph of Section 3 showing the location of log in Figs. 6.17 in white box. B) Drawing of Section 3 showing the measurements for dip and dip direction of stratigraphic beds in white boxes. The measurements from the diamictic Unit 3 are plotted on a stereograph to the left where red dots are from Unit 2 (gravel) and black dots are from Unit 3 (diamict). Samples are marked with S3-CS-U1 and S3-CS-U2.	74
Fig. 6-17. Stratigraphic log of Section 3. Clast shape data with C40 diagrams and frequency for striae, bullet-shaped clasts and facets on clasts. RA index shows the percentage of angular and very angular clasts in the sample (Benn and Ballantyne, 1993).	75
Fig. 6-18. A) Shows Section 3 with white boxes indicating the location of figures B-D. B) The crosscutting sand-lense that truncates through a large part of Unit 3. C) Boundary between Unit 2 and Unit 3. D) Gravel and sand layers with ripples. E) Diamict drapes over the gravel and sand units.....	76
Fig. 6-19. A) Photograph of Section 4 showing the location of log in Fig. 6.20 in white box. B) Drawing of Section 4 showing the measurements for dip and dip direction of stratigraphic beds. The measurements are plotted on a stereograph to the right where black dots are from diamictic layers in Unit 3.	80
Fig. 6-20. Stratigraphic log for Section 4.	81
Fig. 6-21. A) Shows Section 4 with white boxes indicating the location of figures B-J. B) The boundary between Unit 2 and 3 showing locations for frames G, D and H. C) The boundary between Unit 1, 2 and 3. D) A section on the distal side showing bottom Unit 1 with a boundary to Unit 3, skipping Unit 2, which does not extend to this end of the section. E) Disrupted layers of sand and silt. F) Overhanging diamict and irregularly stratified and lense-rich sand, gravel and diamict. G) Boundary between Units 4 and 5. H) A close-up of disrupted fines and sand in Unit 2. I) Dissipation structure in Unit 2. J) Interfingering of sorted and diamict layers in distal part of the section.	82
Fig. 6-22. Large clasts are a common surface feature on top of the ridges.	84
Fig. 6-23. Covariance plots and angularity histograms for surface clasts of five ridges.	84

Fig. 7-1. Juxtaposition of transverse ridges and drumlins/MSGs in Tunguheiði. The transverse ridges tend to be lined up into rows of ridges in the direction of the drumlins/MSGs and are often superimposed upon the streamlined landforms. 87

Fig. 7-2. Sequential model for the formation of ribbed moraines in Hauksstaðaheiði. The model is based on the sedimentology, geomorphology and landscape associations for the Hauksstaðaheiði ribbed moraines..... 92

List of Tables

Table 1. Sedimentary characteristics of ribbed moraines	32
Table 2. Lithofacies codes for field description of glacial diamicts and associated sediments, modified from Krüger and Kjær (1999). The data chart from Krüger and Kjær (1999) was used as a guide for the logs and facies description.....	47
Table 3. Morphological statistics for the transverse ridges in Hauksstaðaheiði	55

Abbreviations

IIS: Icelandic Ice Sheet

SIS: Scandinavian Ice Sheet

LIS: Laurentide Ice Sheet

BIIS: British-Irish Ice Sheet

WAIS: West-Antarctic Ice Sheet

MSGs: Mega Scale Glacial Lineations

LGM: Last Glacial Maximum

DEM: Digital Elevation Model

YD: Younger Dryas

Acknowledgements

I would like to thank my excellent supervisors, Ívar Örn Benediktsson and Ólafur Ingólfsson for their expert supervision and constructive criticism. Their enthusiasm on the topic is inspiring and has kept me motivated and excited about the project over these past two years. Giving good feedback is a skill which they have mastered, it is amazing how each meeting left me full of ideas every time. Such great moral support is invaluable.

For input, discussions on the topic, coffee breaks in Askja and help during field work and data processing I would like to thank Nína Aradóttir. I would also like to thank Sigurrós Arnardóttir, Skafti Brynjólfsson, Anders Schomacker, Wesley Farnsworth, Ben Popken, Till Wenzel and Genevieve Nadeau Bonin for being helpful, insightful and good company during field trips in 2018 and 2019.

I want to thank my dear friends Rob Askew for great proofreading and his helpful youtube video reviews and Daniel Ben Yehoshua for reading and very useful conversations about the formation model.

Special thanks go to my amazing friend Sif who was the field assistant of my dreams. Not only was she a great companion but her section cleaning skills, boulder measuring abilities and sample collecting were unmatched despite below average weather conditions. Field work in Hauksstaðabeiði would not have been the same without you, Sif.

I want to thank my boyfriend Mike who has been patient with me through the entire process and has proved to be the rock that I needed by my side. Thanks to my sister, Soffía, who keeps my life interesting and always provides extreme moral support. I want to thank my parents, Kristín and Helgi, and my sister Birta, who inspire me every day and are the best support network I could ask for. Thanks go to dear Lotta, who took me for regular walks each day, no matter the weather. I also want to thank all my great friends who made me go outside when I most needed it.

1 Introduction

Throughout the major glaciations of the Quaternary, much, if not all, of Iceland was repeatedly covered by an extensive ice sheet, termed the Icelandic Ice Sheet (IIS) (Norðdahl, 1991; Norðdahl, 2005). The Last Glacial Maximum (LGM), where the IIS was at its largest, was reached around 24.4-18.6 cal. ka BP (Jóhannesson, 1997; Andrews, 2000; Spagnolo and Clark, 2009; Norðdahl and Ingólfsson, 2015; Pétursson et al., 2015). During that time, the ice sheet is thought to have been up to 1500-2000 m thick in places and drained by large outlet glaciers and/or ice streams (Norðdahl, 1991; Norðdahl, 2005; Hubbard, 2006; Hubbard et al., 2006; Patton et al., 2017). It is well established that during the LGM Iceland was covered with an ice sheet which probably extended to the edge of the continental shelf surrounding the island. According to bathymetric data on the shelf around Iceland, end moraines occur far offshore and in many areas on the shelf edge (Spagnolo and Clark, 2009; Patton et al., 2017) (See B in *Fig. 1-1*). Despite a relatively long period of study of the extent of the IIS, there are still rather large gaps in datasets and glacial geological mapping in Iceland. It is still unclear exactly how extensive the IIS was at different times, and which dynamics controlled and contributed to its collapse. The deglaciation started around 18.6 cal. ka BP and was very rapid between 15.0 and 13.8 cal. ka BP (Andrews, 2000; Jennings, 2000; Norðdahl and Ingólfsson, 2015; Pétursson et al., 2015) due to rapid global eustatic sea-level rise, causing extreme calving, grounding-line retreat and overall destabilization of the marine sections of the IIS (Ingólfsson, 1991; Norðdahl, 1991; Syvitski et al., 1999; Andrews, 2000; Ingólfsson and Norðdahl, 2001; Norðdahl, 2005; Norðdahl, 2008; Geirsdóttir et al., 2009; Norðdahl, 2012; Norðdahl and Ingólfsson, 2015; Pétursson et al., 2015; Patton et al., 2017). During the Younger Dryas (YD) stadial, which started around 13.0 cal. ka BP, the ice sheet advanced significantly (Ingólfsson, 1991; Pétursson et al., 2015; Patton et al., 2017). A final readvance of the IIS occurred during Preboreal, at 11.2 cal. ka BP just inside the YD maximum position (Pétursson et al., 2015; Patton et al., 2017). Subsequent regression of the ice sheet and transgression of relative sea level occurred and finalized the collapse of the IIS which was mostly deglaciated at 8.7 cal. ka BP (Norðdahl, 2008; Pétursson et al., 2015).

The IIS extent, evolution, and dynamics since the LGM have been reconstructed through numerical modelling, which incorporates previous research and field data (Hubbard et al., 2006; Patton et al., 2017). However, as stated by Patton et al. (2017) information and research is sparse, and as such the models are constrained by limited datasets. These datapoints have mainly been scattered around the western, southern and northern parts of Iceland as well as offshore records from the Icelandic continental shelf (Ingólfsson, 1991; Norðdahl, 1991; Andrews, 2000; Norðdahl, 2008; Geirsdóttir et al., 2009; Pétursson et al., 2015; Patton et al., 2017). Up until recently, there has been a significant lack of data to fully understand the ice sheet evolution in the eastern and northeastern parts of Iceland, although Sæmundsson (1995) and Norðdahl et al. (2019) shed light on the deglaciation in this region through shoreline displacement in Vopnafjörður and the development of the glacial lake Lögurinn, respectively. This research is ongoing, and much work remains to be done in order to give a clearer picture of the last glaciation and deglaciation in Iceland.

Imprints from palaeo-ice streaming or streamlined landforms have been mapped in NW-Iceland using aerial imagery and digital elevation models (DEM) (Principato et al., 2016). These landforms strongly indicate the presence of palaeo-ice streaming in N-Iceland into Húnaflói (Principato et al., 2016). Principato et al. (2016) suggest that a topographically controlled ice stream flowing into Húnaflói created these streamlined landforms during the LGM. Research of another ice stream, located in Bárðardalur, north Iceland is ongoing but widespread imprints of streamlined landforms have been identified in the region by remote sensing methods (McKenzie et al., 2017; Benediktsson et al., 2018). These studies have put a new focus on studying the IIS by quantifying streamlined glacial bedforms paired with spatial analysis and therefore identifying and describing palaeo-ice streaming in north Iceland in detail. The model results of Patton et al. (2017) also indicate fast ice flow across north and northeast Iceland. According to their model and the geomorphology map from Spagnolo and Clark (2009) (See B in *Fig. 1-1*), one of the larger ice streams of the IIS would have flowed into the Vopnafjörður trough (Spagnolo and Clark, 2009; Patton et al., 2017). Ice streams have not been studied in detail in Iceland but shedding light on their behavior will improve understanding of the IIS development as well as the mechanisms of fast ice flow.

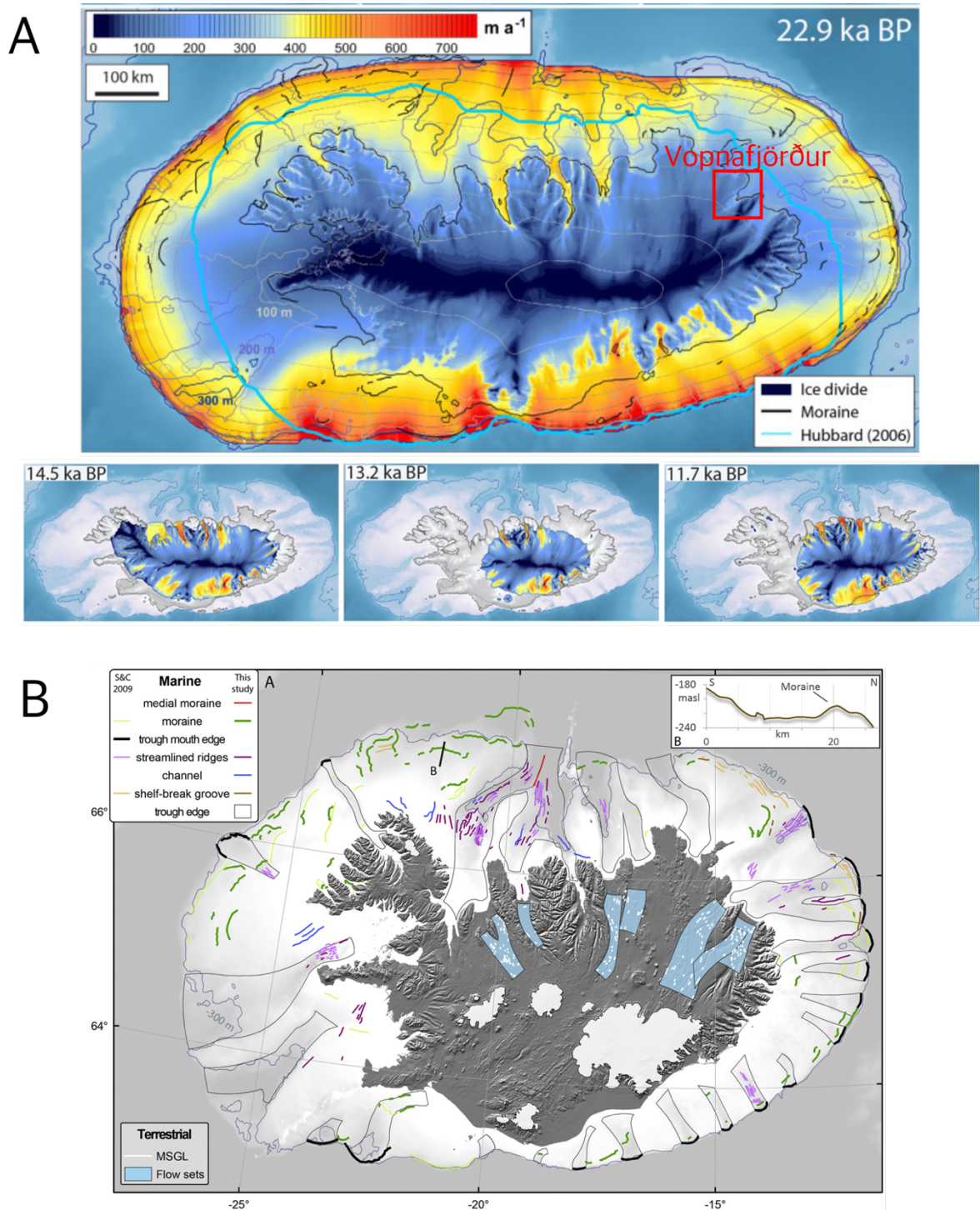


Fig. 1-1. A) Surface ice velocities between LGM (22.9 cal. ka BP) and 11.7 cal. ka BP estimated by Patton et al. (2017), compared with the Hubbard (2006) reconstruction of the IIS. Time slices show the IIS extent from the LGM, 14.5 cal. ka BP, Bølling retreat at 13.2 cal. ka BP and the YD stadial (11.7 cal. ka BP). The Fig. also shows ice divides and their evolution over this time period. The Dimmifjallgarður and Smjörfjöll mountain ranges isolate Vopnafjörður at the LGM according to this model. B) Geomorphology map of the Icelandic continental shelf by Spagnolo and Clark (2009) and edited by Patton et al. (2017). The map shows the main flow sets within the IIS, indicating fast ice flow or ice streaming.

1.1 Objective and motivation of this study

As mentioned above, empirical data that can highlight the extent, dynamics and mechanics, and consequently constrain modelling of the IIS, are significantly sparse. Field observations are particularly lacking in northeast Iceland, where current models rely on limited datasets. The objective of this study is to map and describe transverse ridges in the Vopnafjörður region, northeast Iceland, coupled with analysis of remote sensing datasets. A mechanism of the formation of these ridges is presented and tested against current models and hypotheses of ribbed moraine formation. This project is the first to describe these landforms from Iceland.

This project will further enhance the data available and the knowledge base for understanding the IIS during the LGM by providing a previously missing piece of the puzzle in northeast Iceland. This carries implications for subglacial processes, both in the interior of the IIS and ice streams throughout northeast Iceland since these areas were potentially very significant drainage routes within the IIS. Furthermore, it is important to study the geological and geomorphological products of ice streams in order to gain a better understanding of their flow, onset zones, and overall behavioral patterns. Studying palaeo-ice streams through these methods can also shed light on processes at work in current ice streams in the Antarctic and Greenland ice sheets.

2 Ice streams

Ice streams are defined as corridors of fast flowing ice within an ice sheet. They can be hundreds of kilometers long and tens of kilometers wide, flowing several hundred meters per year. This fast flow allows them to drain an ice sheet of massive amounts of ice and sediments which makes them important for ice sheet stability (Bennett, 2003). All modern ice streams are marine-terminating (Livingstone et al., 2012), but terrestrial ice streams are well-known from the palaeo-setting, such as the Laurentide Ice Sheet (LIS) (Margold et al., 2015). Marine-terminating ice streams discharge approximately 40% of the total volume for ablation of the West Antarctic Ice Sheet (WAIS) and have therefore been intensively studied for decades due to their importance in the stability of the WAIS (Alley and Bindschadler, 2001; Bennett, 2003). Today, ice streams in Antarctica drain vast amounts of ice into the ocean but around 90% of Antarctica's annual mass loss is through ice streams (Bentley and Giovinetto, 1991; Bamber et al., 2000) and approximately 50% in Greenland where there is more surface melt contributing to mass loss (van den Broeke et al., 2009). Ice streams can therefore significantly impact global sea level (Hughes, 1973b; Mercer, 1978; Alley et al., 2005; Shepherd, 2012; Joughin, 2014). This shows that ice streams are a critical component regarding the currently warming climate, their contribution to ice sheet mass loss, sea level rise and how they are impacted by warming ocean temperatures and retreating grounding line, which has the potential to break up ice shelves at accelerating rates (Hughes, 1973a; Weertman, 1974; Mercer, 1978; Alley and Bindschadler, 2001; Alley et al., 2005; Shepherd, 2012; Hanna, 2013; Joughin, 2014). Ice streams can be either constrained by topography (topographic ice streams) or areas of surrounding, slow moving ice (pure ice streams), today occurring in the Siple Coast, Antarctica (Stokes and Clark, 1999). These types of ice streams can behave in different ways and show variability, both spatially and temporally. Ice stream's fast flow is the result of various factors but common explanations are mostly directed either towards a weak, deformable bed of sediments that allows the stream to flow freely or to pre-existing topography that allows the ice stream to drain an ice sheet and flow fast (Margold et al., 2015). Ice streams have shown behavior suggesting that they can switch on and off, or even change their flow trajectory (Margold et al., 2015), a phenomenon which is currently unexplained.

Ice stream's subglacial conditions are almost impossible to physically observe in an active setting and research on them is mostly done with geophysical methods and through remote sensing (See overview paper by Stokes (2018)). Due to the constraints that ice streams provide in modern settings, glaciological and glacial geological research has put a large focus on studying the environments, evolution and geomorphological imprints palaeo-ice streams (Stokes and Clark, 1999; Stokes and Clark, 2001; Livingstone et al., 2012; Margold et al., 2015). The beds of Pleistocene ice sheets are easily accessible and thus can provide insight into processes operating underneath the currently fast flowing ice in Antarctica and Greenland.

Palaeo-ice streams leave sedimentary and geomorphological imprints that have been widely dated and analyzed in order to reconstruct the last deglaciation of the continental ice sheets (Livingstone et al., 2012; Margold et al., 2015). Some modern ice streams have shown signs of stagnation and reactivation, which has also been recorded in palaeo-ice

streams. The key research questions are yet to be answered. These include how basal conditions influence ice flow, what the exact genesis and role of subglacial landforms associated with ice streams is, why ice streams shut down or reactivate and how ice stream behavior can affect ice sheet stability. Determining the processes that trigger and control flow and retreat of marine-terminating, palaeo-ice streams is therefore an important task. Studying ice streams will further enhance the understanding of future predictions of contemporary ice-stream retreat and sea-level rise (Livingstone et al., 2012).

2.1 Geomorphology of ice streams

Ice flow is a leading cause in forming landforms out of pre-existing subglacial material. Landforms typically formed underneath Pleistocene ice sheets include flutes (Boulton, 1976), drumlins (Menzies, 1979), mega-scale glacial lineations (MSGs) (Clark, 1993; Stokes, 2013a) and ribbed moraines (Lundqvist, 1989).

Long elongated and streamlined landforms are believed to be indicative of fast ice flow and have therefore been linked to ice streaming. This has been established by mapping and statistical analysis of their shape, such as elongation ratio, in areas where previous fast ice flow can be estimated spatially. These landforms and features mostly include MSGs and drumlins, and it is suggested that landforms with an elongation ratio of higher than 10:1 are formed under fast ice flow (Stokes, 2002). These observations can potentially help with identifying ice streams and shed light on flow dynamics and stability of palaeo-ice sheets. It has been suggested that lineations, such as drumlins and MSGs, are end members of a subglacial continuum of flow aligned landforms (Ely et al., 2016). An example of ice stream geomorphology from Graham et al. (2009) is shown in *Fig. 2-1*.

Drumlins are long, elongated and subglacially formed landforms that have a streamlined appearance. A drumlin is a hill, generally composed of material of glaciogenic source (Clark et al., 2009). They are a common and widespread feature beneath the Pleistocene ice sheets and are considered to be indicative of fast ice flow or even ice streaming (Stokes, 2002). Pleistocene drumlins tend to occur in swarms but can also occur as single landforms. Drumlin fields occur in regions previously covered by large ice sheets, such as areas of the LIS, SIS and the BISS (Menzies, 1979; Hess, 2009; Knight, 2011; MacLachlan, 2013; Stokes, 2013b; Dowling, 2015; Lamsters, 2015; Eyles, 2016; Knight, 2016). In a modern context, currently active drumlin fields are rare, but a single active drumlin field has been described from the Múlajökull glacier foreland in Iceland (Johnson, 2010; Benediktsson, 2016). However, their formation is still debated and requires further research to shed light on glaciodynamics and subglacial processes underneath ice sheets.

Mega-Scale Glacial Lineations (MSGs) are a characteristic landform of ice streams and are typically associated with rapid ice flow (Stokes, 2002). They are also often thought to record the final imprint of streaming (Graham et al., 2009). There are a few theories for MSG formation, some of these include ice keel ploughing at the base of soft sediments (Tulaczyk, 2001; Clark C.D., 2003); subglacial erosion of soft sediment from a point source, bedrock or till underneath ice stream (Clark, 1993); and the instability theory taking local subglacial drainage systems into account (Fowler, 2010). Their relation to flow velocity,

sediment supply, transport and deposition at the bed is unclear, as is whether they are transient features, changing with bed conditions or stable features that withstand changes in basal processes. Enhancing MSGL formation understanding is important in order to create a clearer picture of how ice streams flow.

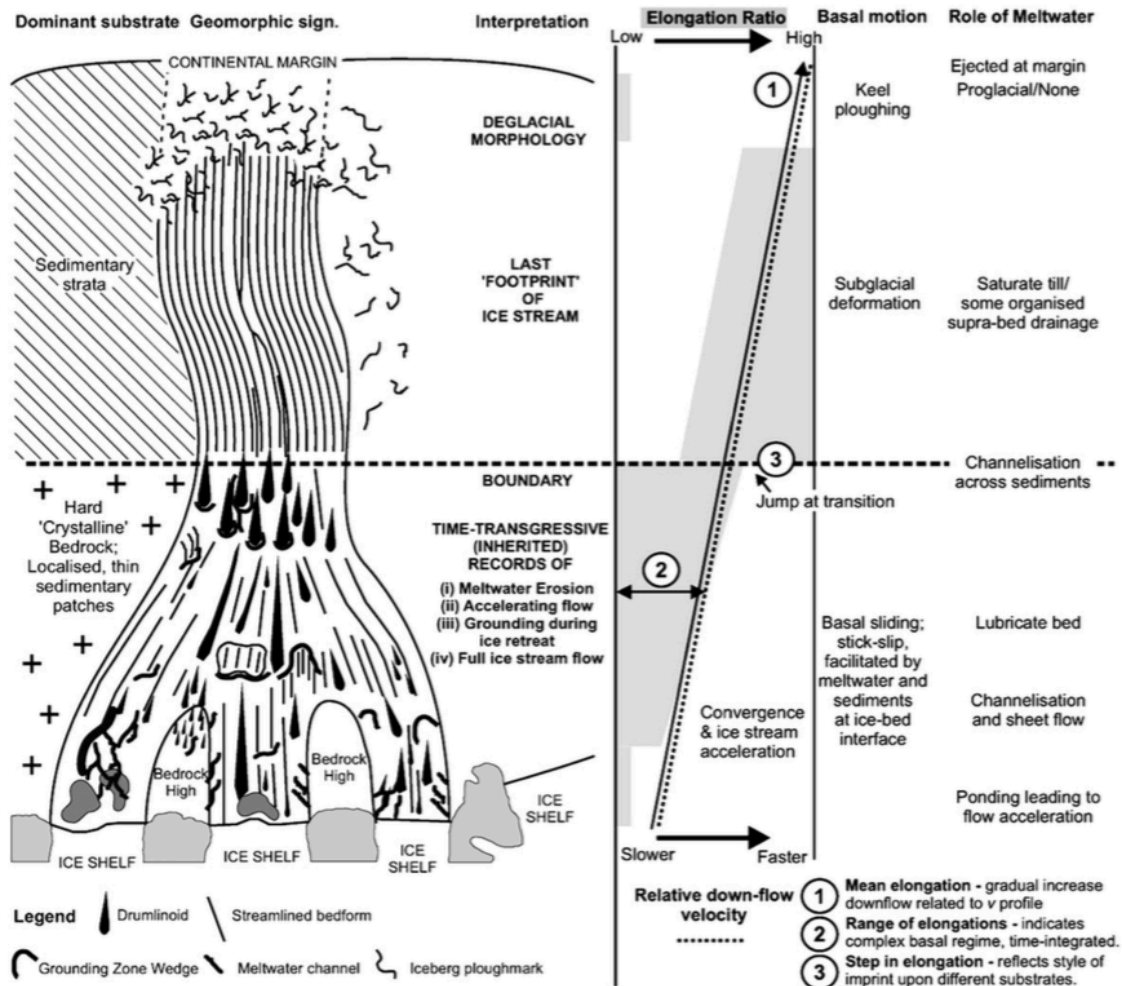


Fig. 2-1. A conceptual model for palaeo-ice stream geomorphology on the west-Antarctic continental shelf, from Graham et al. (2009). This Fig. highlights the time-transgressive landform evolution.

3 Ribbed moraines

Ribbed moraines are clusters of ridges generally orientated transverse to ice flow, resembling waves or ripples in the landscape. The ridges are typically found in the core areas of former ice sheets, although they are not restricted to those areas and are sometimes found closer to the glacier margin, at the coast or within the main trunk-flow zones of ice streams (Dunlop and Clark, 2006; Stokes et al., 2016).

Ribbed moraines consist of short and low relief ridges of less than a km long according to Aylsworth and Shilts (1989a) and less than 10 m in relief, although relief varies between areas (Dunlop and Clark, 2006). Their shape is sometimes irregular, often arcuate with flanks facing down-stream but they have also been recorded with upstream facing flanks (Dunlop and Clark, 2006). The comprehensive analysis of ribbed moraine morphology for the LIS, the Scandinavian Ice Sheet (SIS) and the British-Irish Ice Sheet (BIIS), by Dunlop and Clark (2006) reveal that either side (up-stream or down-stream) has an equal likelihood of being the steeper slope. They also exhibit a complex plan view with a large size range (17-1116 m wide; 1-64 m high; 45-16214 m long; 12-5800 m in spacing). They can be found densely packed or in dispersed clusters and show regular spacing between ridge crests in general (*Fig. 3-1*) (Dunlop and Clark, 2006). Their geomorphology can be extremely varied, not only between study areas but also within one ribbed moraine field, although it is most common that ribbed moraine ridges are similar in dimension to neighboring ridges. They often tend to be situated around the interior of previously glaciated areas (Hättestrand and Kleman, 1999), though they are sometimes found closer to the coast or in marginal settings (Möller, 2006; Lindén et al., 2008). According to the Dunlop and Clark (2006) analysis of ribbed moraine location, they determine that ribbed moraines are not necessarily restricted to specific topographic settings, core glaciation areas or ice divide margins, since they have also been found within ice streams and in their onset zones. They propose that ribbed moraines can be formed at various times during a glacial cycle between the ice divide and the glacier margin.

Ribbed moraines are often called Rogen moraines, deriving its name from a lake in Sweden, where the landforms have been described (Hoppe, 1948; Hughes, 1964a). They have been termed ribbed moraine in North-America (Aylsworth and Shilts, 1989a) and Rogen terrain by Burgess et al. (2003), which generally applies to drumlinized or fluted ribbed moraines. The term ribbed moraine is preferred in most recent studies and therefore is the one used in this study.

These landforms have been described in many palaeo-ice sheet settings. Ribbed moraines are found on the beds of the LIS, the SIS and the BIIS. However, their subglacial origin makes them difficult to identify and describe in modern settings. In some places, ribbed moraines have been linked to the occurrence of drumlins and have been found superimposed on drumlins. Some studies suggest that drumlinization of ribbed moraines indicates a step-like transition between these landforms (Lundqvist, 1989; Dunlop and Clark, 2006).

Ribbed moraines have raised curiosity for researchers for decades now, but their formation and origin are still unclear. Formation of ribbed moraines have been linked to a

variety of aspects of ice sheet behavior, but their origin and formation is still debated. The most prevalent theories are directed at thawing beds (Hättestrand, 1997; Hättestrand and Kleman, 1999), freezing beds (Sollid and Sorbel, 1984), the onset of ice streams or their shutdown (Dyke et al., 1992; Stokes, 2006), changes in ice flow direction (Boulton, 1987; Clark and Walder, 1994), or subglacial outburst floods (Fisher and Shaw, 1992).

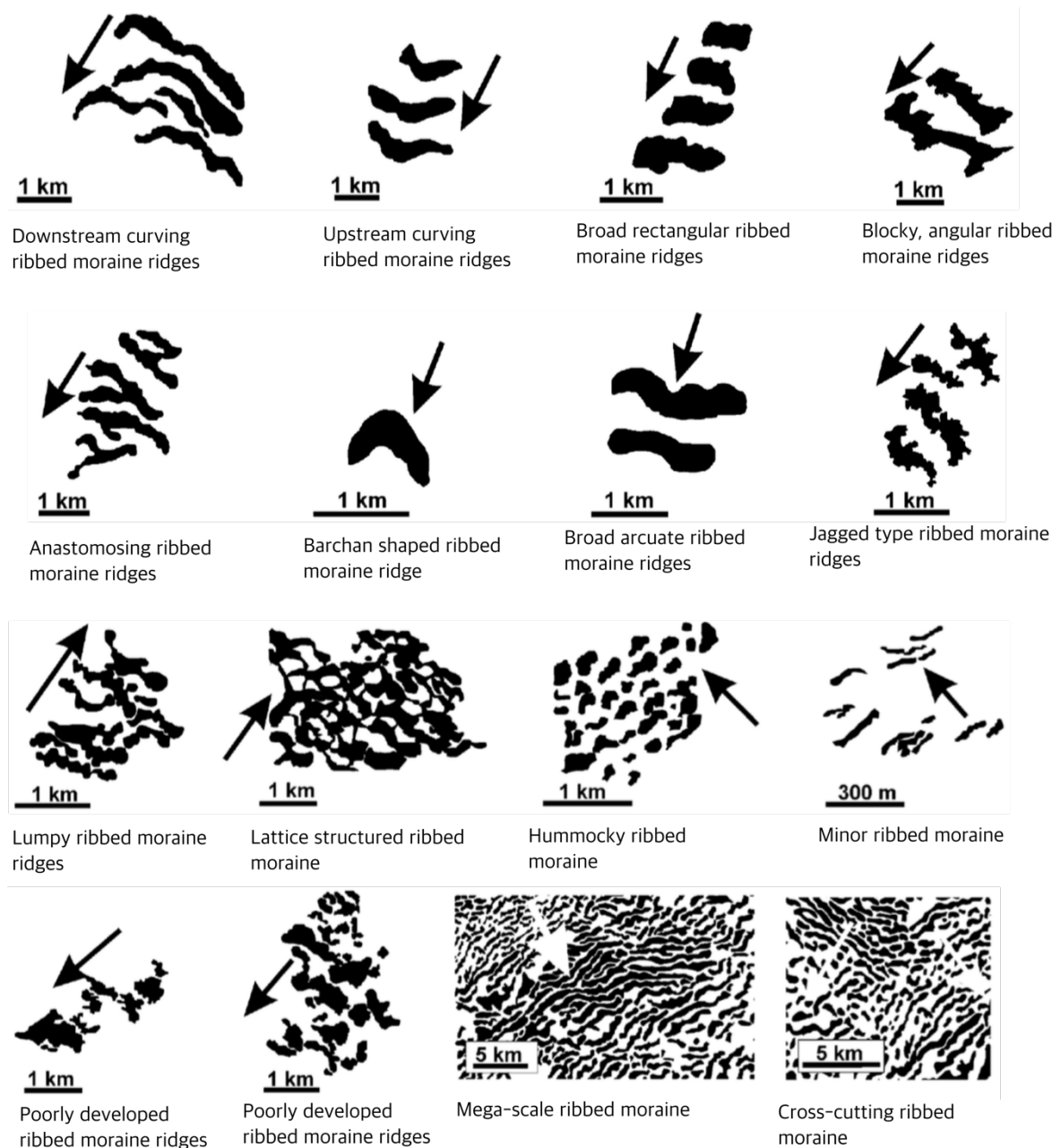


Fig. 3-1. Classification scheme of ribbed moraine geomorphology modified from Dunlop and Clark (2006).

3.1 Importance of studying ribbed moraines

Because of the lack of understanding and limited proof of formation, ribbed moraines have not often been used to reconstruct past ice-sheets (Hättestrand and Kleman, 1999). Other subglacial landforms have been used, such as drumlins, terminal and lateral moraines, eskers, and other ice-marginal landforms (Hättestrand, 1997). Ribbed moraines do occur in the interior of former ice sheets, but their genesis and subglacial glaciological conditions are poorly understood. An increased understanding of ribbed moraines can potentially shed light on their importance and formation and according to Hättestrand (1997), studying their formation and genesis has implications for tracing cold-based areas of ice sheets, where a transition to melting conditions occurred during deglaciation. Although that point of view is a subject of debate (Dunlop and Clark, 2006).

So far, ribbed moraines have been described in many formerly glaciated areas, such as North America (Hughes, 1964b; Aylsworth and Shilts, 1989a; Bouchard, 1989; Fisher and Shaw, 1992; Stokes, 2006), Scandinavia (Lundqvist, 1969a; Lundqvist, 1989; Hättestrand, 1997; Lundqvist, 1997; Raunholm et al., 2003; Möller, 2006), Ireland (Knight and McCabe, 1997; Clark and Meehan, 2001) and Scotland (Finlayson and Bradwell, 2008). The landforms have not previously been described in Iceland. This thesis presents new examples of potential ribbed moraine fields (transverse ridges) from Vopnafjörður, northeast Iceland.

3.2 Previous research on ribbed moraines

Many studies and useful observations have been made on ribbed moraines, but no unifying theory has yet been agreed upon. The landforms were first described by (Högbom, 1885; Högbom, 1894) in central Sweden, who only noted their internal composition. The first hypotheses suggested they formed as a series of end moraines (Frödin, 1913; Högbom, 1920; Frödin, 1925; Beskow, 1935) or of a marginal/near-marginal glacial origin (Frödin, 1954; Lundqvist and Svensson, 1957; Henderson, 1959; Craig, 1965; Fromm, 1965; Cowan, 1968). Lundqvist (1935; 1937; 1943; 1951) suggested a dead-ice origin, arguing that ribbed moraines were made from supraglacial material that slumped into transverse crevasses creating a ribbed-like pattern. Mannerfelt (1942; 1945), Granlund (1943) and Kurimo (1980) were in favor of Lundqvist's theory of this areal stagnation. Another explanation related their formation to calving ice margins (Hughes, 1964a). Hoppe (1948) suggested a near-marginal deposition of material followed by ice-front oscillations.

The subglacial origin of ribbed moraines was not suggested until Lundqvist (1969a) put forward a compilation of observations. He recorded specific lodgement characteristics of till, eskers overlying the ridges, drumlinizations and flutings on the ridge surfaces, which are all features strongly suggesting a subglacial origin. Since then, most studies have favored this with varying versions of exactly what factors and processes are dominant in their formation.

One of the first conceptual models presented was by Bouchard (1986; 1989). The model assumed that the ribbed moraines were formed in near-marginal, topographical bedrock

basins where a down-glacier obstacle causes development of shear planes in the debris-rich, basal ice which would then stack into up-glacier dipping slices. The model was not able to explain morphological characteristics such as the arcuate form of ribbed moraine. Lundqvist (1989; 1997) suggested the primary ridge structure in ribbed moraines to reflect pre-existing features which had been subsequently drumlinized under the ice sheet. Boulton (1987) concurs with Lundqvist to some degree, explaining that pre-existing ridges would have been subglacial folds or drumlins, formed under a different ice flow direction followed by a 90° change in ice-flow under deforming bed conditions. Aario (1977a; 1977b; 1987) concluded that ribbed moraines were formed under wavy ice flow while drumlinoid features were formed under the effect of basal spiral ice flow. Meltwater-flood theories were presented by Fisher and Shaw (1992) and Beaney and Shaw (2000), suggesting that ribbed moraines were formed during subglacial outburst floods as ripple-like cavity infills eroded into basal ice (Fisher and Shaw, 1992; Shaw, 2002).

A numerical formation model was made for ribbed moraine formation, in order to make predictions that are quantitative and that can be tested. The Bed Ribbing Instability Explanation (BRIE) theory argues that ribbed moraines are produced by the natural instability formed in the coupled flow of ice and till (Dunlop et al., 2008; Chapwanya et al., 2011). Transverse subglacial ridges grow spontaneously under certain parameter combinations which predict their wavelengths (crest spacing). BRIE does manage to predict the ribbed moraine patterns and wavelengths correctly and testing failed to prove the model false. The conclusion of the study from Dunlop et al. (2008) is that the BRIE is a viable explanation of ribbed moraine formation although they also state it is largely ignorant from the subglacial conditions that ribbed moraines are formed in.

Two main competing theories for ribbed moraine formation have been suggested through the years: the fracturing theory, and the shear and stack theory. Below, these two theories are presented in more detail:

- i. The fracturing theory (Hättestrand, 1997; Hättestrand and Kleman, 1999) (*Fig. 3-2*):

Extensional flow causes fracturing of till sheets at the (polythermal) boundary of a thawing glacier bed between cold based and warm based glacier or between ice streaming and ice divide. Lundqvist (1969a) presented the original theory on extensional flow where less plastic, debris-rich basal ice fractured transverse to ice flow by strong, tensional forces induced by topography. Hättestrand (1997) and Hättestrand and Kleman (1999) theorized that the transition zone from a cold-based core of ice sheets to warm-based conditions would result in high tensional stresses and extensional ice flow. That would lead to detachment of the pre-existing till sheet and boudinage-like fracturing at this transition zone, creating ribbed moraines (*Fig. 3-2*). The key to this theory is the presence of competent or incompetent sediment drift sheet, causing brittle or ductile deformation of subglacial sediments. During retreat of a cold-based ice boundary, a phase-change surface (PCS) rises through the bedrock, pre-existing sediment sheet and to the ice-bed interface (Hughes, 1973a). Local extensional flow occurs at the frozen-thawed boundary, which is retreating due to increase in basal flow velocity (Kleman and Borgström, 1994). When the PCS reaches the bedrock-drift sheet boundary,

deformation can take place at the interface and ribbed moraines form. If the PCS is below bedrock, no geomorphic processes will act on the drift sheet. If the PCS rises to the ice-drift boundary, drumlinization or fluting of ridges can start.

Hättestrand (1997) and Hättestrand and Kleman (1999) suggest that ribbed moraine distribution can be used to map former ice sheet areas that underwent changes from a frozen bed to a warm bed and that ribbed moraine formation is linked to that temporal and spatial transition from frozen to thawed bed conditions. They also propose that frozen bed areas were larger in earlier stages of glaciation based on the transgressive inward morphology of the landforms downstream cold-based areas. Finlayson and Bradwell (2008) agree with the fracturing theory, although they also state that the shear and stack theory could stand under compressive flow. The landforms they study are in the lee of a topographical obstruction, where extensional ice flow would have likely been dominant. They also observe that the spacing between ridge crests increases downstream, which they claim to indicate formation associated with extensional processes.

According to *Hättestrand (1997)* his theory supports the following ribbed moraine characteristics:

- Ribbed moraines are only found in core areas of ice sheets (Schytt, 1974; Hooke, 1977; Sollid and Sorbel, 1984; Dyke, 1993; Huybrechts and T'siobbel, 1995; Heine and McTigue, 1996).
- A heterogenous internal composition of the ridges. The morphology-shaping process is unrelated to internal composition in this model (Lundqvist, 1989).
- Ribbed moraines are frequently composed of the same material as the surrounding area or a potential pre-existing drift sheet (Henderson, 1959; Cowan, 1968).
- Till sheet is often thin or absent between ridges (Wastenson, 1983) which can be expected if the PCS is situated near the bedrock-drift interface.
- Drumlinization of ribbed moraines is common and they also commonly transition into drumlins (Lee, 1959; Hughes, 1964b; Hoppe, 1968; Lundqvist, 1969a).
- Glaciotectonism is frequent in ribbed moraines (Shaw, 1979; Bouchard, 1980; Dredge et al., 1986; Bouchard, 1989; Lundqvist, 1989).
- Ridges commonly fit together as a jig-saw puzzle (Lundqvist, 1969a; Bouchard, 1989; Hättestrand, 1997), which they suggest indicates extensional flow and fracturing of a sediment drift sheet.

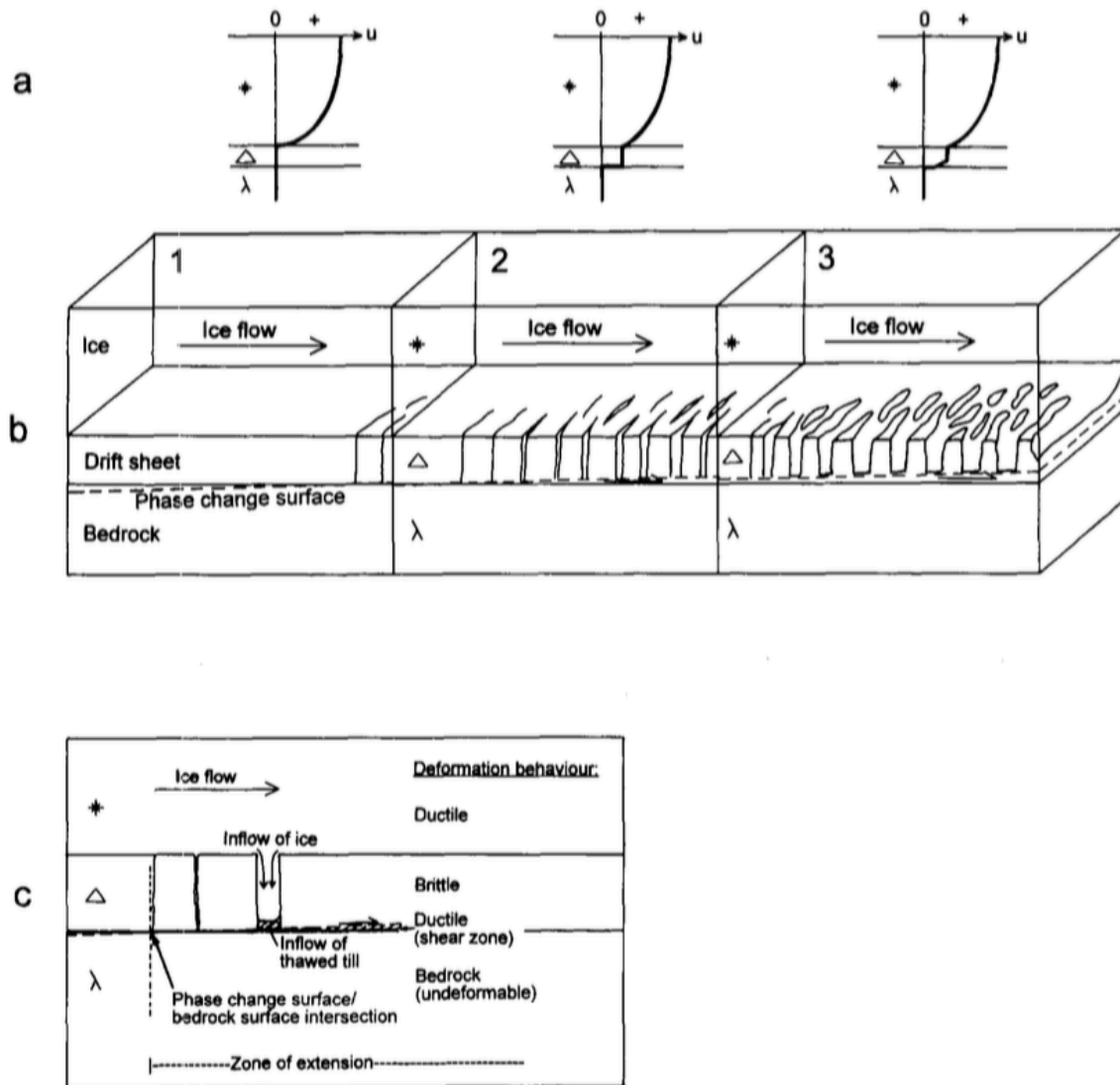


Fig. 3-2. The fracturing model of ribbed moraine formation model taken from Hättestrand (1997) proposes that they result from the rise of a pressure melting isotherm (PCS) through a glacier bed. (a) Ice flow velocity (u) for stages 1-3 which is shown in (b). (b) Time slice boxes (1-3), showing how pre-existing drift sheet develops into ribbed moraines with different stages of underlying drift sheet. The frozen drift ribs detach as soon as the pressure melting isotherm reaches the bedrock surface. (c) The fracture zone where the drift sheet has experienced detachment and extension as ice velocity increased.

- ii. *The shear and stack theory* (Shaw, 1979; Aylsworth and Shilts, 1989a; Bouchard, 1989; Lindén et al., 2008):

Till slabs or near-base englacial material experiences subglacial folding and thrust stacking due to compressive ice flow with subsequent lee side cavity infill and subglacial melt-out. The shear and stack theory has been presented in different variations by e.g. Shaw (1979), Bouchard (1980; 1989), Lee (1959), Dredge et al. (1986), Aylsworth and Shilts (1989a), Dyke et al. (1992), Sollid and Sorbel (1984) and Lindén et al. (2008). Some of these studies suggest a compressive flow due to

topographic obstructions at the down-stream end of rock basins (Högbom, 1885; Bouchard, 1980; Minell, 1980; Sollid and Sorbel, 1984; Bouchard, 1989). Others argue that a large amount of near-basal debris can decrease the plastic behavior of the ice, increasing compression and basal shearing of the debris-rich ice due to a low ice-surface gradient and climatic deterioration (Dredge et al., 1986). Another theory proposed that ridges were formed far from the ice-margin, as water-soaked debris was entrained into the glacier sole and sheared into ridges during an expansion of a frozen core area under the ice sheet (Sollid and Sorbel, 1984). Dyke et al. (1992) also suggested that ribbed moraines form in a transition zone from cold- to warm-based conditions but explained by alternating sticking and sliding conditions causing stacking of debris. Lindén et al. (2008) proposed an alternative hypothesis taking internal structures and sedimentary composition into account while comparing with ridge morphology. They argue that basal water pressure depended on seasonal variations in meltwater recharge of the subglacial system causing temporal and spatial changes in rheology and deformation on the bed (*Fig. 3-3*). These changes would stem from bed conditions fluctuating between rigid and deforming, leading to localized folding and thrusting in the rigid bed transition zone where glaciotectionic stress was greater than bed strength. They suggest that none to several ridges can be built during this bed-rheology cycle. Möller (2006) proposed a model in which the sediment comprising a Rogen moraine was already present in the form of a ridge but was later shaped into a Rogen moraine.

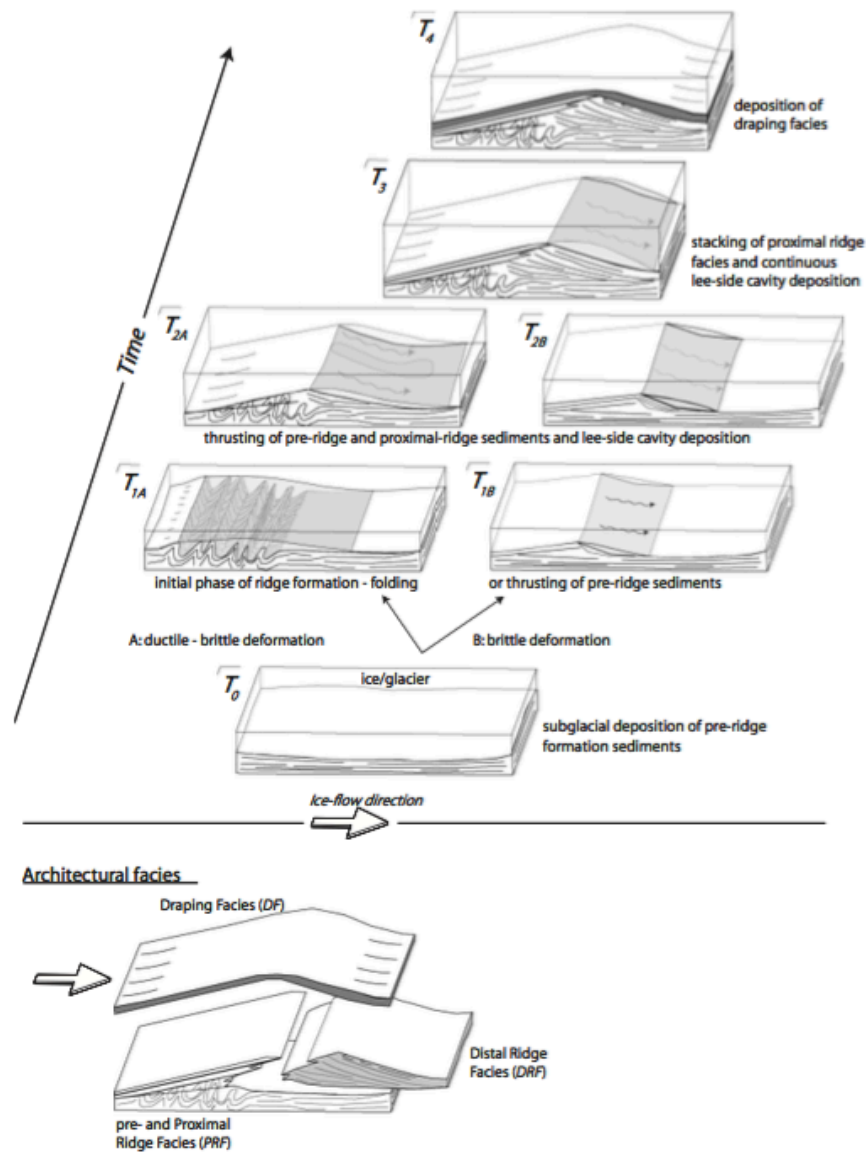


Fig. 3-3. The shear and stack model from Lindén et al. (2008). T_0 : pre-existing sequences of laminated sediments are deposited in valley areas. T_{1A} : ridge starts forming due to bed compression where pre-existing sediments fold and thrust (T_{1B}) in ice-flow direction causing a transverse thickening of the bed, forming an obstacle to the ice-flow and causing a lee-side cavity to form parallel to the ridge developed. Ridge forms in stages T_2 - T_3 with folding followed by erosion and thrust sheet stacking of sediment (T_{2A}). T_{2B} shows a brittle deformation case where ridge forms only through thrust-fault stacking. Distal cavity infilling starts, with a variable deposition of glaciofluvial sediments including suspension of fine-grained sediment to high flow velocity gravels of traction load interbedded with stratified and massive diamicts. The diamicts are interpreted to be deposited from sediment gravity flows into the lee-side cavity from the deforming bed. Larger clasts are interpreted as drop stones. Lee-side cavity sediments include small-scale normal faulting and reverse faulting due to extensional and compressional faulting. T_4 is the draping stage where the ridge is smoothed with erosion, creating an unconformity in the sediments and then draped over by a diamict with a high clast orientation.

Möller (2006) and Lindén et al. (2008) agree with Kurimo (1980) and Lundqvist (1989) on a polygenetic origin of ribbed moraines due to the variety in their internal composition, size, shape and spatial distribution. They propose that the term ribbed moraine is used purely as a descriptive, morphological term encompassing a polygenetic group of glacial landforms. This opposes Dunlop and Clark (2006) who suggest a unifying hypothesis explaining ribbed moraine formation. Hättestrand (1997) and Hättestrand and Kleman (1999) concur, stating that different variations have widely similar distribution patterns and orientations in context with ice flow and ice sheet distribution which, in turn, suggests a single formation process. They argue that the distribution pattern and orientation of different types of ribbed moraines indicate that the morphologies are variations of a single genetic landform (Hättestrand, 1997). They also suggest that all types of ribbed moraine ridges are compatible with the fracturing theory as opposed to the shear and stack theory, which they believe fails to explain features in the distribution pattern and morphology of ribbed moraines. Hättestrand (1997) also showed that the distribution patterns of different morphological varieties of ribbed moraine was similar in terms of patterns and orientation towards the ice flow indicating a similar formation process throughout the field and a monogenetic landform formation.

3.3 Internal characteristics of ribbed moraines

Ribbed moraines have a vast range of internal composition. They are commonly composed of the same material as their surroundings (Cowan, 1968; Lundqvist, 1969a). Lundqvist (1969a; 1997) noted that the most common material in ribbed moraines is subglacial till. *Table 1* presents an overview of ribbed moraine sedimentary composition throughout the literature and in part based on *Table 1* from Hättestrand (1997) with the addition of later studies.

Table 1. 9Sedimentary characteristics of ribbed moraines

Material	Locality	Reference
Loose, massive, sandy, stratified diamicton with clasts of local lithology and beds of sorted sand. Shear structures and microfaulting exist with some bullet shaped, faceted and striated clasts.	Northern Scotland	Finlayson and Bradwell (2008)
Fissile, till-cored ribbed moraines.	West/Central Labrador, Canada	Cowan (1968)
Matrix-supported diamict alternating with interbedded gravel and sand containing erosional surfaces, lenses, indicating sediment reworking or debris-flows.	Avalon Peninsula, Newfoundland	Fisher and Shaw (1992)
Ridge surfaces have large boulders which are not in the sections. Gravelly, sandy diamicton, interbedded with sorted sediments, beds of sandy silt and clast horizons.	Dalarna, Central Sweden	Möller (2006)
Diamict and stratified sorted material showing signs of glaciotectionics in sorted material.	Northern Sweden	Lindén et al. (2008)

Diamicton overlain by sorted sand and gravel. Clasts show glacial erosion features and the unit has fractures and thrust structures.	Dubawnt palaeo-ice stream	Stokes (2006)
Boulders on ridge surfaces. Deformed diamict containing sheared sand and gravel. Sand is planar-bedded with small-scale cross-laminations and ripples.	Finland	Sarala (2006)
Diamict with a sandy matrix and large, striated clasts. It is intercalated with lenses of stratified, sorted, and distorted sediment zones, with scattered dropstones and erosive upper contacts.	Jæren, Norway	Raunholm et al. (2003)
Fluvial sediments and compact diamict, with glaciotectionic features	Central Sweden	Lundqvist (1997)
Medium to coarse sand	Quebec, Canada	Ives (1956)
Glaciofluvial sand, interbedded in ablation and basal till	Värmland, Sweden	Lundqvist (1958)
Gravelly sediments	Keewatin, Canada	Aylsworth and Shilts (1989a)
Kalix till, slightly disturbed and fine-grained	Norrbottn, Sweden, Värmland, Sweden	Hoppe (1948); Fromm (1965); Lundqvist (1969a)
Sveg till, diamict with layers of sorted material (subglacial meltout till)	Jämtland, Sweden	Shaw (1979)
Stratified, matrix-supported, fine-grained diamicton (basal melt-out till)	Quebec, Canada	Bouchard (1989)
Sandy-silty till with sorted sediment lenses	Lake Rogen area, Sweden	Wastenson (1983)
Sandy till (clayey till underneath and in surrounding areas)	Jämtland, Sweden	Lundqvist (1969a)
Loose ablation till	Värmland, Sweden	Lundqvist (1958)
Very hard-packed basal till	Jämtland, Sweden	Rasmusson (1951)
Silty till with folded beds of shattered bedrock	Jämtland, Sweden	Minell (1977)
Broken rock with little matrix	Manitoba, Canada	Dredge et al. (1986)
Disaggregated sandstone, without fines	Keewatin, Canada	Aylsworth and Shilts (1989a)
Great variations in internal structure and bedding	Sweden	Lundqvist (1969a); Lundqvist (1997)

3.4 Spatial relationships of ribbed moraines

Ribbed moraines can have a variety of spatial relationships with other landforms and landscapes. They can both be drumlinized or in close proximity to drumlins and MSGs. They have also been observed superimposing streamlined landforms and vice versa (Dyke et al., 1992; Dunlop and Clark, 2006), but the chronology of cross-cutting relationships is often unclear. The study by Dunlop and Clark (2006) included a large dataset and a wide spectrum of ribbed moraines across the Northern hemisphere and compared their size, shape, pattern, spatial relationships, and distribution with results from previous studies. This indicated that ribbed moraine characteristics are more complicated and varied than many previous studies had claimed. *Fig. 3-4* shows examples from Dunlop and Clark (2006) where ribbed moraines are found in proximity to, superimposed on, or adjacent to landforms such as MSGs, drumlins, eskers or crag and tails. Dunlop and Clark (2006) also present a geomorphological overview which indicates that ribbed moraines are generally not associated with any specific type of topographic setting over another and their location is also not bound to downstream or upstream facing slopes.

Ely et al. (2016) propose a theory of a continuum of subglacial landforms where ribbed moraines and mega-scale ribs form a continuum of subglacial ribs. They also present quasi-circular landforms, which their analysis of landform shapes suggests are a stage between transverse bedforms towards streamlined lineations. The increased elongation ratio is thought to indicate increased ice flow rate.

Stokes (2006) mapped ribbed moraines in the Dubawnt Lake palaeo-ice stream tracks that lie on top of MSGs, which appear to be segmented. The re-moulding of MSGs by ribbed moraines indicate that the ribbed moraines are a secondary feature and post-date the MSGs. Stokes et al. (2006) link ribbed moraines to spatial and chronological transition between cold and warm-based ice leading to acceleration and deceleration of ice flow. They suggest that ribbed moraines are signs of ice-stream shut-down and a reversion to frozen bed conditions after a thawing period. However, this study did not include field observations of the ridges and their exact formation remains open to debate.

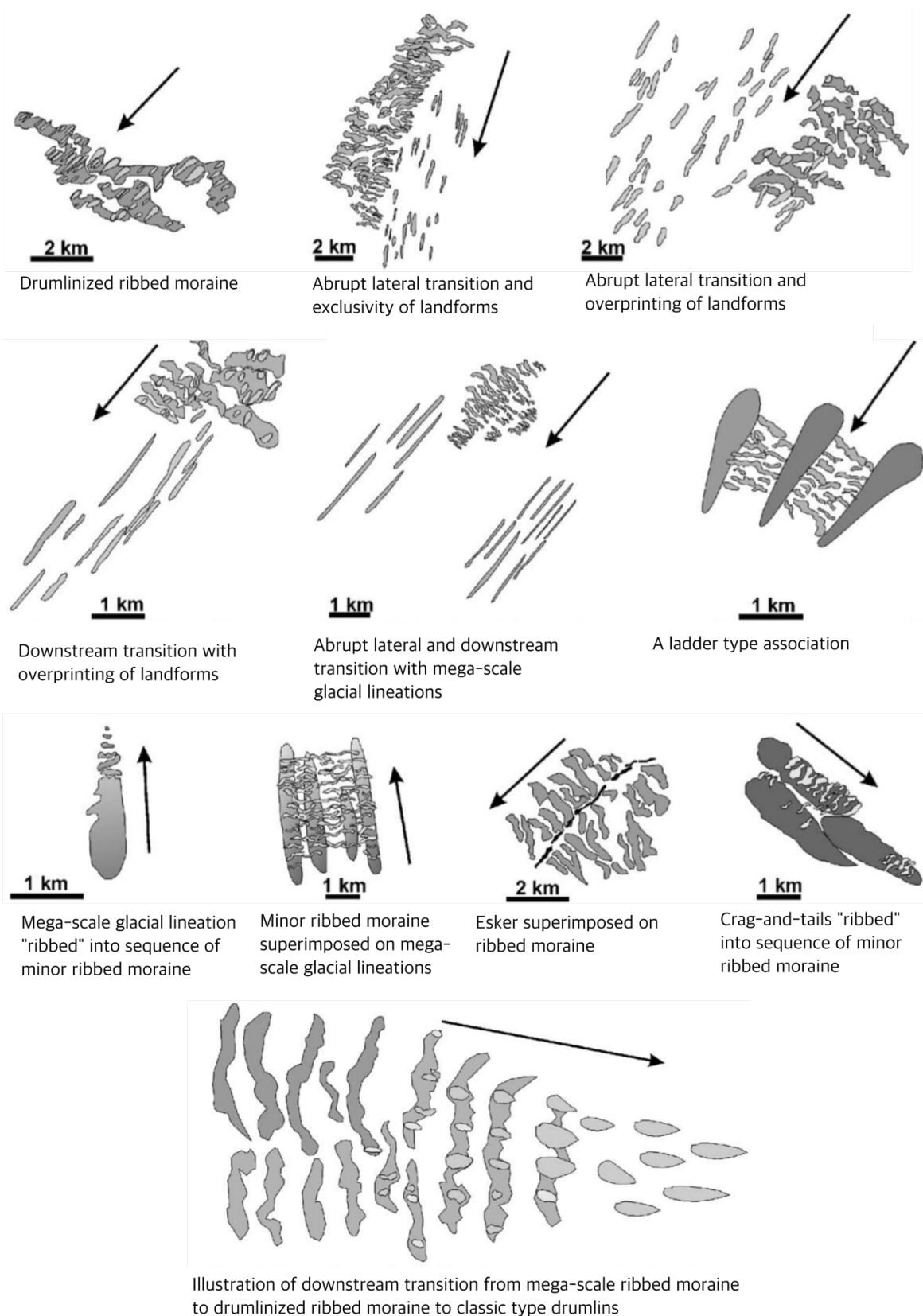


Fig. 3-4. A schematic diagram showing the spatial relationships between ribbed moraines and other glacial landforms. The direction of ice flow is indicated with an arrow. Modified from Dunlop and Clark (2006).

3.5 Ribbed moraines in a modern context

Ribbed moraines and ribbed terrain might have a modern comparative context, but subglacial conditions of glaciers and ice sheets are, for obvious reasons, difficult to explore. This requires a different means of research, thus, various geophysical methods can be applied in order to further the understanding of modern ice stream behavior. The flow of ice streams has been linked to low driving stress at the ice bed, strong lubrication from subglacial till and its high-pressure water content (Alley et al., 1986; Blankenship et al., 1986; Alley et al., 1987; Kamb, 2001). Changes in ice stream dynamics might be caused by changes in basal conditions or long-term climate forcing (Anandakrishnan and Alley, 1997; Tulaczyk et al., 2000; Winberry et al., 2014). Ice streams are sometimes restricted by side drag (Raymond et al., 2001), high basal shear stress or “sticky spots” (MacAyeal, 1989) which may have a role in the so-called stick-slip motion of ice streams (Bindschadler et al., 2003).

Stokes et al., (2016) compared the patterns of ribbed palaeo-ice stream beds from Canada and patterns of high basal shear stress (sticky spots) found with geophysical techniques underneath modern ice streams in Antarctica and Greenland (MacAyeal, 1992; MacAyeal et al., 1995; Price, 2002; Joughin et al., 2004). Their study revealed a similarity and potential connection between these observations. In modern ice streams these features of high basal shear stress are termed ‘traction ribs’ (*Fig. 3-5*) (Sergienko and Hindmarsh, 2013). The features observed at the palaeo-ice streams in Canada may provide insight into the formation of traction ribs underneath modern ice streams. Sergienko and Hindmarsh (2013) hypothesize that even though ribbed moraine is a smaller feature, traction ribs they observed in Pine Island Glacier and Thwaites Glacier in Antarctica are of similar pattern-forming origin to ribbed moraines. They link that theory to differences in bed strength and the effects of subglacial water transport on effective pressure variations. They also suggested that the landforms are only found in the parts of ice sheets where the bed is temperate and has deforming subglacial till. These findings show promise in improving understanding of the behavior of ice streams and the origin and the role of ribbed moraines.

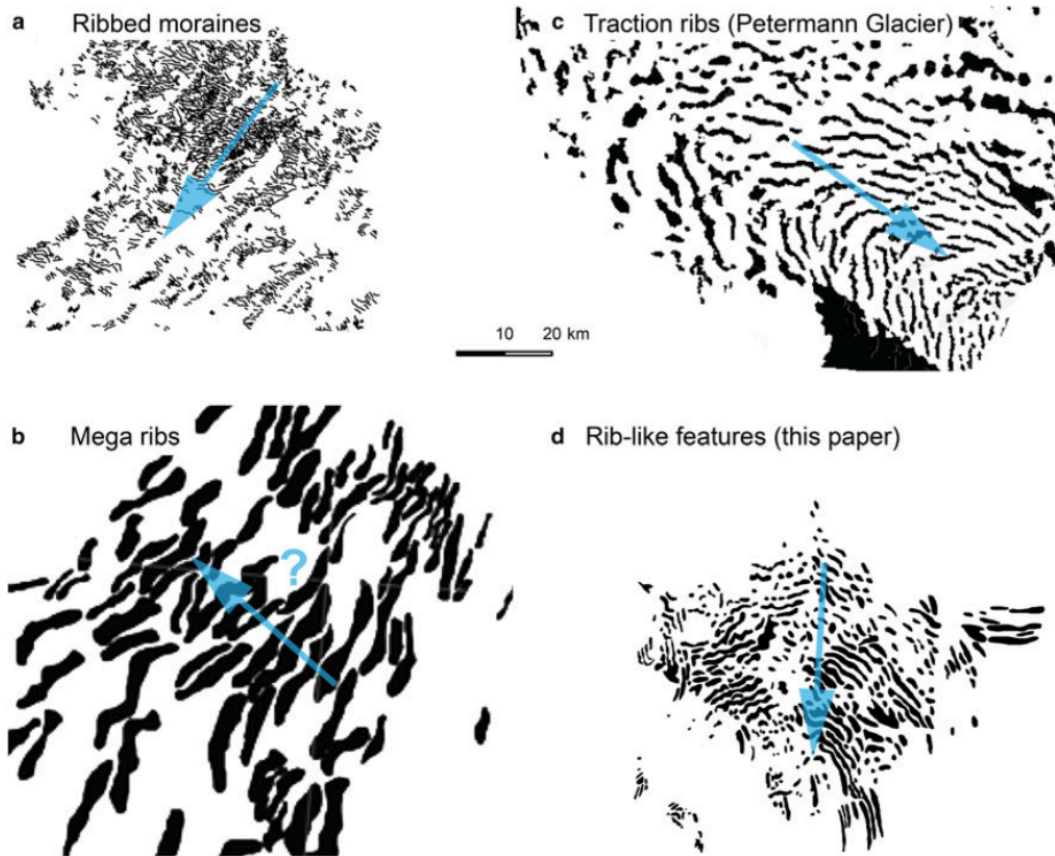


Fig. 3-5. Comparison from Stokes et al. (2016) between types of ribbed features observed in palaeo-settings (a, b and d) and 'traction ribs' (c). They split ribbed palaeo-features into three subcategories; ribbed moraines, mega ribs and the more irregularly patterned rib-like features. Blue arrows show the estimated ice flow direction. In the paper, d and c were compared and authors suggested a continuum of subglacial rib formations.

4 Study area

4.1 Regional setting

The Vopnafjörður fjord is located in the northeast part of Iceland (*Fig. 4-1*). The fjord is up to 20 km wide at its mouth and 22 km long with a southwest-northeast orientation. The mountain ranges Smjörfjöll and Fagradalsfjöll are situated in the southeast part of Vopnafjörður with steep slopes, cirques, and narrow valleys. On the northeast side is Bakkaheiði plateau with gentler sloping hills and abundant north-south trending streamlined landforms, which are clearly visible on aerial and satellite imagery. As a continuation of the southwest trend of Vopnafjörður are three valleys: the Selárdalur valley to the west, Vesturárdalur valley in the center, and Hofsárdalur valley to the east. Vesturárdalsháls is an elongate bedrock high located between Selárdalur and Vesturárdalur and has a streamlined appearance to the northeast. The valleys are wide at their mouths but get narrower inland, gain elevation, and eventually merge with the plateaus, which mark the boundary to the Icelandic highlands (above 300-400 m a.s.l.). The Bustarfell mountain forms a clear start of the highland plateau. Beyond the highland margin, glacial landforms are prominent features in the landscape, with hundreds of streamlined landforms as well as isolated basins with smaller, transverse (to estimated ice flow) landforms. Hauksstaðaheiði (Hauksstaða-plateau) is the area of main focus in this study and is located as a southwest-wards continuation of Selárdalur and Vesturárdalur (*Fig. 4-1*).

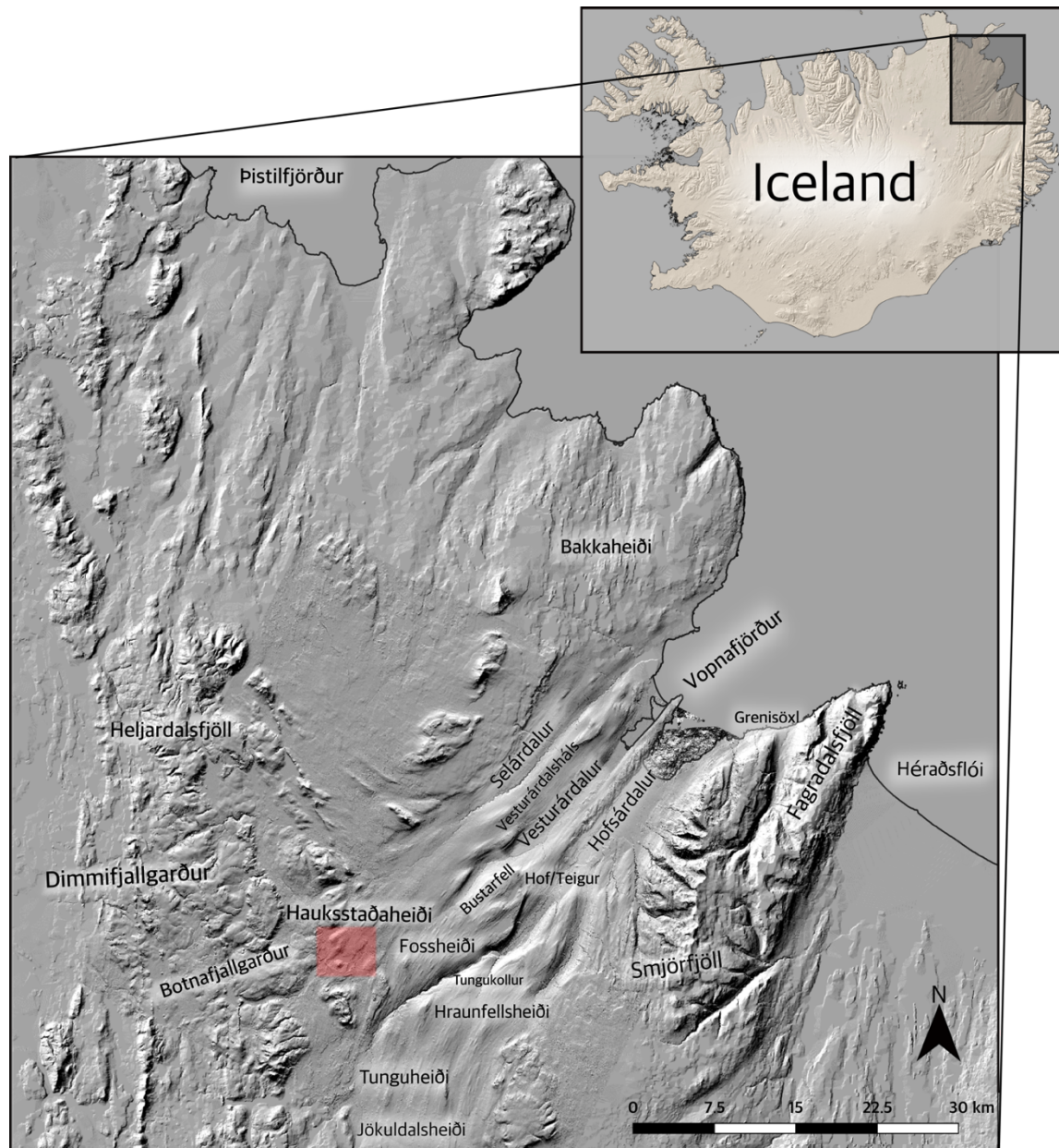


Fig. 4-1. The study area of Vopnafjörður and its location in Iceland. The large map shows the focus area of Hauksstaðaheiði inside the red box but Tunguheiði and Selárdalur were also mapped. Map base is from the ArcticDEM (Porter, 2018) and the National Land Survey of Iceland (Landmælingar Íslands)(LMÍ, 2016).

The Hauksstaðaheiði study area is located in the lower highlands southwest of Vopnafjörður between Dimmifjallgarður mountain range and Vopnafjörður (Fig. 4-1). The landforms studied here are situated in the Leirvatnaskvos basin, at an altitude between 415-528 m a.s.l., which is slightly lower than the surrounding hills and mountains of Hauksstaðaheiði (Fig. 4-2). The Skeljungsa river flows through the basin from Leirvatn to Arnarvatn, eroding the landforms (Fig. 4-3). The Langafell and Leirvatnshnjúkur hills are situated to the west and Hlíðarfell hill to the north. These mountains are part of the Botnafjallgarður massif (Fig. 4-1), which is at the flank of a larger mountain range,

Dimmifjallgarður. Dimmifjallgarður reaches up to 800-900 m a.s.l. at its highest. Dimmifjallgarður has a north-south orientation, which coincides with the plate rift between the North-American and the Eurasian tectonic plates. The mountains are located east off the main rift zone. The mountain range and local bedrock type is largely basaltic (Jóhannesson and Sæmundsson, 2014) but has not been studied extensively. It has been suggested that the ice sheet was cold-based above the mountain range during the LGM (Sæmundsson, 1995) and was potentially the location of an ice divide according to the model by Patton et al. (2017) (Fig. 1-1).



Fig. 4-2. The Hauksstaðaheiði and Leirvatnshnjúkur area with place names taken from www.maps.google.com (Airbus, Landsat/Copernicus, Maxar Technologies, U.S. Geological Survey). The ridges are situated in a vegetated depression in Leirvatnshnjúkur where the Skeljungsa river runs from lake Leirvatn to lake Arnarvatn. The Fig. shows the road as a yellow line, leading to Vopnafjörður.

According to a bedrock geology map from the Icelandic Institute of Natural History (Jóhannesson and Sæmundsson, 2014), the age of the bedrock in the field area at Hauksstaðaheiði plateau and Leirvatnshnjúkur is 3.3-0.8 m.y.. The region is mostly composed of basaltic lavas, but because the rock formed at the start of a climatic cooling, there can also be hyaloclastites, tillites or glaciofluvial sediments present in the strata. This area is situated where the distinctive volcanic, highland plateau landscape starts becoming more eroded towards the coast and deep fjord and valley systems become an increasingly dominant landscape feature to the east (Jóhannesson and Sæmundsson, 2014; Loftmyndir, 2016, 2000). The bedrock closer to the shoreline is older, or from the late- and mid-Miocene. The Hauksstaðaheiði field area is at the border of upper- or lower-Pleistocene lavas and Leirvatnshnjúkur to the west is made of upper-Pleistocene age (younger than 0.8 m.y.). This is where the Dimmifjallgarður mountain range starts and subglacial volcanic

formations (hyaloclastite, pillow lava and sediments) characterize the area. Interglacial and supraglacial basic and intermediate lavas younger than 0.8 m.y. are also found to the south-west of Hauksstaðaheiði.



Fig. 4-3. A view of the Leirvatnsvos basin (looking towards the west). The Skeljungsá river runs from Leirvatn on the left and into Arnarvatn which is not seen on this fig., creating useful sections in the ridges for investigations of internal composition. Section 4 can be seen on the figure.

Other areas of interest are Tunguheiði, Jökuldalsheiði, Hraunfellsheiði and Selárdalur where similar landforms to the ones studied in Hauksstaðaheiði occur. The upper/western part of Selárdalur has a number of transverse landforms and so does the Tunguheiði, Jökuldalsheiði and Hraunfellsheiði area. Streamlined bedforms are common in Tunguheiði, Hraunfellsheiði, Vesturárdalsháls, Bustarfell, Fossheiði and in other areas and are included in maps in this study.

4.2 Previous research/ Glacial history of Vopnafjörður

Very little research has been conducted in the area of Hauksstaðaheiði and no studies have been published with the main focus on glacial geomorphology or ice streaming into Vopnafjörður. Sæmundsson (1995) studied the deglaciation and associated shoreline displacement in Vopnafjörður but most of his research was conducted at the valley floor and shoreline level, with a minor focus on the Vopnafjörður uplands. His research in the area and hypotheses on deglaciation of Northeast Iceland nevertheless proved very useful in order to gain a better perspective on controlling late-glacial processes and timing of deglaciation.

Norðdahl et al. (2019) estimated that the model presented by Patton et al. (2017) shows that at the LGM, the ice sheet extended more than a 100 km beyond the coastline of

Héraðsflói, south of Vopnafjörður. A warm-based ice stream would have flowed at velocities higher than 300 m annually, through Fljótsdalur and into Héraðsflói in the east of Iceland (Norðdahl et al., 2019). Their study finds that the deglaciation of Fljótsdalur-Úthérað coincides with the deglaciation of Iceland in general, caused by Late-Weichselian and early Preboreal climatic warming and changes in ocean dynamics in the North Atlantic. This confirms with (Sæmundsson, 1995) results for Vopnafjörður. Norðdahl et al. (2019) also found that the IIS had retreated into the central parts of Iceland by 9.2 ± 0.2 cal. ka BP, which is when glacio-isostatic uplift in the region had completed.

Fast-flowing ice streams most likely drained into Vopnafjörður during the LGM (Norðdahl, 1983; Sigbjarnarson, 1983; Sæmundsson, 1995; Bourgeois et al., 1998; Hubbard et al., 2006; Patton et al., 2017). According to Bourgeois et al. (1998), the ice divide of the LGM ice sheet for the northeastern part of Iceland extends from the interior of what now is the Vatnajökull ice cap, extending northwards, along Dimmifjallgarður and towards the Heljardalsfjöll mountains, towards Þistilfjörður fjord in the north.

Glacial striae on bedrock observed by Sæmundsson (1995), underlying sedimentary shoreline sequences in the Vopnafjörður valley floor, show a northeasterly ice-flow direction into the fjord. This direction will be referred to as the general flow of ice in this study. Selárdalur shows an easterly ice flow through striae, potentially influenced by the ice divide between Bakkaflói and Vopnafjörður and thought by Sæmundsson (1995) to be the main ice-flow for that area. Younger ice-flow directions are parallel to the valley directions while older ones can have a different directional element indicating less topographic control of ice flow. Sæmundsson (1995) observed striations on the outer coast of Vopnafjörður, 9 km from the Hofsárdalur valley coast suggesting a minimal ice marginal extent during the maximum ice cover of the region. However, it is more likely that the margin reached further out on the shelf.

Sæmundsson (1995) proposed a rapid deglaciation during late Younger Dryas and early Preboreal in the Vopnafjörður region. He also suggested that the ice-margin retreated inside the present coast of Vopnafjörður during late Younger Dryas. The following period of Preboreal was characterized by glacier advances and still stands in southwestern, central North and South Iceland (Norðdahl, 1994). Sæmundsson's radiocarbon dates confirm this for Vopnafjörður, indicating a readvance or still stand at 10.9 cal. ka BP (Pétursson et al., 2015) recorded at Hof-Teigur (*Fig. 4-1*). Rapid deglaciation after the Hof-Teigur event was also confirmed by Sæmundsson (1995) where rapid glacio-isostatic rebound occurred, observed through erosion and deposition in Vopnafjörður. In summary, Sæmundsson (1995) proposes four regional deglaciation events for the Vopnafjörður region:

1. The maximum event: A complete ice cover was over the Vopnafjörður region with the ice margin located off the present coast. The glacier later retreated inside the coastline and ice flow became restrained to local bedrock topography.

2. The Grenisöxl event: The ice margin was located just inside the coast and the sea level was higher than 55 m a.s.l. during late Younger Dryas.
3. The Hof-Teigur event: Ice margins in all valleys had retreated further inside the coast from Grenisöxl in eastern Vopnafjörður or 4-14 km into the three valleys during the early Preboreal.
4. The Bruni event: The ice margins in all three valleys had retreated into the highlands west of Vopnafjörður. Final deglaciation was rapid along with rapid glacio-isostatic rebound. The Vopnafjörður highlands (Tungukollur on Tinguheiði) then became ice free during early Holocene or between 10.0 and 8.7 cal. ka BP (Pétursson et al., 2015).

5 Methods

A variety of methods were used to conduct the research on Hauksstaðaheiði with field observations, measurements, sampling, sedimentological analysis and geomorphological mapping with geographical information systems (GIS). The research site on Hauksstaðaheiði was identified with help from the ArcticDEM (Porter, 2018) and aerial imagery (Loftmyndir, 2000, 2016). This was then verified during a reconnaissance in the field in July 2018 when some of the studied sections were also identified. During fieldwork in August 2019 more sections were discovered and finally four sections were mapped and studied over the course of a week.

5.1 Geomorphological mapping

The Hauksstaðaheiði landforms were mapped in detail with GIS (*ArcMap 10.4.1* and *QGIS 2.18.2*). Other areas in the region (Tunguheiði heath and Selárdalur valley) where similar ridges are present were also mapped, but in less detail. This was done using mainly aerial imagery from *Loftmyndir ehf.*, the *ESRI Basemap* from *ArcMap* and the *ArcticDEM* (Porter, 2018) from the Polar Geospatial Center using the ISN93 coordinate system as the primary layer system.

The *ArcticDEM* provides a 2x2 m pixel resolution making it easier than ever to map the extent of landforms such as the ridges investigated in this study, which are on the scale of tens of meters. The *IcelandDEM* was used, which consists of a mosaic of the *ArcticDEM* with improved positioning and robust mosaicking, carried out by the National Land Survey of Iceland, the Icelandic Meteorological Office and the Polar Geospatial Center. In order to get the most precise outline of the ridges, the *IcelandDEM* was extracted into hillshade and slope maps.

Loftmyndir ehf provide detailed aerial imagery for Iceland online, with good quality imagery for the Vopnafjörður highland region. The images used for this study are from 2016, 2013 and 2000 with a pixel resolution of up to 1 m. The ridges are easily spotted from aerial photos due to their rocky surface contrasting with green, vegetated surroundings, which made it easy to map through visual interpretation (*Fig. 4-2*). The ridges themselves appear brown and gravelly while the flat depressions between are green, vegetated and often wet. Therefore, aerial imagery was an essential tool along with the hillshade and slope raster maps to get a precise outline of the ridges.

Mapping was conducted in the GIS-lab at the University of Iceland where access to *ArcMap* imagery from *Loftmyndir ehf* is provided. Each ridge was drawn as a polygon and a shapefile was made for each ribbed moraine area (Hauksstaðaheiði, Selárdalur and Tunguheiði). For ridge statistics on width and length each polygon was framed by a

rectangle which measured their width, length and directional element with the feature „Minimum bounding geometry“. This information was moved into *Excel* for further statistical analysis. The relief of the Hauksstaðaheiði ridges was established by using „Interpolate shape“, then „Add Z Information“, which would then appear as the ridge relief from its surrounding lowland in the layer attribute table. The ridges are potentially larger than presented here because they were mapped from the relief (slope) differences and by aerial imagery using differences in vegetation.

Various maps were constructed showing the Hauksstaðaheiði landforms in detail with a different focus such as their relief, crest direction trend and shape. A large-scale map was also made, showing the ridges with respect to streamlined features in Bustarfell/Fossheiði, Tunguheiði and Vesturárdalsháls. For this map, transverse ridges in Selárdalur, Tunguheiði, Jökuldalsheiði and Hraunfellsheiði were also mapped in order to shed light on the distribution of transverse ridges in the region and the relationship with streamlined landforms and potential ice streaming. Shapefiles for streamlined landforms were acquired from Nína Aradóttir, a PhD candidate at the University of Iceland. A ridge relief map, showing the relief of each individual ridge was also created.

Two elevation profiles were drawn through the Leirvatnsvos basin using a plugin in *QGIS* and are presented as a map as well as the elevation profile. The distances between the ridge crests on the elevation profiles were measured crest to crest with a decameter accuracy. Another map was aimed at showing the transverse trend for the Hauksstaðaheiði ridges, where polylines were drawn along the crest of each ridge and their directional trend calculated in *QGIS*.

5.2 Field work

The Hauksstaðaheiði field site is a remote area located in the margin of the Botnafjallgarður/Dimmifjallgarður massifs. Accessing the area and the sections investigated required a high clearance, 4WD vehicle and an additional hike of up to 5 km one way to the closest section carrying the gear necessary for cleaning and investigating the sections. The field excursion in July 2018 was aimed towards general scouting of the Vopnafjörður region and Hauksstaðaheiði ridges and surrounding landscape. The ridges' characteristics were examined in the field in order to confirm previous observations from remote sensing. The landforms were thoroughly photographed from the valley floor and from topographic highs to the east of the Leirvatnsvos basin.

In 2019, a full day was used to identify all available natural sections by hiking around Hauksstaðaheiði and Leirvatnsvos. The landforms have been eroded by the Skeljungská river, leaving several usable sections revealing the interior of the ridges. Four large sections were used for sedimentary investigations. The remaining days were used to

clean/excavate, sketch, photograph, log, sample and measure the four sections. Clast morphology samples were taken from Sections 1-3.



Fig. 5-1. Sketching Section 1, with a string grid for reference.

Each section was excavated with the aim to expose as much of the interior as possible leaving enough time to investigate. Each section was first measured and scaled properly putting in markers for drawing and photographing. For scale, strings were lined up at different intervals depending on ridge size, forming a grid-like pattern to scale (*Fig. 5-1*). The sections were photographed and drawn in detail on site. Characteristics were sketched into field books and each feature thoroughly described. Then each section was logged using the Krüger and Kjær (1999) lithofacies code system (**Error! Reference source not found.**). The Benn and Evans (2004), *A Practical Guide to the Study of Glacial Sediments*, was useful as a guide for operating in the field. Dip and dip direction of layers and features were measured with a compass and an inbuilt clinometer. Measurements were distributed across the section if possible, in order to give an overview of the section's layers. These measurements were later plotted into the program *Stereonet 10.1.6* creating a stereograph showing the directional elements of the interior of the ridges. The plots created from *Stereonet* corrected for a 11° magnetic variation for this part of Iceland. Clast samples (CS) were collected for sections 1-3: two samples from Section 1 (S1-CS-U1/S1-CS-U2), three samples from Section 2 (S2-CS-U1/S2-CS-U2/S2-CS-U3) and two samples from Section 3 (S3-CS-U1/S3-CS-U2).

Table 2. Lithofacies codes for field description of glacial diamicts and associated sediments, modified from Krüger and Kjær (1999). The data chart from Krüger and Kjær (1999) was used as a guide for the logs and facies description.

Diamict sediments		Sorted sediments	
D	Diamict	B	Boulders
<i>General appearance:</i>		Bh	Boulders, horizontally bedded
m	Massive, homogenous	Gm	Gravel, massive
g	Graded	Gh	Gravel, horizontally laminated
b/s	Banded/Stratified	Gt	Gravel, trough cross-bedded
h	Homogenous	Gp	Gravel, planar cross-bedded
<i>Clast/matrix relationship:</i>		Sm	Sand, massive
(c)	Clast-supported	Sh	Sand, horizontally laminated
(m ₁)	Matrix-supported, clast poor	St	Sand, trough cross-bedded
(m ₂)	Matrix-supported, moderate	Sp	Sand, planar cross-bedded
(m ₃)	Matrix-supported, clast rich	Sr	Sand, ripple cross laminated
<i>Granulometric composition of matrix:</i>		Fm	Fines (silt, clay), massive
C	Coarse-grained, sandy-gravelly	Fl	Fines (silt, clay), laminated
M	Medium-grained, silty-sandy		
F	Fine-grained, clayey-silty		
<i>Consistence when moist:</i>			
1	Loose, not compacted		
2	Friable, easy to excavate		
3	Firm, difficult to excavate		
4	Extremely firm		

5.3 Laboratory analyses

5.3.1 Clast morphology

Clast sampling was done for sections 1, 2 and 3, where the aim was to get clast samples from each major unit in the sections, measure and examine the morphology of the clasts. Two clast samples (CS) were taken from section 1 and 3 each with one diamict sample and one gravel sample. Three samples were taken from section 2 where two diamict units were detected as well as the underlying sand and gravel unit. Methods from Benn and Evans (2004) were used in the field and in the sample analysis. The samples were gathered by hand-picking 50 clasts from the section within a 50x50 cm frame. For each clast, the length of the a-, b-, and c-axes were measured. Their roundness class was classified according to the Powers (1953) roundness diagram (*Fig. 5-2*). Each clast was examined for any striae,

facets or bullet-shape features. On the logs in Chapter 6.2, samples are marked according to the section and the unit collected from, f.ex. S1-CS-U1 (Section 1-Clast Sample-Unit 1).













	Well Rounded	Rounded	Sub-Rounded	Sub-Angular	Angular	Very Angular
Low Sphericity	 1	 2	 3	 4	 5	 6
High Sphericity	 7	 8	 9	 10	 11	 12

Fig. 5-2. Roundness diagram used for determining morphology for each clast (Powers, 1953).

These measurements can be used to calculate C40, RA and RWR values. The C40 index is the c:a ratio (Benn and Evans, 2004) and gives an indication for how the clast was transported. A ratio of 0.4 and below indicates a subglacial influence on a clast (Benn and Ballantyne, 1993). These values are then put into covariance plots of either angularity (RA diagram) or roundness (RWR diagram) depending on which quality was more prominent in the sample (Lukas, 2013). Each clast population was then plotted in triangular covariance diagrams according to the Sneed and Folk (1958) (*Fig. 5-3*) method using a TRI-PLOT (triangular diagram plotting spreadsheet) from Graham and Midgley (2000).

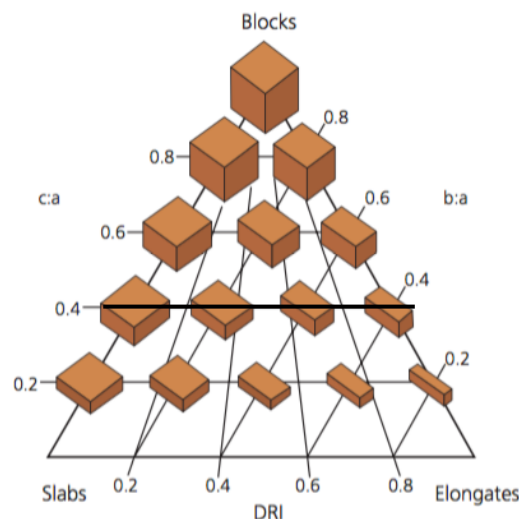


Fig. 5-3. Sneed and Folk shape continuum diagram modified from Benn and Evans (2004). The C40 0.4 line indicates that sediments shaped below have undergone significant erosion.

5.3.2 Sections and logs

The original field-sketches of sections and logs were redrawn and digitized in *Inkscape*, an open-source graphic editing program. Images of the sections were used to adjust the scale of the section drawings and presented alongside the drawings on figures in Chapter 6.2. The section drawings in Chapter 6.2 show the orientation of the sections and landforms, sample points, lithofacies codes, directional elements for layers and descriptions of sediments. The legend for all sketches and logs in Chapter 6 is seen in *Fig. 5-4*.

Legend



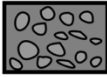
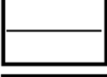
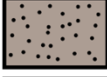
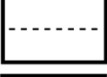

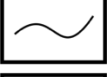

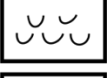



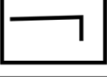



	Bedrock		Bedding
	Gravel		Sharp boundary
	Sand		Gradational boundary
	Diamict units (except S2-D2)		Sharp conformable boundary
	S2-D2 Diamict unit		Fissility
	Fines (clay/silt)		Ripples
	Clasts/Boulders		Unconformity
	Water dissipation structures		Section X- Clast Sample- Unit X
			Lense

Fig. 5-4 Legend for logs and section drawings.

6 Geomorphology and sedimentology of ribbed moraines

All data from geomorphological mapping, field measurements and sedimentological analysis are presented in this chapter. The first part presents maps of the ridge distribution and geomorphology along with statistics on shape and form, and the second part deals with sedimentology and internal architecture.

6.1 Geomorphology

Here, various geomorphological maps of the Vopnafjörður and Hauksstaðaheiði region are presented, showing the ribbed moraine distribution compared with streamlined landforms and landscape, their position in Hauksstaðaheiði, ridge relief and a map with ridge crests and their directional element. The mapping revealed 241 transverse landforms and yielded information on the statistics of ridge geometry such as width, length and relief. The ridges follow a basin almost consistently down-valley but also extend to the flanks of the basin. *Fig. 6-1* presents a wider glacial geomorphological perspective of the entire Vopnafjörður region and *Fig. 6-2* provides an overview of the transverse ridges on Hauksstaðaheiði.

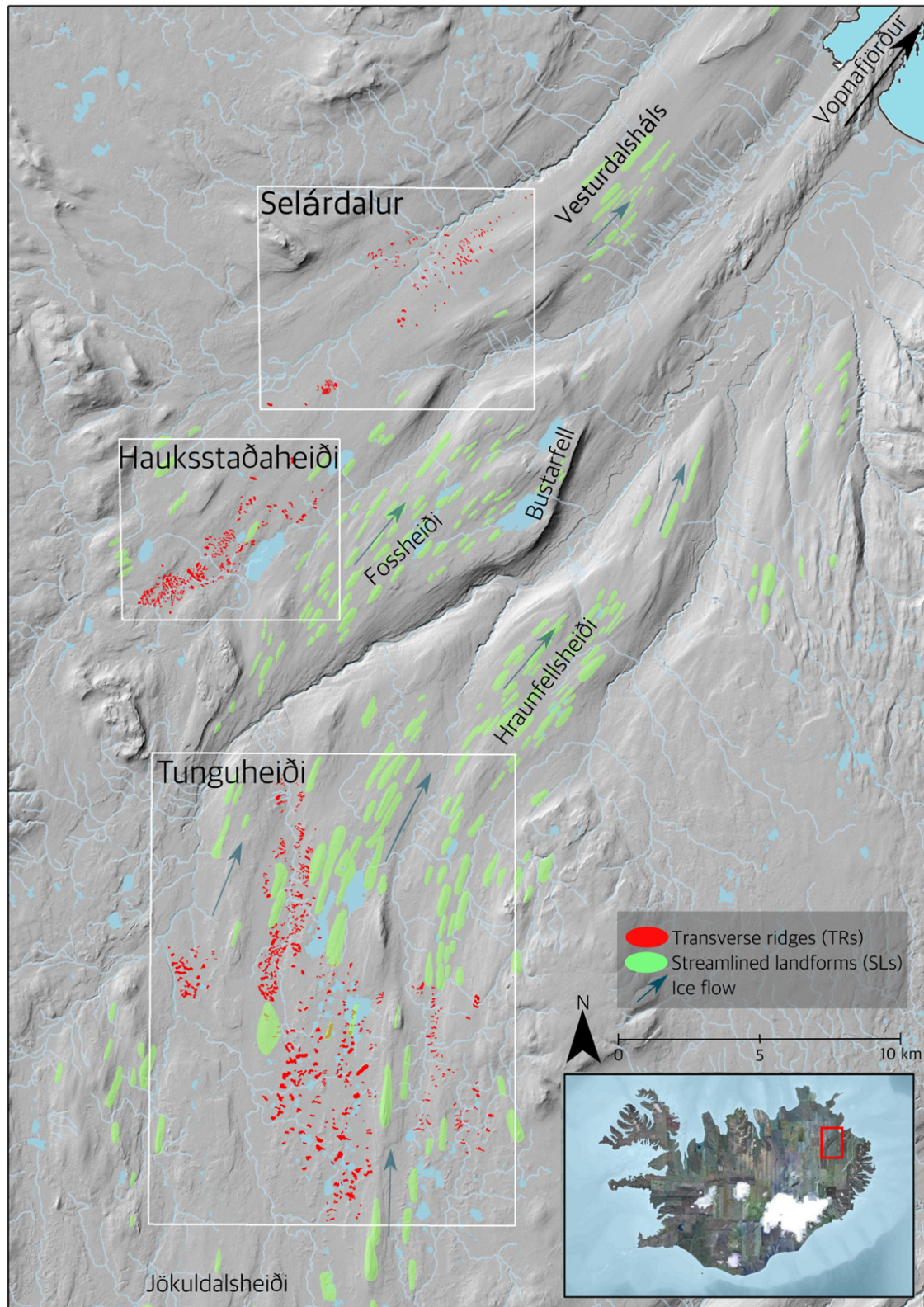


Fig. 6-1. An overview map showing glaciogenic landforms in the interior of Vopnafjörður and geomorphology at the highland margin. The transverse ridges (to estimated ice flow (Sæmundsson, 1995) in Tunguheiði, Hauksstaðaheiði and Selárdalur are shown here along with streamlined landforms. Blue arrows signify general ice flow directions. The streamlined landforms are densely packed on Bustarfell, Fossheiði and Hraunfellsheiði. It is

notable that the areas with highest density of transverse ridges are situated at higher altitudes or inland of the most densely spaced streamlined landforms, forming a belt at the highland margin.

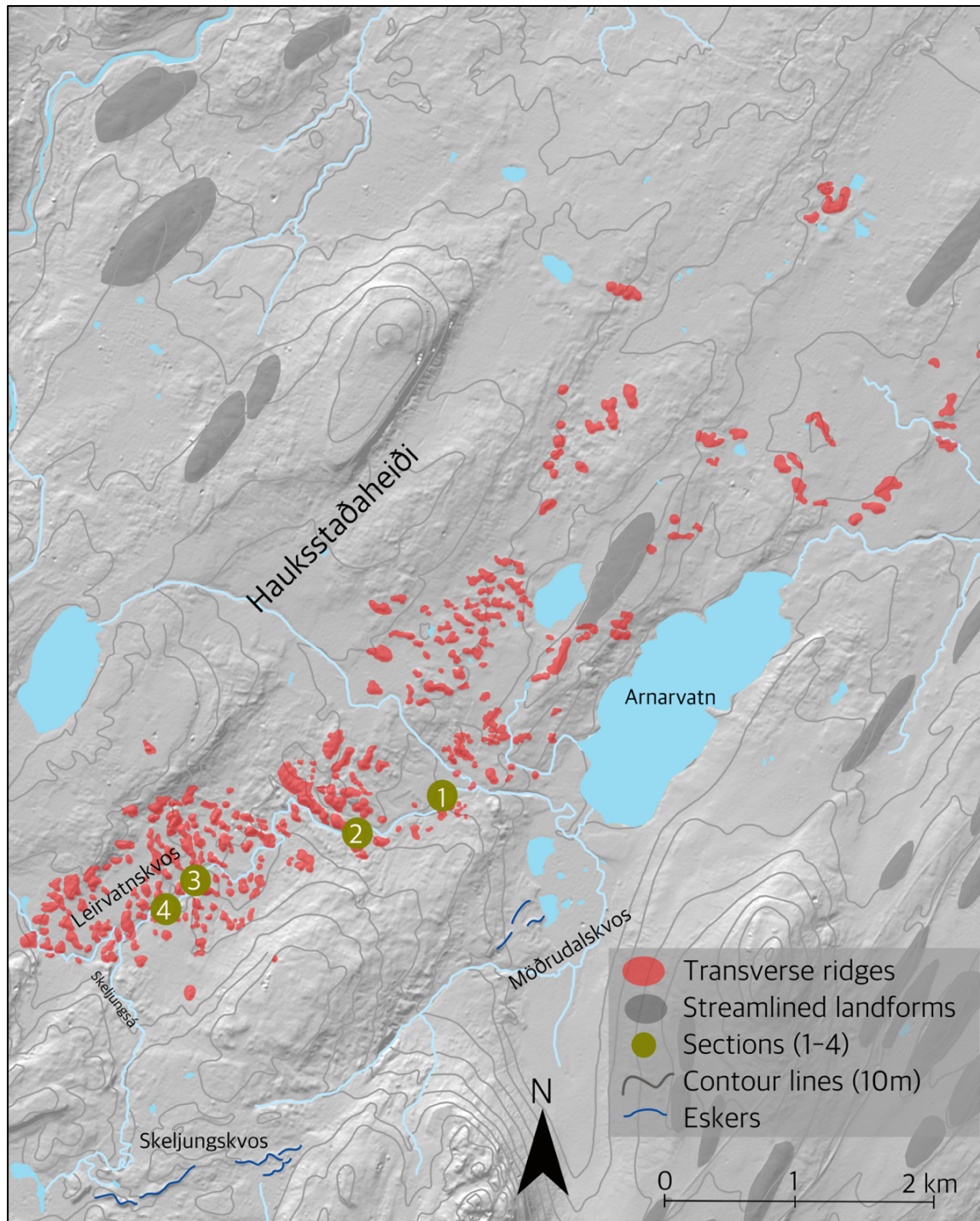


Fig. 6-2. Transverse ridges on Hauksstaðaheiði shown in relation to streamlined bedforms in the area and eskers. In the upstream part of the Leirvatnsvos depression, the ridges are most densely distributed. It is notable that the most densely situated ridges also have a distinct transverse alignment.

A map of glaciogenic landforms in the Vopnafjörður region, presented above shows the distribution of transverse ridge sets groups in relation to groups of streamlined landforms (*Fig. 6-1*). The Hauksstaðaheiði transverse ridges were mapped in detail but Tunguheiði and Selárdalur transverse ridges were mapped in order to bring forward an overview and context of the presence of transverse ridges in the region. Transverse ridges on Hauksstaðaheiði are prominent features in the landscape with a clear transverse orientation and shape compared to most ridges mapped in Selárdalur and Tunguheiði. Streamlined landforms are also common features for the Vopnafjörður region and are presented here as a supplement into this study to give further insight into the spatial relationships between transverse and streamlined landforms in palaeo-ice sheet environments.

The Hauksstaðaheiði transverse ridges are located in a shallow depression east of Botnafjallgarður and Dimmifjallgarður. The basin is bordered by gentle hills and heaths (*Fig. 6-2*). The transverse ridges have a distinct transverse ridge orientation (to the inferred ice streaming) in the valley basin of Leirvatnaskvos, whereas ridges uphill to the sides and downstream from the basin have a less pronounced transverse morphology and are rather irregular and somewhat circular sediment mounds.

The transverse ridges are also located approximately 4 km west of the Fossheiði area where streamlined landforms are very closely spaced. Where the transverse ridges are situated on Hauksstaðaheiði, there are few streamlined landforms present and lateral change in bedforms can be considered non-transitional from streamlined landforms on Fossheiði to transverse ridges on Hauksstaðaheiði (*Fig. 6-2*). On Fossheiði and Bustarfell, streamlined landforms are a dominant landscape feature and no transverse ridges are visible. Streamlined landforms are found in gently sloping terrain and are mostly located inland from the three Vopnafjörður valleys, on the highland plateau.

On Tunguheiði, the ridges are mostly located south of streamlined landforms but are dispersed among streamlined landforms in places further north. Some ridges on Tunguheiði even superimpose streamlined landforms (*Fig. 6-1*). The streamlined landforms are occasionally broken up into circular and transverse ridges and somewhat chaotic transverse ridge fields with a low but visible transverse to circular nature.

It is notable that the three ridge sets on Hauksstaðaheiði, Tunguheiði and Selárdalur are located up-valley from the groups of streamlined landforms. The transverse ridge areas together cover a region forming a belt of transverse landforms up-valley (south, southwest and west) from the areas where streamlined landforms are most densely located (*Fig. 6-1*).

To the east of Hauksstaðaheiði/Leirvatnaskvos, lies the Möðrudalskvos basin (*Fig. 6-2*). There are landforms in Möðrudalskvos which differ in shape and size from the transverse and streamlined landforms. They are smaller with irregular or meandering morphology, pointing slightly down-valley and contain well-rounded surface clasts. This is the only other landform identified between the fields of transverse and streamlined landforms. The ridges can be traced up-valley and into Skeljungskvos.

6.1.1 Ridge geometry

In the field, as well as through interpretation of aerial data, the ridges are easy to identify. Their distinct, rocky, gravelly surface is contrasted by the surrounding vegetated flatlands (Fig. 6-3). Using aerial imagery was therefore crucial in order to identify and map the bounds of the ridges. In all, 241 ridges were mapped in Hauksstaðaheiði and statistics calculated only from those. The average relief of the ridges is 6.4 m with a highest relief of 19.3 m and the lowest 0.8 m. The ridges are the tallest in the Leirvatnsvos basin where they reach up to 19.3 m above the surroundings (Fig. 6-4). The ridges in Leirvatnsvos are also more closely spaced than elsewhere in the area.

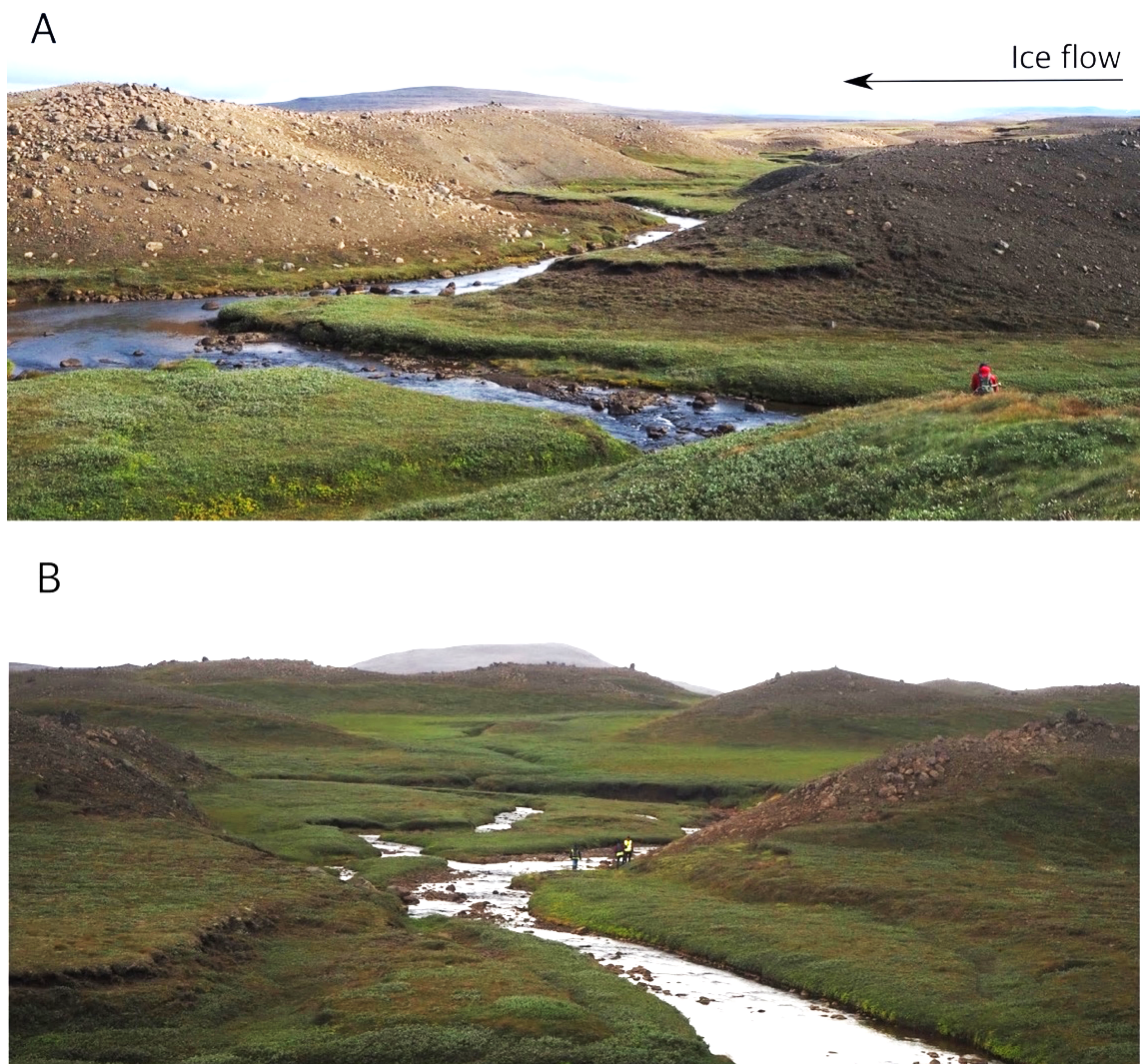


Fig. 6-3. Skeljungsá river runs between the Leirvatnsvos ridges. People (approx. 1.7 m) indicate the scale of the ridges which range up to 19.3 m. The ridge crests have a gravelly and rocky appearance compared to the surrounding, vegetated lowlands. A) A perpendicular view of the ridges in Leirvatnsvos along the ridge crests towards the southeast. B) An upstream view of the ridges in Leirvatnsvos towards the southwest with Leirvatnshnjúkur in the background.

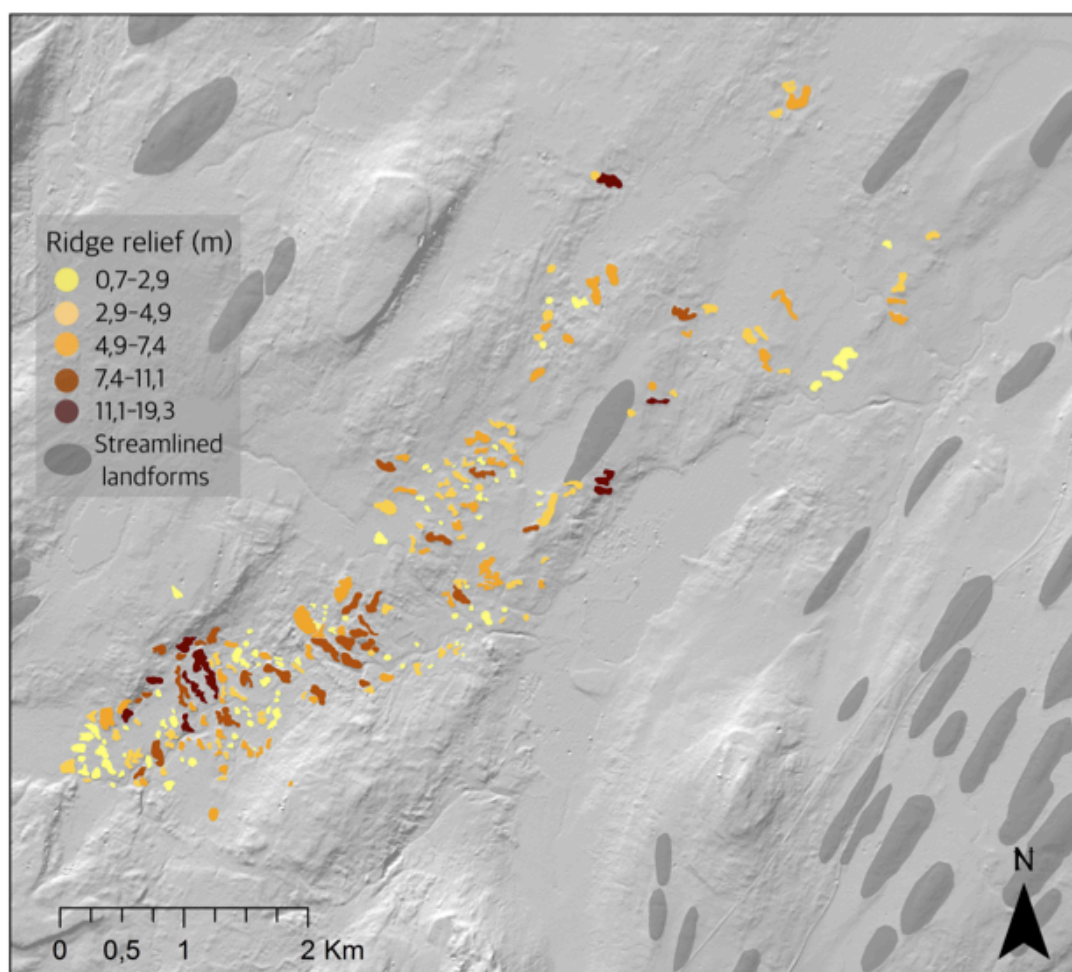


Fig. 6-4. A map showing the relief of individual ridges. Most of the tallest ridges are located in the Leirvatnsvos basin and ridges with lower relief occur on the basin flanks and further down-stream.

The morphometric statistics of the Hauksstaðaheiði ridges are presented in *Table 3*. This includes their average, median, standard deviation and range for their length, width, relief and elongation ratio. *Fig. 6-5* shows the morphometrics of the ridges on Hauksstaðaheiði including the normal frequency distribution of the morphometrics for the ridge length, width, relief and elongation ratio, as well as the ratio between length and width.

Table 3. Morphological statistics for the transverse ridges in Hauksstaðaheiði

	Length (m)	Width (m)	Relief (m)	Elongation Ratio
Average	112.0	66.0	6.4	1.69
Median	95.1	63.1	5.8	1.61
Standard Deviation	61.1	26.7	3.3	0.52
Range	24.7-427.8	18.9-172.0	0.8-19.3	-

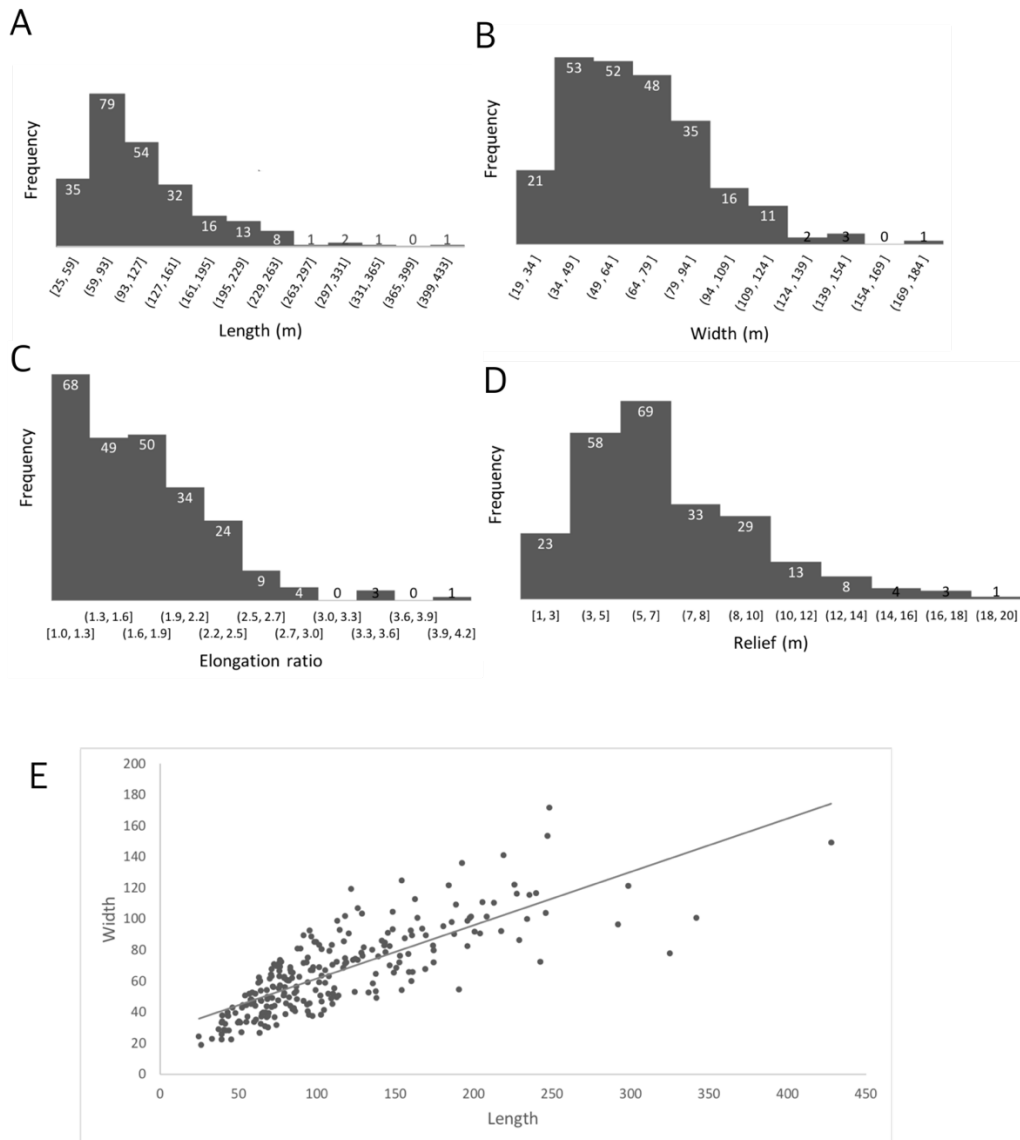


Fig. 6-5. Normal frequency distribution of ridge morphometrics on Hauksstaðheiði showing their length (A), width (B), elongation ratio (C) and relief (D). Elongation ratio graph (E) shows a strong correlation between length and width of the ridges. The line in (E) graph shows the trendline of the graph.

6.1.2 Ridge spacing

Terrain cross-profiles were made downstream through the crests of the most prominent ridges in order to estimate ridge spacing. The elevation drop for the profiles is approximately 140-160 m. The profiles show that spacing between ridges ranges from 60 to 500 m (Fig. 6-6). Mean spacing between the ridges is 145 m for Profile 1 and 204 m for Profile 2. From 0-3 km, the ridges are more densely situated, with average spacing of around 126 m for Profile 1 and around 160 m for Profile 2. From 3-7 km, the average spacing is 165 m for Profile 1 and 264 m for Profile 1. The tallest ridges are between km 1-3 on both profiles. Profile 1 shows higher ridge density throughout, ranging from 5

ridges/km (km 4-5) to 10 ridges/km (km 1-2). Profile 2 has lower relief ridges and a lower ridge density ranging from 3 ridges/km (km 3-6) to 7 ridges/km (km 0-1 and 2-3). This shows that the ridge density is generally higher in the upstream part of the profiles.

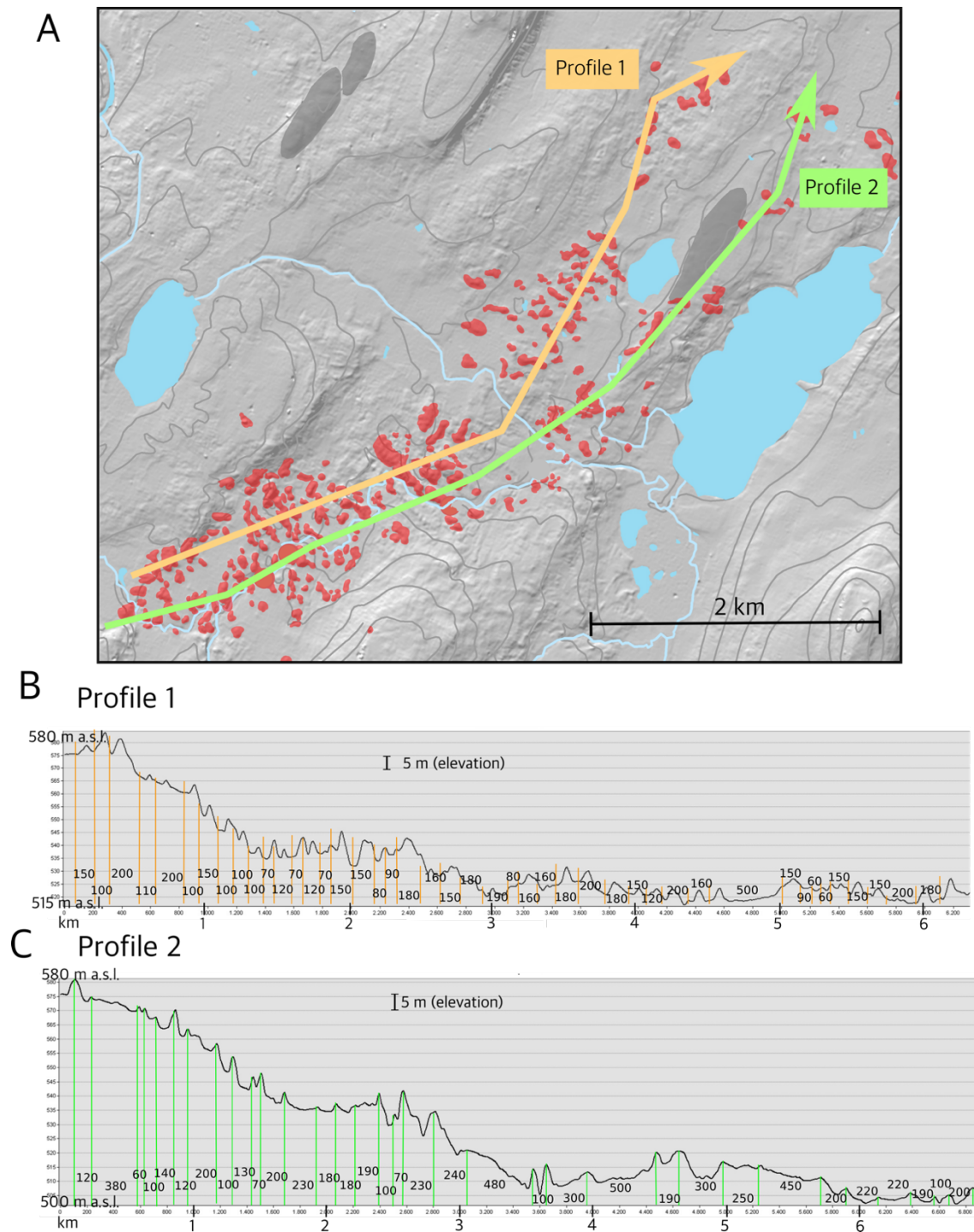


Fig. 6-6. A) Map showing terrain cross-profiles across the main segments of the ridge system in Hauksstaðaheiði. B) Graph showing Profile 1 seen in A above. C) Graph showing Profile 2 seen in A above. Gray, horizontal lines indicate 5 m in elevation. The profiles have vertical indicator lines and the numbers between the indicator lines show a roughly estimated spacing between ridge crests. The profiles show the downslope evolution of ridge relief and spacing. Grey horizontal lines on graphs indicate 10 m in elevation.

6.1.3 Ridge shape

The ridges have a slight arcuate shape; however, some ridges have outer flanks pointing down-valley. This is not a dominant feature overall but can be seen in some of the larger ridges in the Leirvatnsvos basin and in areas with the highest ridge density. Judging from the profiles in *Fig. 6-6*, there is no visible up-ice or down-ice geometry or signs of difference in steepness on proximal and distal sides. The ridge crests are generally curved and broad.

6.1.4 Ridge trend

A ridge direction trend analysis was made in order to shed further light on their general orientation transverse to ice flow. This required a separate mapping effort with mapping only the ridge crests. A rose diagram produced by using the *QGIS Line Direction Histogram Plugin*, shows the directional trend of 241 ridge crests mapped on Hauksstaðaheiði (*Fig. 6-7*). The ridges in the Leirvatnsvos basin appear to have a distinct, transverse orientation compared to more irregularly shaped ridges further down-valley and to the sides of the basin (*Fig. 6-7*).

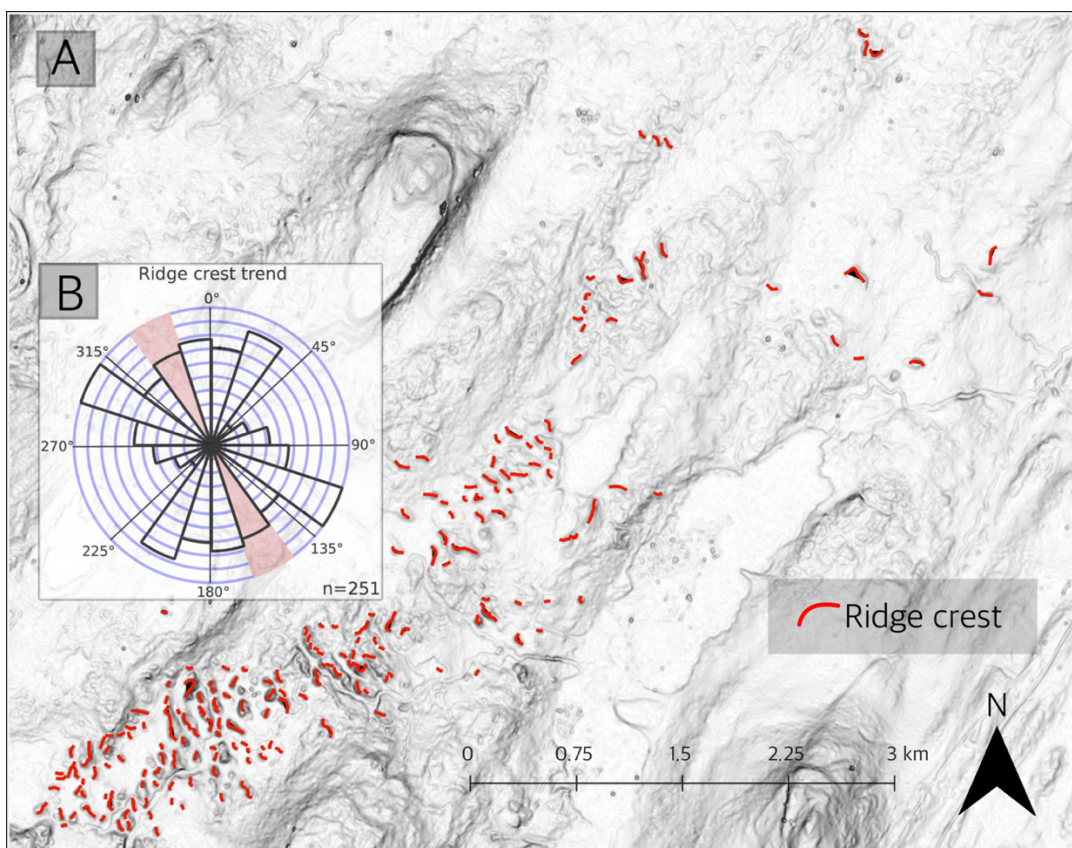


Fig. 6-7. Ridge trend map. A) Shows a map of ridge crests. The rose diagram (B) shows directional trends for 251 ridge crest lines and has a general trend between 135° and 180°. The pink line in the rose diagram shows the direction mean for the transverse ridges.

6.1.5 Interpretation and discussion

The transverse ridges as interpreted as ribbed moraines as they are strikingly similar to the previously featured ribbed moraine (Chapter 3) in terms of morphometry and morphology (Lundqvist, 1969a; Aylsworth and Shilts, 1989a; Bouchard, 1989; Hättestrand, 1997; Hättestrand and Kleman, 1999; Dunlop and Clark, 2006). The streamlined landforms on Bustarfell, Fossheiði, Tunguheiði and Hraunfellsheiði are here interpreted as drumlins and MSGL based on their shape and elongation ratio (Aylsworth and Shilts, 1989b; Clark, 1993; Stokes, 2002). The landforms in Möðrudalskvos and Skeljungskvos (*Fig. 6-2* Fig. 6-2) are interpreted here as eskers. This is due to their meandering shape and sorted surface appearance with rounded clasts (Clark and Walder, 1994; Warren and Ashley, 1994).

The three ridge assemblages of Hauksstaðaheiði, Tunguheiði and Selárdalur are all located upstream from the valleys Selárdalur, Vesturárdalur and Hofsárdalur, which lead into the main Vopnafjörður trough (Sæmundsson, 1995; Patton et al., 2017). The transverse ridges on Hauksstaðaheiði occur in a shallow trough between the Dimmifjallgarður/Botnafjallgarður mountain range to the northwest and Bustarfell/Fossheiði drumlin field in the southeast. Streamlined landforms such as drumlins and MSGLS have been linked to ice streaming or fast ice flow. This leads to the conclusion that an ice stream flowed from an ice divide at the Dimmifjallgarður mountain range through the Vopnafjörður trough at some time during the last glaciation (Hubbard et al., 2006; Patton et al., 2017).

Whether the formation of the ribbed moraines was controlled by the surrounding topography and landscape remains unanswered. As stated before, the three ribbed moraine areas are located near the highland margin, upstream from the Vopnafjörður trough. These areas are also located upstream from drumlin/MSGSL fields and can be described as some sort of a “transition zone” towards drumlin/MSGSL fields. This could indicate that there is a spatial factor involved in where each landform type is situated. This finding is in line with studies that also document such clear transitions between landform types (*Fig. 3-4*).

Another interesting observation is that the ribbed moraines on Tunguheiði are superimposed on the pre-existing drumlins/MSGLS. In places they fragment the drumlins/MSGLS, and form sets of ridges with a linear direction trend aligned with streamlined landforms in the area. This indicates that the ribbed moraines on Tunguheiði formed after the drumlins and MSGL fields and hence are a secondary feature to drumlins.

The ridges are tallest and most densely situated in the Leirvatnskvos basin. The basin might have collected more sediments than surrounding areas, providing material for ridge formation. Crest spacing is similar throughout the ribbed moraine field although a difference can be seen for profile 2, where the spacing increases down-stream (*Fig. 6-6*). The difference is, however, not significant enough to make concluding interpretations from

that observation, but Hättestrand and Kleman (1999) suggested that this might indicate displacement of subglacial material due to extensional flow.

Ribbed terrain can be seen on the flanks of Leirvatnsvos basin. These ridges are not located in a basin but on the hillside and are less pronounced in the landscape than the ridges in the Leirvatnsvos basin as the ridges are irregularly shaped and vegetation does not separate the ridges in the same way. This makes the ridges on the flanks more difficult to identify with remote sensing data, but surface material is very similar to what is found on regularly spaced, transverse, ribbed moraines in Leirvatnsvos. Further field work would be useful in order to determine the scope of ribbed terrain in the area. Directional landforms can be difficult to plot since not all ridges have a clear ridge crest. This is why *Fig. 6-7* plots all ridge crests with a broad distribution of ridge orientations. The ridges have a clear transverse element to them in the southernmost section of Leirvatnsvos where the crests are the most distinct. In *Fig. 6-8*, a directional element has been plotted for selected landforms centered in Leirvatnsvos basin, with only the longest and most pronounced transverse ridges included. The selection shows a narrower trend range, plotting between 90°-225°, with the main trendline at 160°-180°. A possible explanation for this difference in directions could be that the ridges have been preserved to a varying degree, resulting in some ridges having undergone more post-glacial erosion than others or the possibility that there was more sediment supply in the basin than on the flanks. Why the ridges form at such regularly spaced intervals is unclear and requires further research on glacier dynamics.

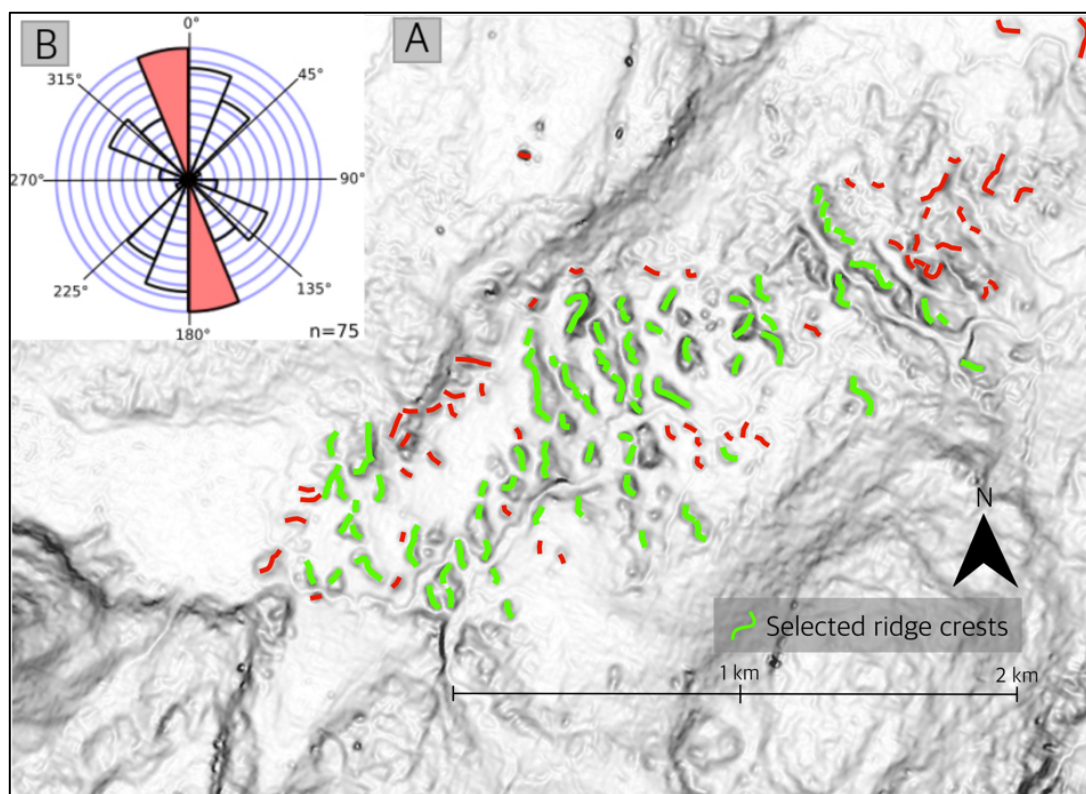


Fig. 6-8. A) map showing a clearer direction trend for selected ridge crests (green lines) in Leirvatnsvos that have a particularly clear transverse orientation. B) Rose diagram for the selected ridge crests. The pink line in the rose diagram shows the direction mean for the transverse ridges. The red lines in A represent ridges that were not included in the selection.

6.2 Sedimentology

There are only a few natural sections where sediments are exposed through the ridges at Hauksstaðaheiði. The river Skeljungská has exposed four ridge sections which give insight into the sedimentary architecture and composition of the ridges and brings us a step closer towards understanding their origin. This chapter presents field and laboratory data from the four sections. This includes section drawings, measurements of directional elements, stratigraphic logs, photographs, lithofacies descriptions and clast analysis (C40 and angularity). Each unit is described and interpreted, and each section is in turn interpreted when all data have been presented. The final chapter goes through five random ridge surface clast measurements where their shape and angularity are discussed in comparison to the ridge internal composition.

6.2.1 Section 1

Section 1 is located at the northernmost location of the four sections and furthest downstream of Skeljungská (Fig. 6-2). The GPS coordinates are 65.58719; -15.42504 ± 5m at an approximate elevation of 438 m a.s.l.. The orientation of the section is 236° and the ridge trend is 135°. The ridge is 7 m high and 20 m wide. Strings were lined up for the height

at 5 m intervals and one string across at 5 m height for the width. Measurements of dip/dip direction of stratigraphic beds were made at seven locations in the section, from the proximal to the distal parts. Two clast samples are from Unit 1 (S1-CS-U1) and Unit 2 (S1-CS-U2) (*Fig. 6-9*).

Unit 1: Coarse gravel (Gh/Sr)

Unit 1 is mostly composed of coarse gravel with interbedded, stratified sand and gravel lenses (*Fig. 6-10; Fig. 6-11*). There is also some small-scale deformation visible. Unit 1 is divided into five sub-units. The uppermost *sub-unit 1.5* is approximately 2 m thick and has a grading boundary with the slightly coarser gravel unit below. *Sub-unit 1.4* is abundant with large clasts grading downward from sand at the top towards larger clasts at the bottom of unit. The layer has stratification, partly rippled sand lenses and occasional large boulders. This layer has a sharp boundary to *sub-unit 1.3*, which is primarily fine to medium sand with some coarser sand and gravel lenses. It contains vague but slightly deformed ripples. This unit shows signs of fissility closer to the proximal edge of the section, near to the diamict layer where the overlying gravel units are thinner. It shows more fissility than the overlying diamict. *Sub-unit 1.3* has a grading boundary with *sub-unit 1.2*, which is a stratified coarse gravel layer with an occasional large clast and thin sand laminations of up to 1 cm thick in between gravel stratifications (*Fig. 6-11*). At the bottom of the section there is a hard gravel *sub-unit 1.1* extending throughout the entire section and forming a dense bed underneath.

Interpretation

Unit 1 is interpreted to be an originally fluvially deposited unit of sand and gravel (Miall, 1977; Miall, 1985). It is possible that this unit was later overridden by glacial ice. There are no striae or bullet shapes found within the gravel (*Fig. 6-10*). The fissility in the uppermost gravel unit is an unusual characteristic for sorted sediments but indicates subglacial deformation of the fluvial sediments (Krüger and Kjær, 1999; Evans et al., 2006).

Unit 2: Matrix to clast supported diamict ($D_{m/b/s}C(m_3/c)_4$)

This diamictic unit (Unit 2) drapes over the underlying gravel Unit 1 throughout the section (*Fig. 6-9; Fig. 6-10; Fig. 6-11*). Unit 2 is mostly covered with scree but was also partly excavated in order to document its properties (*Fig. 6-9*). The uppermost part of the diamict is homogenous, fissile, slightly banded or stratified and containing varying clasts that are subrounded to very angular. The unit is extremely firm, coarse grained and ranges from

being clast-supported to matrix-supported and clast rich. The boundary to the lower unit is sharp and conformable (*Fig. 6-10*).

Interpretation

The diamictic Unit 2 is here interpreted as a subglacial traction till because of its fissility and consistency, in particular (Krüger and Kjær, 1999; van der Meer et al., 2003; Evans et al., 2006). The boundary to the underlying unit is sharp and conformable and indicates that unit 2 was deposited after unit 1.

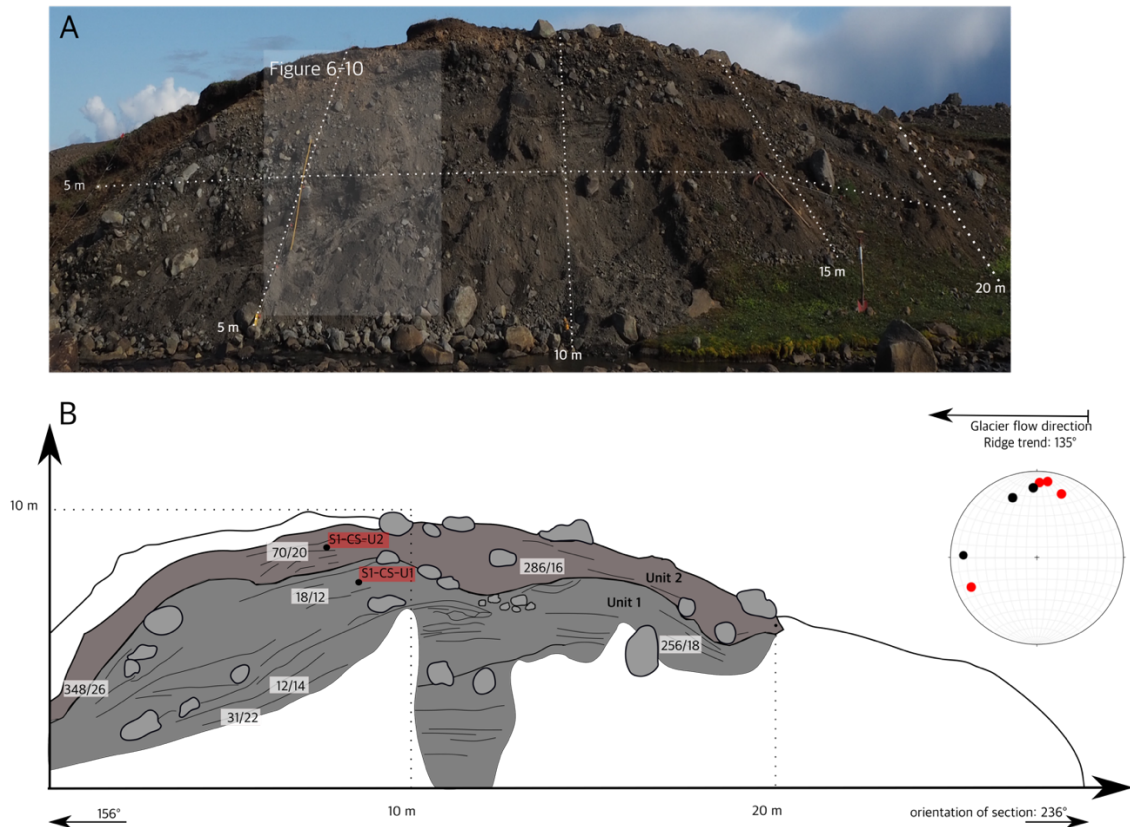


Fig. 6-9. A) Photograph of Section 1 showing the location of log in Fig. 6.10 in white box. B) Drawing of Section 1 showing the measurements for dip and dip direction of stratigraphic beds. The measurements are plotted on a stereograph to the right where red dots are from unit 1 and black dots are from unit 2. Samples from both units are marked with S1-CS-U1 and S1-CS-U2.

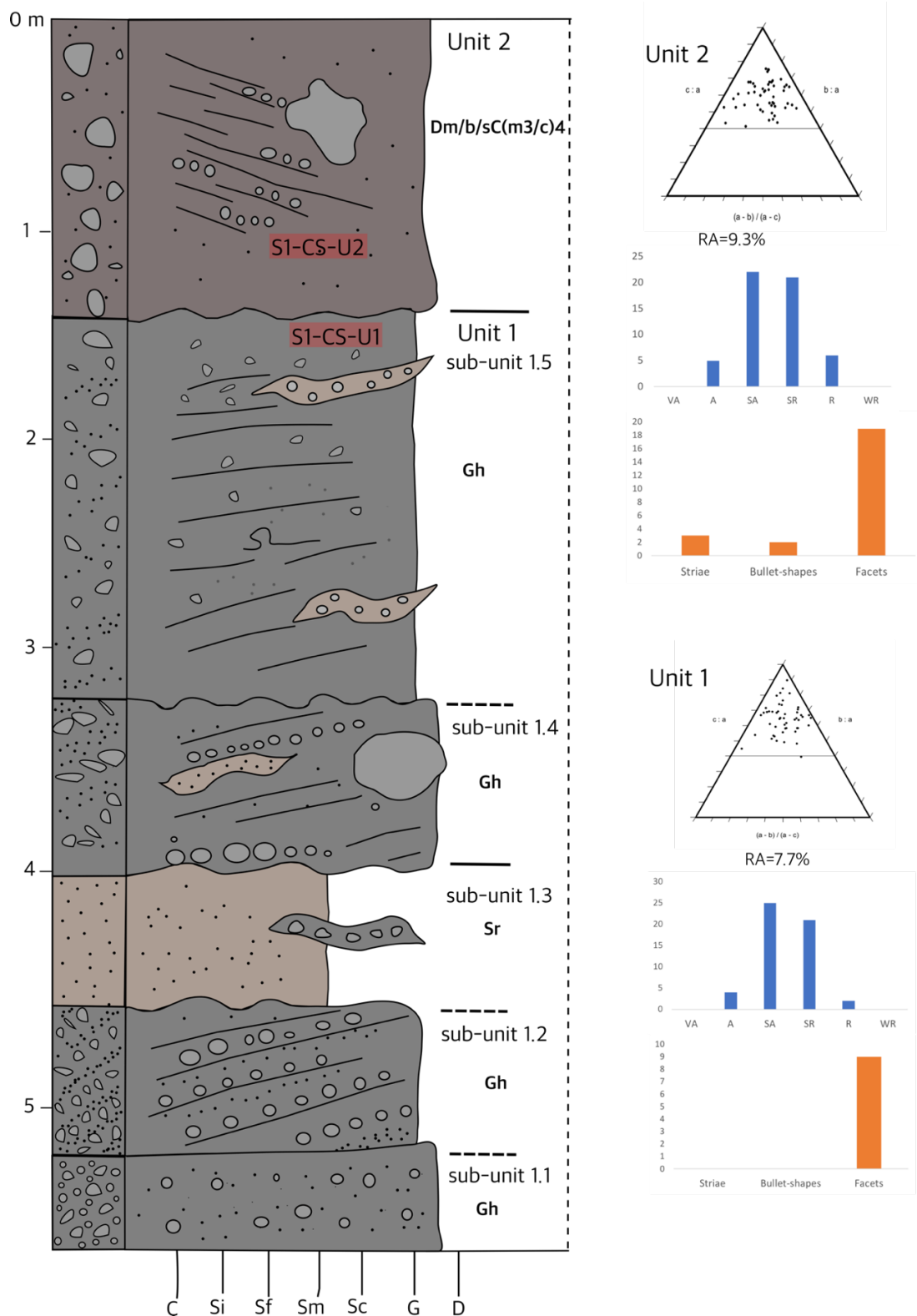


Fig. 6-10. Stratigraphic log of Section 1. Clast shape data with C40 and frequency for striae, bullet-shaped clasts and facets on clasts. RA index shows the percentage of angular and very angular clasts in the sample (Benn and Ballantyne, 1993).

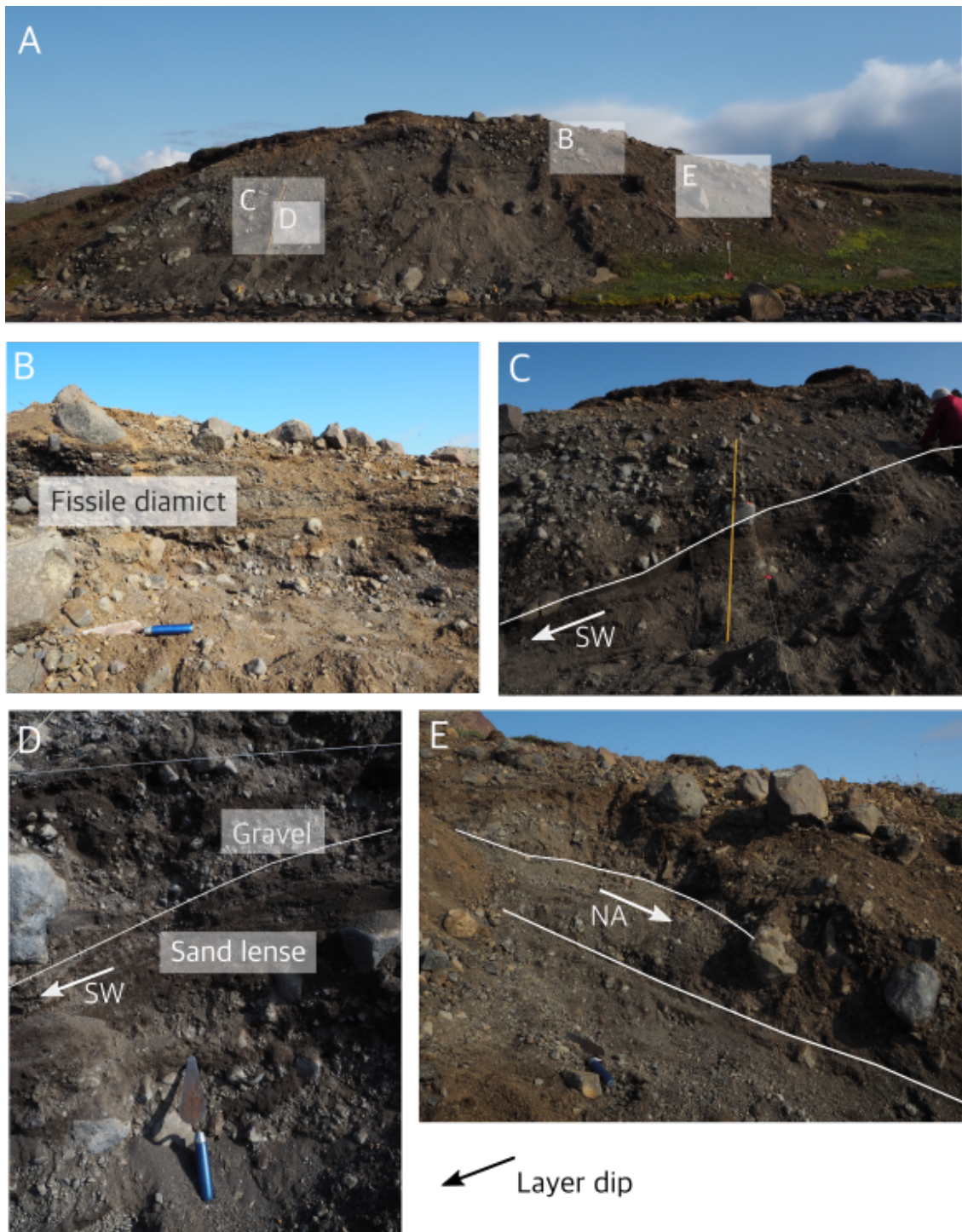


Fig. 6-11 A) Shows Section 1 with white boxes indicating the location of figures B-E. B) Fissile diamict in unit 2 draping over unit 1. C) White line showing the approximate layer dip in the section. D) Gravel and sand lenses within unit 1. E) Layers in unit 1 dipping towards the proximal end of the ridge.

Interpretation of Section 1

The till unit in the upper part of the section is interpreted to have been deposited after the gravel unit below. Fissility and facets in the gravel unit indicate that this unit, or at least the top part of it, was compacted and deformed by glacier flow. The sharp and conformable boundary between the units indicates that the till was deposited by a glacier on top of the fluvial units without disturbing the pre-existing sediments significantly, leaving minimal traces on the pre-existing sediments.

6.2.2 Section 2

This section is located upstream from Section 1, next to the Skeljungsa river. The GPS coordinates are 65.58501, -15.44002 \pm 2m at an approximate elevation of 458 m a.s.l.. The orientation of the section is 30° and the ridge trend is 335°. The section is up to 15 m high and 50 m wide. The section is split into roughly three units, two diamict units on top of an assemblage of gravel and sand units, which are here classified as one unit. Two logs were made for this section in two spots where layers could be traced across the section (*Fig. 6-13* and *Fig. 6-14*). Measurements of dip/dip direction of stratigraphic beds were made at two locations in the section in the uppermost diamict unit. Three samples are from Unit 1 (S2-CS-U1), Unit 2 (S2-CS-U2) and Unit 3 (S2-CS-U3) (*Fig. 6-12*).

Unit 1: Sand and gravel series (Gm and Sm/Sh)

Unit 1 is composed of a series of gravel and sand layers with horizontally laminated sand and gravel layers truncated in between each other (*Fig. 6-14*). The uppermost part of unit 1 is truncated by unit 2 with an unconformable boundary (See C and D in *Fig. 6-15* and *Fig. 6-12*). This gravel and sand unit grades downward into a matrix supported gravel with a sandy matrix and continues grading down into more granular gravel. The unit grades into a clast supported gravel at around 5.5 m down the log (*Fig. 6-14*). There are some sand lenses in that lower section with a massive appearance as well as horizontal lamination.

Interpretation

Unit 1 is interpreted to be an originally fluvially deposited sand and gravel (Miall, 1977; Miall, 1985). After deposition, the sediments were truncated by glacial ice, leaving striae and facets on clasts as well as an erosional upper boundary (*Fig. 6-14*) (Krüger and Kjær, 1999; Evans et al., 2006). The sediments could also have been deposited as glacial sediments and subsequently reworked by fluvial processes, which can also explain striae and facets on clasts.

Unit 2: Massive, homogenous diamict ($D_mM/C(c)4$)

Unit 2 has a massive, homogenous appearance. Its matrix ranges from coarse grained or sandy/gravelly to a medium grained or silty/sandy matrix composition (*FigGG. 6-13*). This unit is only clast supported and has an extremely firm consistence. There is also a slight color difference between the two diamict units (Unit 2 and 3) (See E in *Fig. 6-15*). Unit 2 truncates Unit 1 below and has an unconformable basal contact (See C and D in *Fig. 6-15* and *Fig. 6-12*).

Interpretation

The diamictic Unit 2 (*FigGG. 6-13*) is interpreted as subglacial traction till mainly based on the presence of striations, facets and bullet-shaped clasts within the unit (Krüger and Kjær, 1999; van der Meer et al., 2003; Evans et al., 2006). The lower boundary with Unit 1 is interpreted here as an erosional contact where glacial ice truncated pre-existing fluvial sediments, leaving the overlying till unit.

Unit 3: Firm, fissile and matrix/clast supported diamict ($D_{b/s}C(m_3)4$)

Unit 3 is slightly banded or stratified but no other structures were observed. It has a coarse grained, sandy matrix but is very clast rich and even clast supported in places. The clasts range from rounded to very angular. The unit is extremely firm overall and shows delicate fissility. Striations, facets and bullet-shaped clasts were found in the clast sample (*FigGG. 6-13*). The boundary with the lower diamict unit is a gradational boundary (See E in *Fig. 6-15*). Diamict unit 3 resembles unit 2 in Section 1.

Interpretation

The diamictic Unit 3 (*FigGG. 6-13*) is interpreted as a subglacial traction till mainly based on the presence of striations, facets and bullet-shaped clasts within the unit as well as fissility visible in places (Krüger and Kjær, 1999; van der Meer et al., 2003; Evans et al., 2006).

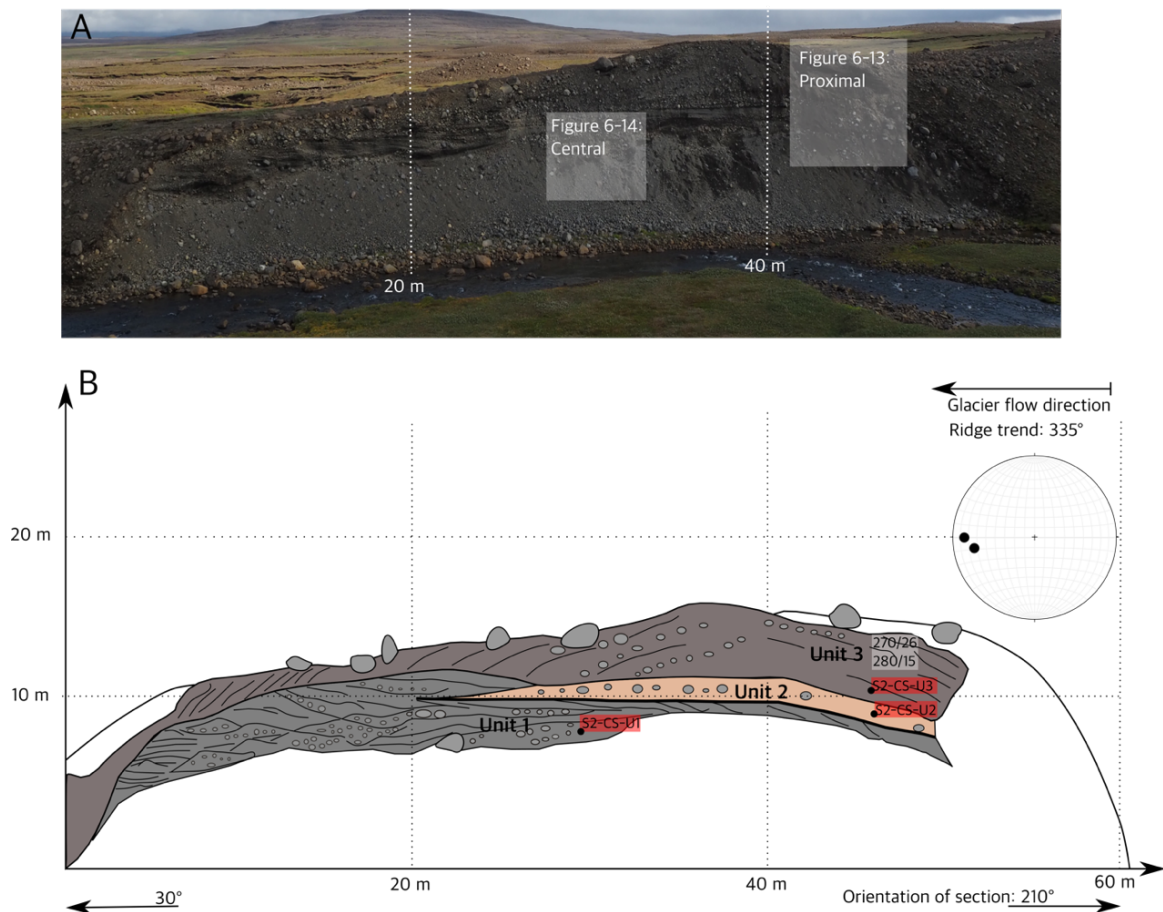
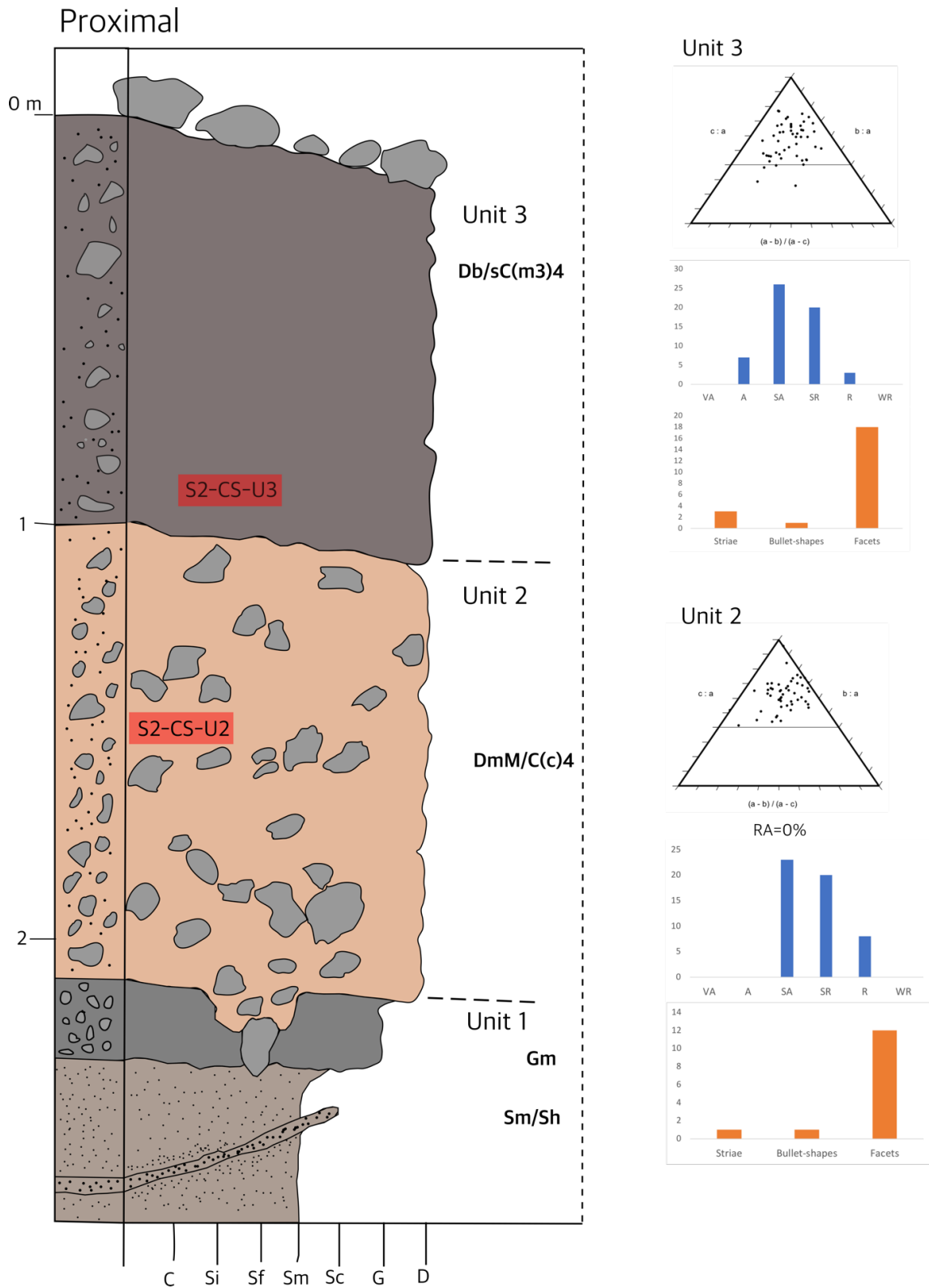


Fig. 6-12 A) Photograph of Section 2 showing the location of log in Figs. 6.13; 6.14 in white boxes. B) Drawing of Section 2 showing the measurements for dip and dip direction of stratigraphic beds in white boxes. The measurements from the diamictic Unit 3 are plotted on a stereograph to the right as black dots. Samples from all units are marked with S2-CS-U1, S2-CS-U2 and S2-CS-U3. Topmost diamict has stratification but no other structures. A sand layer can be traced across from the proximal side of section and its upper boundary is truncated by the lower diamict. A large part of the center of the diamict Unit 3 is scree but continues towards the distal side. The lower diamict and gravel/sand boundaries are unclear but can be traced into the Unit 3 where they are discontinued, indicating that the surface (marked with a bold line in Fig.) is eroded.



FigGG. 6-13. Stratigraphic log of Section 2, proximal log. Clast shape data with C40 diagrams and frequency for striae, bullet-shaped clasts and facets on clasts. RA index shows the percentage of angular and very angular clasts in the sample (Benn and Ballantyne, 1993).

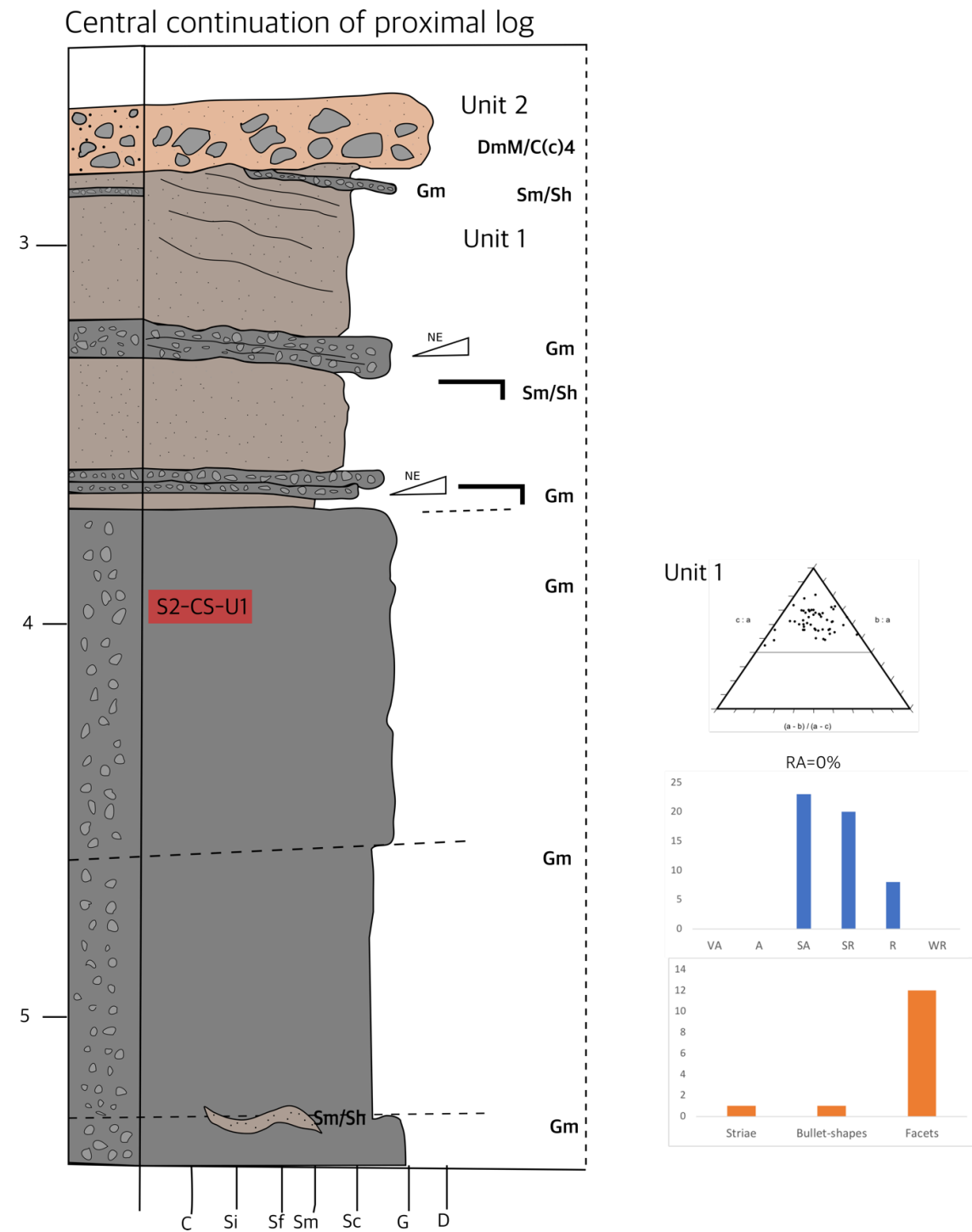


Fig. 6-14. Stratigraphic log of Section 2, central log. Clast shape data with C40 diagrams and frequency for striae, bullet-shaped clasts and facets on clasts. RA index shows the percentage of angular and very angular clasts in the sample (Benn and Ballantyne, 1993).

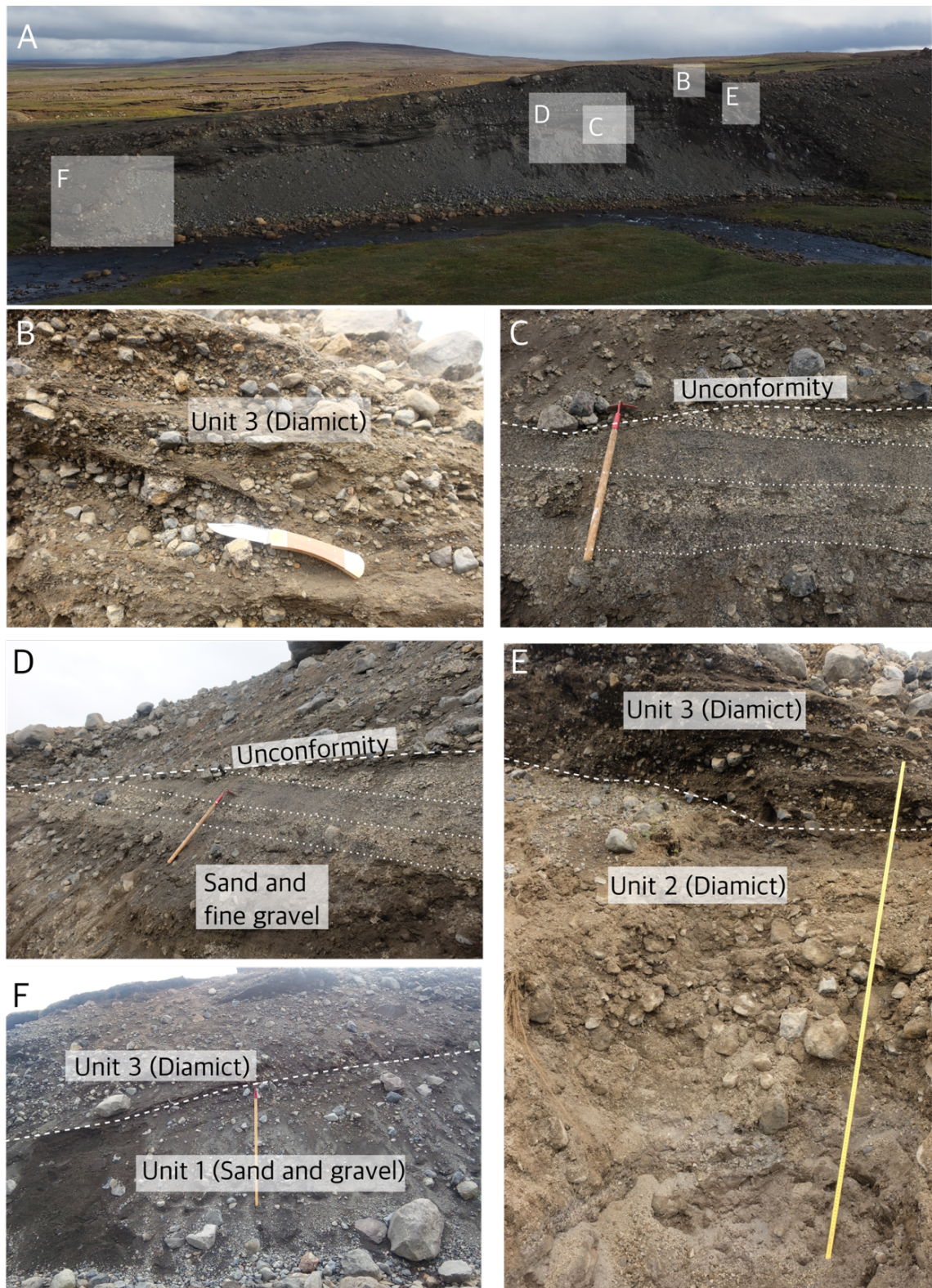


Fig. 6-15 A) Shows Section 2 with white boxes indicating the location of figures B-F. B) Unit 3 is fissile but clast rich. C) A close-up of the unconformity between Unit 3, where overlying diamict unit 2, truncates the underlying sand layers that are discontinued into the diamict unit. D) The unconformity seen for more layers. E) Boundary between Unit 3 and Unit 2. F) Boundary between Unit 2 and Unit 1 towards the distal (down-stream) side of the section.

Interpretation of Section 2

The till units are overlying the fluvial units and are here interpreted to have been deposited after the gravel and sand units below. The fluvial Unit 1 is discontinued upwards into Unit 2 (See C and D in *Fig. 6-12*). This is interpreted as an erosional contact where the glacial till has truncated fluvial sediments. After deposition, the fluvial sediments were truncated by glacial ice, leaving striae and facets on clasts and an eroded contact (Krüger and Kjær, 1999; van der Meer et al., 2003; Evans et al., 2006).

6.2.3 Section 3

Section 3 is located upstream from Section 2, next to Skeljungsá river (*Fig. 6-2*). The GPS coordinates are 65.58266, -15.46619 ± 3 m at an approximate elevation of 482 m a.s.l. The orientation of the section is 24° to 320° and the ridge trend is 113°. The section is 15-20 m wide (15 m was sketched on *Fig. 6-16*) and up to 3 m high in the center (*Fig. 6-16*). The section itself is located at the very edge of the landform. Strings were lined up for the height at 2.5 m intervals. The log (*Fig. 6-17*) was drawn approximately along the 5 m marker (*Fig. 6-16*). The section can be divided into three main units: the upper diamict unit (Unit 3), underlying gravel and sand unit (Unit 2) and a fine grained, stiff unit (Unit 1). Measurements of dip/dip direction of stratigraphic beds were made at seven locations in the section. Two clast samples are from Unit 2 (S3-CS-U2) and Unit 3 (S3-CS-U3) (*Fig. 6-16*).

Unit 1: Fine grained, stiff unit (FI)

Unit 1 is a stiff layer of fines with interbedded sand-lenses, ripples and an occasional larger clast at the bottom of the section. The dip and dip direction were difficult to estimate due to rippling and loose material. This unit is 80 cm thick.

Interpretation

Unit 1 is interpreted as fluvially deposited sediments (Miall, 1977; Miall, 1985). The occasional larger clast might indicate that the unit is actually diamictic and potentially fluvial sediments that have been subsequently reworked by glacier flow (Krüger and Kjær, 1999; Evans et al., 2006).

Unit 2: Stratified gravel, sand and fines (Gh)

Unit 2 is mostly gravel of up to 1 m in thickness, with clear stratification and layering. The layers are either gravel, fine sand or silt but mostly stratified gravel with large clasts, sand horizons and rippled sand lenses. This unit is only seen between 2.5-8 m on the width in the section (*Fig. 6-16*). A 20-30 cm thick, rippled sand layer can be traced throughout the section (See D in *Fig. 6-18*). It has a lower boundary with a traceable gravel layer.

Interpretation

Unit 2 is interpreted to be an originally fluvially deposited unit of sand and gravel (Miall, 1977; Miall, 1985). The diamict was deposited after the fluvial material, potentially causing distortion of pre-existing layers.

Unit 3: Coarse, clast rich diamict ($D_{b/s}$ C(m/c)3)

Unit 3 is a banded/stratified diamict unit with signs of interruption throughout the section. It is coarse grained, sandy/gravelly, firm, fissile and has a clast rich to clast supported matrix. This unit is overhanging in the center (at 7.5 m, *Fig. 6-16(B)*; *Fig. 6-18(E)*) and is stiffer than Unit 2 below. The boundary with Unit 2 is sharp and conformable. On the proximal (upstream) side of the unit there is a stratified, sorted sand vein perpendicular to the general stratification of diamict (See B in *Fig. 6-18* and B in *Fig. 6-16*). Other sand-lenses are aligned with the general stratification of the diamict. Unit 3 drapes over underlying units in the lower left part of the section. This might be explained by the location of the section in the landform (*Fig. 6-16* *Fig. 6-18*).

Interpretation

On basis of fissility, striae, bullet-shapes and faceted clasts Unit 3 is interpreted to be subglacial traction till (van der Meer et al., 2003; Evans et al., 2006). The sand-lense, crosscutting Unit 3 is interpreted as a hydrofracture/water dissipation structure and indicates waterflow from permeable sand into till (Krüger and Kjær, 1999; Rijdsdijk et al., 1999).

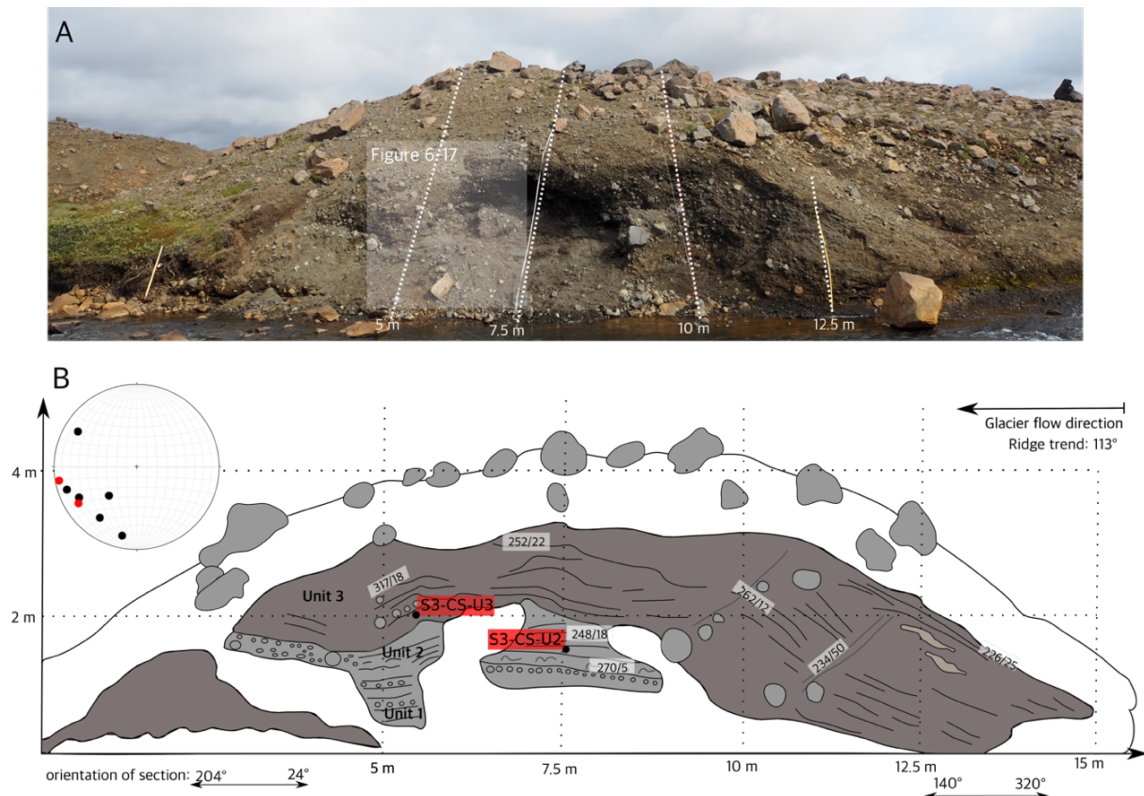


Fig. 6-16 A) Photograph of Section 3 showing the location of log in Figs. 6.17 in white box. B) Drawing of Section 3 showing the measurements for dip and dip direction of stratigraphic beds in white boxes. The measurements from the diamictic Unit 3 are plotted on a stereograph to the left where red dots are from Unit 2 (gravel) and black dots are from Unit 3 (diamict). Samples are marked with S3-CS-U1 and S3-CS-U2.

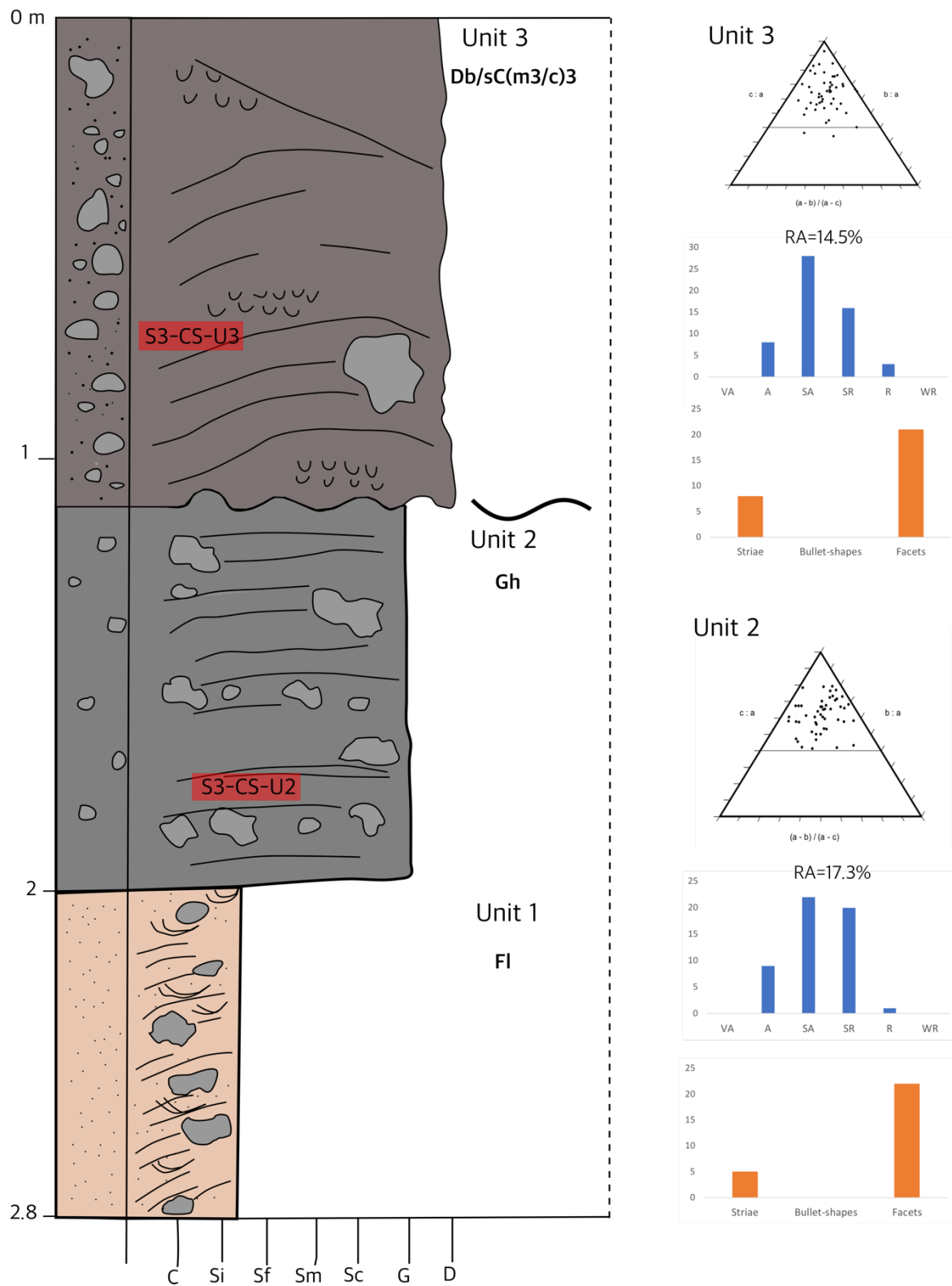


Fig. 6-17. Stratigraphic log of Section 3. Clast shape data with C40 diagrams and frequency for striae, bullet-shaped clasts and facets on clasts. RA index shows the percentage of angular and very angular clasts in the sample (Benn and Ballantyne, 1993).



Fig. 6-18. A) Shows Section 3 with white boxes indicating the location of figures B-D. B) The crosscutting sand-lense that truncates through a large part of Unit 3. C) Boundary between Unit 2 and Unit 3. D) Gravel and sand layers with ripples. E) Diamict drapes over the gravel and sand units.

Interpretation of Section 3

The till Unit 3 is interpreted to have been deposited after the underlying Units 1 and 2. The fluvial Units 1 and 2 seem to have experienced some disturbance. The presence of hydrofractures in till unit indicates that permeable layers contained water which burst into the till unit under large pressure gradients (Rijsdijk et al., 1999; van der Meer et al., 2009). The ridge has likely been eroded at the very edge and therefore the till unit drapes over underlying units, providing only a small window into the landform.

6.2.4 Section 4

Section 4 is located at the southernmost location of the four sections and is situated next to the Skeljungsá river (*Fig. 6-2*). The GPS coordinates are 65.58106, -15.47081 at an approximate elevation of 484 m a.s.l. The orientation of the section is 93° but changes to 146° at 30 m. The ridge trend is 317°. The section is 35-40 m wide and up to 19 m high (*Fig. 6-19*). The section is not a perpendicular cross-section of the landform which might give a distorted view into the interior of the ridge. Due to the lack of such large natural sections and the abundance of interesting features and information found in this section there was reason to document it. The units in this section are more difficult to distinguish apart than in sections 1-3 where stratigraphy was more straightforward. Complex sequences of interbedded lenses of sorted sediments and diamictic is descriptive for the section. All layers on the distal (downstream) side of the section have a dipping trend to the southeast. Measurements of dip/dip direction of stratigraphic beds were made at eight locations in the section, in the central to distal parts (*Fig. 6-19*). No clast samples were taken from Section 4.

Unit 1: Stratified diamict ($D_{b/s}C/F(m_2)^{3/4}$)

Unit 1 is a stratified diamict unit with medium to fine grained matrix. The unit is matrix supported, has a moderate number of clasts and is generally firm to extremely firm. It has clasts up to 10 cm and frequent sand and silt lenses. The unit has a lower boundary with bedrock. The bedrock was only visible in one location of the section and could not be inspected thoroughly in terms of potential erosional features or contact with overlying unit.

Interpretation

Unit 1 is here interpreted as subglacial traction till based on the similarities to other fissile units (3 and 5) in the section (Krüger and Kjær, 1999; van der Meer et al., 2003; Evans et al., 2006).

Unit 2: Laminated silt and fine sand (Fl/Sh with a Sr layer)

Unit 2 is composed of dense, laminated silt and fine sand with frequent sand lenses and small clasts of up to 3 cm. Sediments are distorted in places and layers are frequently cut off by others (See E in *Fig. 6-21*). Stratification of layers is unclear. The unit is discontinued to the right and might be a large lense which is hard to say with such a small window into the section.

Interpretation

Unit 2 is interpreted here to be fluviially deposited sorted sediments (Miall, 1977; Miall, 1985). The layers are highly distorted, and their original structure has likely been displaced by glacial flow.

Unit 3: Matrix supported and fine grained diamict ($D_mF(m_1)4$)

This diamict unit that can be traced across the distal, lower part of the section. It has an extremely hard, massive, homogenous appearance and a fine grained, fissile matrix with few clasts. The unit contains sorted lenses of sand and gravel, similar to underlying units.

Interpretation

Unit 3 can be interpreted as subglacial traction till due to its fissility (Krüger and Kjær, 1999; van der Meer et al., 2003; Evans et al., 2006).

Unit 4: Lenses of sand, gravel and laminated fines (Gh/Sh)

Unit 4 contains deformed but laminated silt and sand layers. Grading upwards, there are coarser grained sorted materials with sand lenses in between fine, massive diamict layers containing larger clasts that can be traced across the section. In the upper part of Unit 4, there are stratified sand and gravel layers with ripples that can be traced across the section with massive diamict layers interfingering with these layers of sorted material (See G and J in *Fig. 6-21*). Boundaries are gradational and units and layers quite often interfinger with each other. Gravel and sand units tend to show signs of displacement. In general, Unit 4 is irregularly stratified/banded with gravel, sand, fines and diamict lenses. There is often some kind of interbedding between sorted sediments and diamict above. A silty dissipation structure is visible in this unit (See I in *Fig. 6-21*).

Interpretation

The distorted, lensed, sorted materials are interpreted as fluvial sediments (Miall, 1977; Miall, 1985). The presence of silty dissipation structures in till unit is interpreted as a water dissipation structure, indicating that permeable layers (sand and gravel) contained water which burst into the unit under large pressure gradients (Rijsdijk et al., 1999; van der Meer et al., 2003).

Unit 5: Stratified, clast rich diamict ($D_{b/s}C(c/m_3)3$)

Unit 5 consists of a dense diamict with frequent lenses of sorted material, large clasts and boulders. It is slightly overhanging which indicates that this unit is harder than underlying ones (See F and G in *Fig. 6-21*). The uppermost diamict is banded/stratified, very firm, coarse grained and clast rich to clast supported. The clasts in this unit range from subangular to angular. Gravel lenses show cross bedding and lamination and some lenses show rippling as well as horizons of thin silty layers. The lenses of sorted material decrease upwards in frequency and at the very top of the unit there are no sorted lenses within the diamict. Unit 5 is similar in characteristics to diamict units in previous sections.

Interpretation

Unit 5 is interpreted as subglacial traction till because of its fissility, and similarities in appearance in comparison with till units in sections 1-3 (van der Meer et al., 2003; Evans et al., 2006). The unit shows signs of mixing with underlying sediments and distortion of originally deposited sediments.

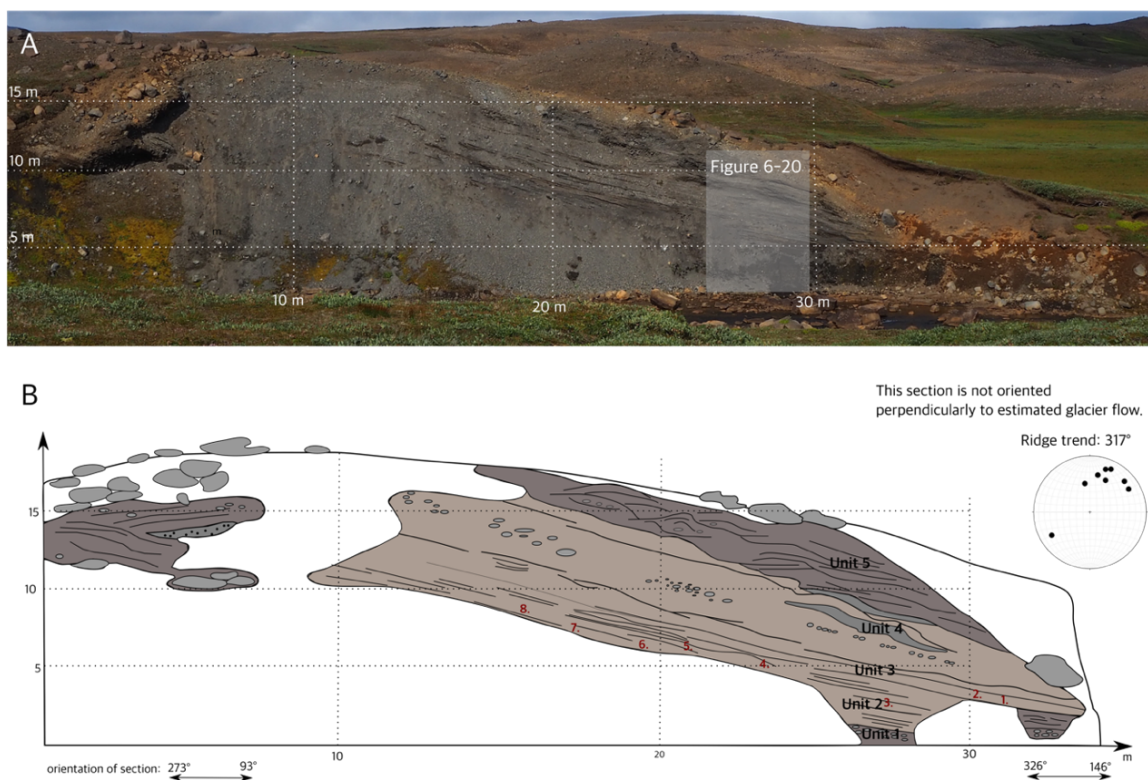


Fig. 6-19. A) Photograph of Section 4 showing the location of log in Fig. 6.20 in white box. B) Drawing of Section 4 showing the measurements for dip and dip direction of stratigraphic beds. The measurements are plotted on a stereograph to the right where black dots are from diamictic layers in Unit 3.

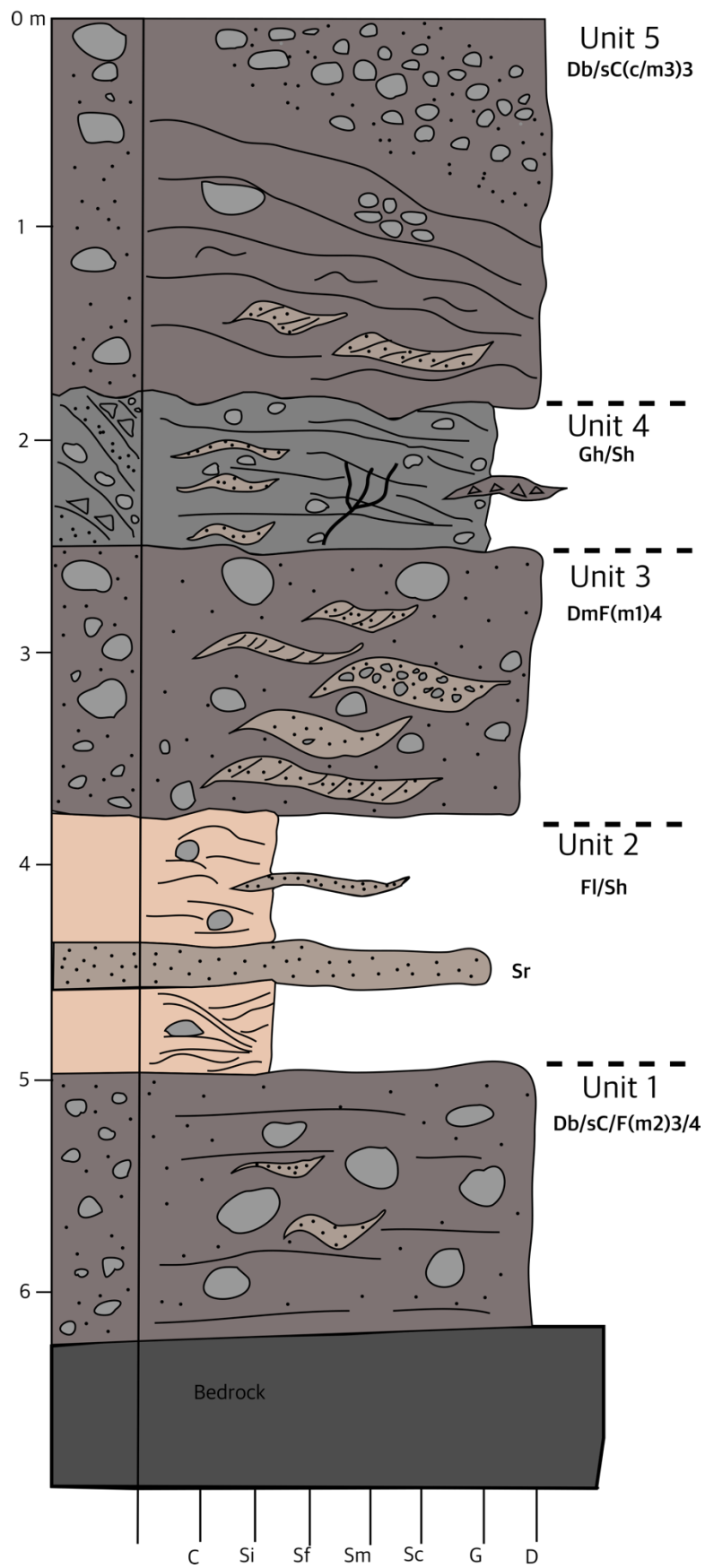


Fig. 6-20. Stratigraphic log for Section 4.



Fig. 6-21. A) Shows Section 4 with white boxes indicating the location of figures B-J. B) The boundary between Unit 2 and 3 showing locations for frames G, D and H. C) The boundary between Unit 1, 2 and 3. D) A section on the distal side showing bottom Unit 1 with a boundary to Unit 3, skipping Unit 2, which does not extend to this end of the section. E) Disrupted layers of sand and silt. F) Overhanging diamict and irregularly stratified and lense-rich sand, gravel and diamict. G) Boundary between Units 4 and 5. H) A close-up of disrupted fines and sand in Unit 2. I) Dissipation structure in Unit 2. J) Interfingering of sorted and diamict layers in distal part of the section.

Interpretation of Section 4

Section 4 is larger and more complex than Sections 1-3. The units and their boundaries are vague and difficult to distinguish, making it hard to put the different units into a chronological order. For example, the uppermost unit (Unit 5) is interpreted as till, and the same applies to the bottom unit (Unit 1). In between there are lenses of fluvial sediments and till of varying grain sizes but some of the large ones are described here as separate units. The section seems to be dominantly and irregularly lensed which might indicate that all units and lenses have been displaced from original position and draped over by till. Section 4 might have undergone ductile deformation with a significant amount of material mixing. No major folds or tectonic features were observed in the section, but this might also be explained by the angle at which the section is and the view that is presented into the landform. There are visible signs of distortion where water dissipation structures, small-scale deformation on bedding structures in sand and fines and general layer distortion indicate movement of material. Bedrock lies underneath the section and might indicate that the pre-existing, fluvial sediment sheet in the area is not very thick. Fluvial sediments are likely to have been deposited in the area before glacier overrode the area and deposited till on top. Later, both fluvial sediments and till were disturbed and mixed together, draping a final till bed on top.

6.2.5 Ridge surface clast measurements

The ridges are commonly covered with large boulders on the surface. The boulders are generally much larger than the clasts found in the ridge sections, which made them an interesting topic for further investigation. A random selection of clasts on top of five ridges in proximity to the sections described above, were measured in terms of a, b and c axes. Their angularity was also estimated. This data has been plotted into C40 diagrams as well as angularity histograms (*Fig. 6-23*). These show that the surface clasts are generally blocky and angular to sub-angular in shape. The results from ridge surface measurements reveal that subangular to angular clasts are more frequent on ridge surfaces than rounded to subrounded and no well-rounded clasts were observed.



Fig. 6-22. Large clasts are a common surface feature on top of the ridges.

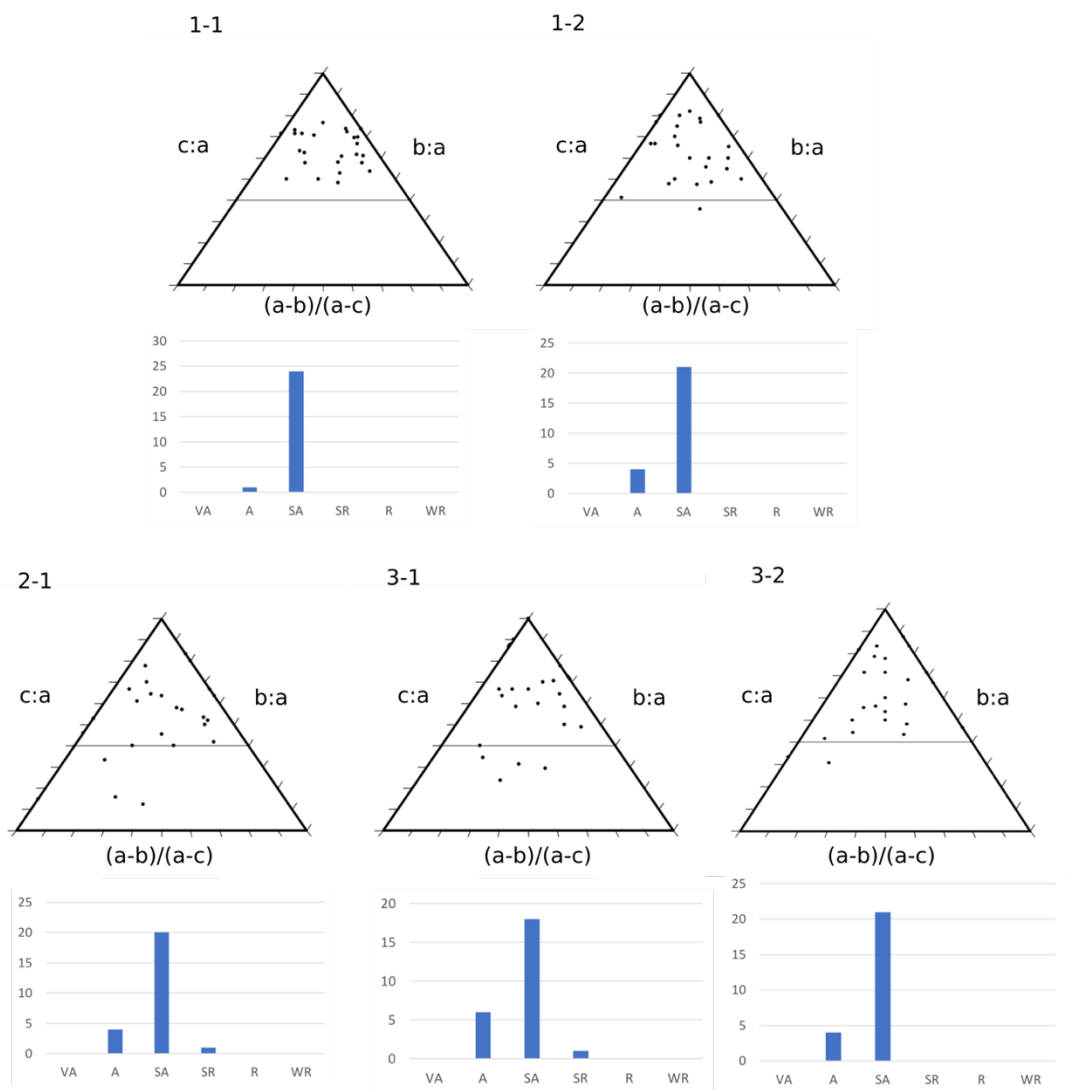


Fig. 6-23. Covariance plots and angularity histograms for surface clasts of five ridges.

Interpretation of surface clast results

The results from surface clast analysis indicates that the large, blocky clasts were either transported a short distance and experienced little rounding (Powers, 1953; Hambrey and Ehrmann, 2004) or were transported supra- or englacially (Benn and Evans, 2010). The clasts were likely transported englacially since eskers in the area (*Fig. 6-2*) do not have the same surface clast characteristics as the ribbed moraines which could be assumed if the clasts were transported supraglacially. However, the clast angularity indicates that they were probably transported a short distance.

7 Discussion

This study presents a comprehensive overview of the geomorphology and sedimentology of transverse ridges in the Vopnafjörður region, northeast Iceland. The ridges at Hauksstaðaheiði have been interpreted as ribbed moraines based on their transverse orientation, shape, size, distribution and topographic position. They fit well with previous studies on ribbed moraine characteristics at key sites in e.g. Scandinavia and North America (*Fig. 3-1*) and are interpreted to have formed subglacially. Ribbed moraines vary widely in internal composition and geomorphological characteristics making it difficult to pinpoint a single formation mechanism for all ribbed moraine landscapes. In this chapter the main findings of the study are discussed and a model for their formation is presented and compared with existing formation hypotheses.

7.1 Ridge characteristics

The location of the ridges at the highland plateau margin and upglacier from the main areas of streamlined terrain suggests that the ridges were formed within the onset zones of ice streaming near the ice divides of the IIS. This kind of setting for ribbed moraine formation has previously been proposed by e.g. Dyke et al. (1992); Hättestrand and Kleman (1999); Stokes (2006); Finlayson and Bradwell (2008) and Angelis and Kleman (2008).

The ridges are located in depressions/basins where hydrological influences can be expected by the discharge and collection of water in subglacial sediments. Normal stress and overburden pressure is high as well as pore-water pressure within subglacial sediments. Eskers in the Möðrudalskvos basin, are located between the ribbed moraine field in Leirvatnkvos and the Fossheiði drumlin field. Eskers are indicative of subglacial water flow (Warren and Ashley, 1994) and have been observed to occur close by ribbed moraines (Hättestrand and Kleman, 1999; Dunlop and Clark, 2006; Angelis and Kleman, 2008). This is in line with evidence found in the ribbed moraines such as hydrofractures/water dissipation structures.

The ribbed moraine ridge sets (Tunguheiði, Hauksstaðaheiði and Selárdalur) are located upstream of drumlin and MSGL flow sets (

Fig. 6-1). This indicates that the ridges are located at or form a boundary between fast (thawed conditions with drumlins and MSGLs) and slow ice flow (frozen conditions or ice divides such as Dimmifjallgarður)(Dyke et al., 1992; Hättestrand and Kleman, 1999; Dunlop and Clark, 2006).

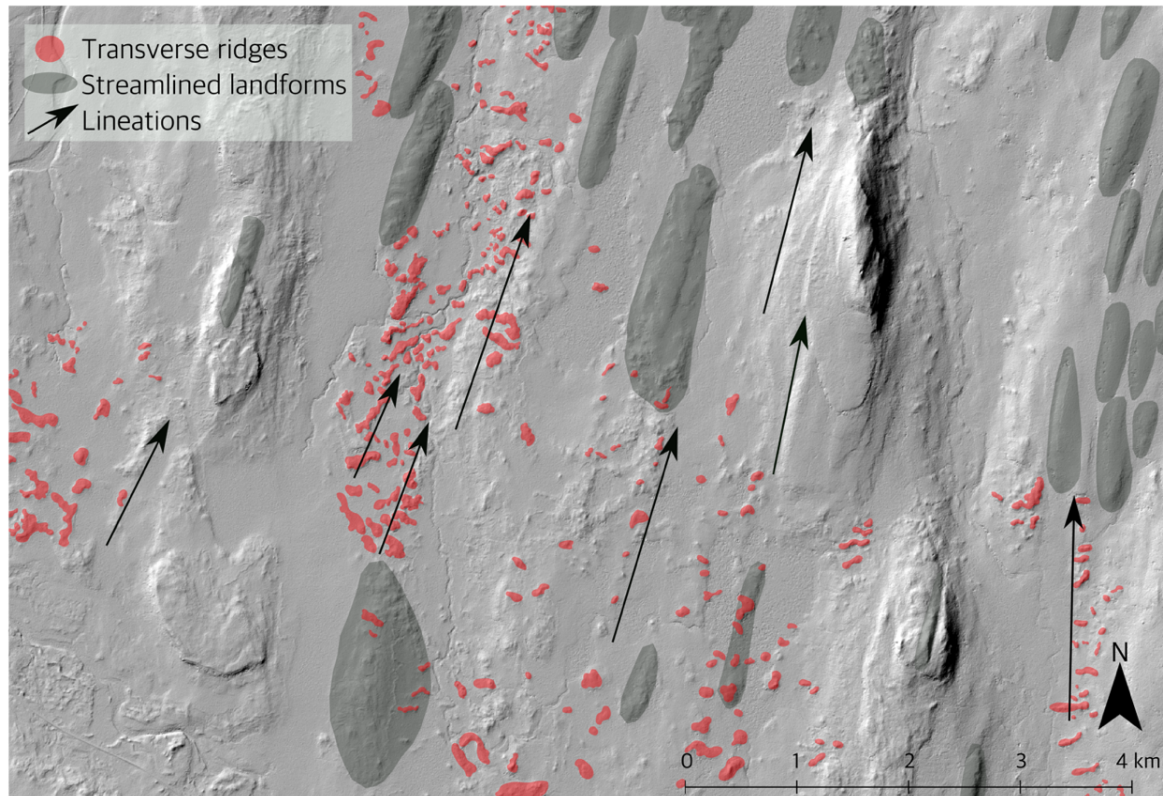


Fig. 7-1. Juxtaposition of transverse ridges (ribbed moraines) and drumlins/MSGLs in Tunguheiði. The transverse ridges tend to be lined up into rows of ridges in the direction of the drumlins/MSGLs and are often superimposed upon the streamlined landforms.

Hättestrand (1997) suggested that drumlins often superimpose ribbed moraines and that ribbed moraines often transition into drumlins (Lee, 1959; Hughes, 1964b; Hoppe, 1968; Lundqvist, 1969a). The opposite is observed, where ribbed moraines superimpose and fragment drumlins/MSGLs in Tunguheiði which is also observed by Stokes (2008) (Fig. 7-1). This pattern continues onto Hraunfellsheiði. The ribbed moraines in Tunguheiði commonly fragment drumlins and MSGLs into circular and transverse ridges. They cover a large part of upper Tunguheiði and tend to line up into rows of ridges, aligned with the streamlined NE trend of the region similar to what was observed by e.g. Aylsworth and Shilts (1989a). This suggests that they could be re-moulded from streamlined landforms (Fig. 7-1). This indicates that the ribbed moraines in Tunguheiði and potentially across the Vopnafjörður region are a secondary feature to drumlins and MSGLs, which is clearly a significant future topic of research (Dyke et al., 1992). The superimposition of ribbed moraines on streamlined landforms in Tunguheiði possibly points out that ribbed moraines formed following a decrease in ice streaming into Vopnafjörður during deglaciation of the area (Aylsworth and Shilts, 1989a). This relationship between streamlined landforms and ribbed moraines in the Vopnafjörður region needs to be further investigated since it might bring forward important implications of ribbed moraine formation and ice stream dynamics during deglaciation.

The Hauksstaðaheiði ribbed moraines vary in shape but their regular, dense spacing and transverse orientation is prominent in Leirvatnsvos. This might have resulted from a greater sediment supply in the basin, while flanks might have had less material to build

landforms from. The smaller, more fragmented ridges can also be interpreted as hummocky remnants from a more extensive and prominent ribbed moraine field as their shape varies greatly, potentially indicating that they have been eroded.

The internal characteristics of the Hauksstaðaheiði ribbed moraines show signs of disturbance and small-scale glaciotectionics which corresponds to other studies that have documented ribbed moraine sedimentology (*Table 1*). They have distorted fluvial composition, interbedded with till and draped with subglacial till. Hydrofractures/water dissipation structures cross-cut both fluvial and till units. These structures are indicative of water flow during deposition of the ridges (van der Meer et al., 2009). The ridge surfaces are covered with large, angular boulders and clasts. Their angularity suggests minimal glacial erosion and a short transport distance of clasts. The presence of eskers close by which have a washed surface with sorted material indicates that the highly angular surface boulders on the ribbed moraines were deposited subglacially. Further work is needed to confirm these interpretations. In addition, it would be beneficial to investigate sections in Tunguheiði and Selárdalur.

7.2 Comparison with previous studies

The criteria for ribbed moraine characteristics put forward by Hättestrand (1997) and presented in Chapter 3.2, applies to the Hauksstaðaheiði ribbed moraine field to a limited degree. Here, the ridges are likely composed of the same material as the surroundings or pre-existing sediments. The drift sheet between the landforms was not observed but is likely to have been thin as indicated by exposed bedrock in Section 4. They have neither been observed drumlinized or transitioning into drumlins. Glaciotectionism is limited in terms of folding and faulting but displacement of sediment is clear. A jig-saw puzzle pattern between ridges was not observed, however due to their location, it is likely that extensional flow played a role in ridge formation.

Table 1 shows the internal characteristics of a large amount of ribbed moraine studies that have noted their sedimentology. Their sedimentology can be very varied although it is interesting to see how many studies have a similar composition and characteristics as the Hauksstaðaheiði ridges (Shaw, 1979; Lundqvist, 1997; Raunholm et al., 2003; Möller, 2006; Sarala, 2006; Finlayson and Bradwell, 2008; Lindén et al., 2008). In fact, a large portion of the ridges mentioned in *Table 1* are composed of sorted material (fluvial) and diamict (till) and a few note glaciotectionism as claimed a frequent ribbed moraine characteristic by (Hättestrand, 1997). Similarly, the Hauksstaðaheiði sections can be described this way: Lenses of fluvial sediments, draped by and interbedded with till, showing signs of distortion, erosional surfaces and water dissipation structures/hydrofractures. Although Hättestrand (1997) and Lundqvist (1989) claim that the internal composition of the ridges is unrelated to the morphology-shaping process of ridge moraine formation, it is interesting to see such similarities between studies from a wide range of regions as well as time periods. However, it is argued here that the ridges are formed from pre-existing, local sediments and their formation is controlled by external processes. Further investigating the internal composition of ribbed moraines on a larger scale might nevertheless provide an interesting angle on ribbed moraine studies.

Large surface boulders are here interpreted as a part of the originally deposited till in the ribbed moraines. Finer material was then eroded away during and after stagnation by dead ice processes and/or fluvial processes which left large boulders as lag deposits. This could indicate that ribbed moraines are a common product from a passive retreat of an ice sheet/ice stream since their morphology correlates well with hummocky terrain as observed by Burgess et al. (2003). A passive retreat is more plausible than an active one since no signs of ice-marginal processes are visible. Sarala (2006) and Möller (2006) observed similar large surface boulders which were not found inside the landforms. Möller (2006) inferred that the boulders were quarried upstream and transported englacially and finally draping them onto the already formed ridges during deglaciation. Sarala (2006) interpreted the coarse surfaces as bedrock quarried from upstream of each ribbed moraine ridge, depositing rock fragments and boulders onto the next ridge under high pressure. These two hypotheses are difficult to test with the Hauksstaðaheiði ribbed moraines since clast lithologies were not described and is less feasible in this bedrock setting. Samples collected from the ridges were homogenous although no further investigations were made, or any focus put on this.

Fig. 3-1 shows a classification scheme of ribbed moraine geomorphology from Dunlop and Clark (2006). The Hauksstaðaheiði and Tunguheiði ribbed moraine fields do not always have a distinct transverse shape but their shapes are similar to those termed “Lumpy ribbed moraine ridges” and “hummocky ribbed moraine” by Dunlop and Clark (2006).

The focus area of this study is located downstream from the topographic high, Dimmifjallgarður, where extensional ice flow may have operated down-glacier of a cold-based ice divide. Due to the potential for extensional flow in the downstream end of a topographical obstruction, the fracturing and extensional theory from Hättestrand (1997) is a likely explanation. Evidence supporting the “shearing and stacking” theory are folds and faulting which are not observed to any large degree in the Hauksstaðaheiði ridges. Therefore, it is difficult to attribute “shearing and stacking” to the ribbed moraines in Hauksstaðaheiði. The ridges in Hauksstaðaheiði, Tunguheiði and Selárdalur are all formed in narrow but shallow depressions or tracks. The Hauksstaðaheiði ribbed moraines are in a depression between an area where ice flow was most likely fast and a supposedly cold-based ice divide. Extensional ice flow in the region was therefore likely, causing fracturing of sediments in Hauksstaðaheiði where a slow, cold-based glacier was integrating into a warm-based, fast-flowing ice stream. This agrees with the observations of Finlayson and Bradwell (2008) who suggest that the ridges could be formed by fracturing and extension by slow moving ice integrating into a fast corridor of ice, thus making lateral changes in flow velocity an important factor in ridge formation.

Hättestrand (1997) suggests that a change in bed thermic conditions from cold-based to warm-based can cause the sediment sheet to partially thaw and break up into boudins. The basal shear stress increases with faster ice flow and creates a patchwork of cold and warm based ice zones, piling sediments up into ribbed moraines with the help of water flowing towards lower pressure. Here, the fracturing model is applied to the Hauksstaðaheiði ridges. Blocks of fluvial material and till remained frozen during displacement into ridges and were deposited and interbedded in a ductile way as they moved towards a thawing bed. Finlayson and Bradwell (2008) note similar characteristics, where ridges are located in a shallow depression upstream from deep valley troughs,

making them likely to have experienced a lateral and longitudinal gradient in ice flow velocity as described before.

A number of studies have suggested that ribbed moraine ridges are formed at a late stage during deglaciation (Hättestrand and Kleman, 1999; Finlayson and Bradwell, 2008). This is proposed because of the ridge's morphology and position inside the glacier's greatest extent. Their location in Hauksstaðaheiði suggests that they could have formed at the onset of ice streaming (Dyke et al., 1992).

7.3 Model of ribbed moraine formation

The morphological and sedimentological data in this study suggest that the ribbed moraine ridges in Hauksstaðaheiði were formed through the collection of pre-existing material underneath transverse crevasses at the boundary of an ice stream and ice divide (Fig. 7-2).

Before ridge formation, Hauksstaðaheiði was ice free with a river running in the shallow valley of Leirvatnsvos. The fluvial material observed in the lower part of the ridges was deposited on top of bedrock (Fig. 7-2, A). Subsequently, the basin was overridden by a glacier, as suggested by the overlying subglacial traction till. The fluvial sediments became covered with, and sometimes eroded by, subglacial till, creating unconformities between the two units. Drumlins and MSGs were formed in the region in e.g. Fossheiði and Tunguheiði (Fig. 7-2, B).

Drumlins and MSGs in the highlands south of Vopnafjörður were probably formed by an ice stream. The Dimmifjallgarður ice divide, however, caused imbalances between the fast-flowing ice stream and the cold-based ice divide. This caused ice in the transition zone between the two areas to experience extensional ice flow, which in turn caused the formation of transverse crevasses (Nye, 1952). The crevasses formed as a result of tensile stresses pulling ice apart in Hauksstaðaheiði between an ice divide and an ice stream. Subglacial water found its way to the Hauksstaðaheiði basins where sediments became water saturated and deformable (Fig. 7-2, C).

When crevasses formed at the surface there was lower normal stress on the bed beneath. Porewater pressure built up in the sand and gravel because of the sealing of the dense till unit above. Eventually the seal broke and finer sediments burst into overlying sediments, creating water escape structures (as observed in sections 3 and 4). The seal unit in Section 3 is till and sand/gravel in Section 4. These structures seem to be moving upwards, from lower units of corresponding material. This supports the hypothesis that subglacial water found the lowest pressure and partly frozen rafts of fluvial and subglacial traction till lenses were dislocated into ridges located below extensional crevasses (Fig. 7-2, D). The sediments in the ridges are generally dipping away from the center of the ridges where the least overburden pressure is expected to be. The ribbed moraines are here thought to have formed during deglaciation as the ice stream was slowing down, which is confirmed by the superimposed ribbed moraines on drumlins/MSGs in Tunguheiði. During this stage, the cold-based region was potentially expanding towards the coast, as the ice stream shut down and fast flow in the region had stopped (Stokes, 2006). This might also explain why

ribbed moraines commonly superimpose and fragment pre-existing drumlins and MSGs in Tunguheiði.

The ice stream shut down and experienced passive retreat as a result. As the glacier stagnated to the ridge level, the coarse ridge surfaces were eroded by dead ice and fluvial processes when the glacier had fully retreated. The surface would then presumably have experienced erosion of finer materials during and after deglaciation, leaving only larger, coarse clasts on the surface as lag deposits (*Fig. 7-2, E-F*). However, the surface clasts have a slightly greater angularity element than clasts sampled from the interior of the sections. This till layer could have been transported a shorter distance than the underlying till.

The Hauksstaðaheiði, Leirvatnsvos basin became a river environment again (*Fig. 7-2, F*). Erosion of the ridges occurred, leaving open sections and segmented ridges behind. The river might have caused fragmentation of the ridges into disorganized, less transverse features. There is a possibility that the ridges could also have been decomposed during the very last stages of ice stagnation or deglaciation in the area (*Fig. 7-2, F*).

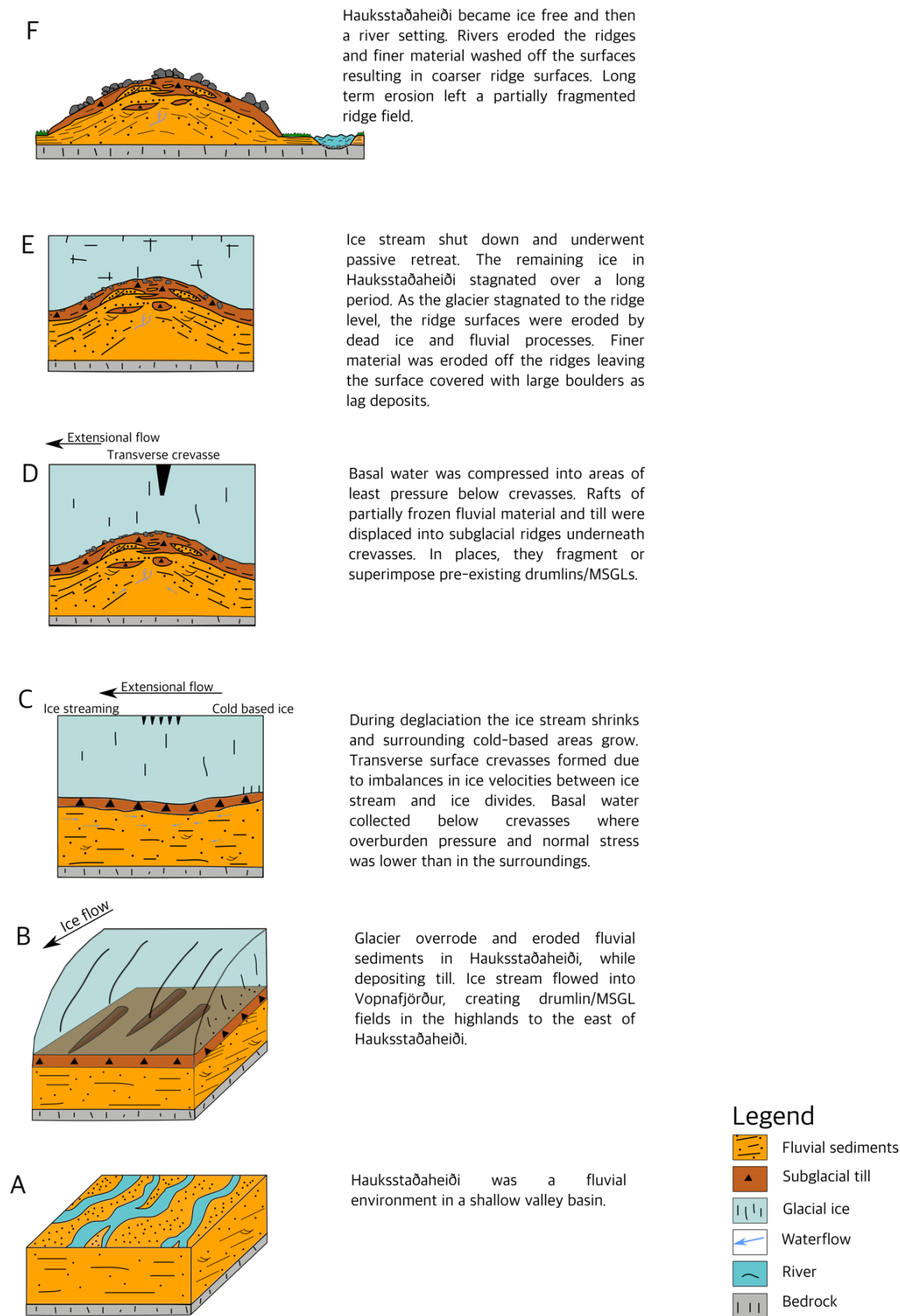


Fig. 7-2. Sequential model for the formation of ribbed moraines in Hauksstaðaheiði. The model is based on the sedimentology, geomorphology and landscape associations for the Hauksstaðaheiði ribbed moraines.

It is unclear whether one model or more can explain the formation of ribbed moraines and this study will certainly not attempt to claim either. The landforms have different characteristics to those described by a number of studies and their geomorphology does not correspond to all ribbed moraine morphologies. It is also clear that their environmental associations and surroundings are not applicable between all ribbed moraine sites as stated by Dunlop and Clark (2006). Hättestrand and Kleman (1999) and Dunlop and Clark (2006) suggest that a single formation hypothesis will be the most successful in order to explain the formation of ribbed moraines and their vast diversity. Whether ribbed moraine formation is related to basal water flow, ice velocity or pressure gradients and unrelated to pre-existing sediments or their specific surrounding landscape is hard to determine. It will not be argued here further since there is little evidence to why the ridges should have a poly- or monogenetic origin of formation. Until that is established, the term ribbed moraine should only be used as a morphological term as proposed by Möller (2006). Further research is required in order to establish a formation mechanism for ribbed moraines. A comprehensive, interdisciplinary approach would be most successful where glacial geology, geomorphology, glaciology and geophysical methods are considered. Such research would surely provide the most accurate explanation to the formation of these ambiguous landforms that ribbed moraines remain to be.

8 Conclusion

- I. The shape, size and topographical setting of the ridges in Hauksstaðaheiði, Tunguheiði and Selárdalur suggest that they are ribbed moraines.
- II. Detailed mapping and statistical analysis of the Hauksstaðaheiði ribbed moraines reveals that the ridges have a dominant transverse orientation to the estimated ice flow direction towards the northeast. Their shape is irregular with an average length, width and height of 112.0 m, 66.0 m and 6.4 m. Their average spacing is 125-160 m but is considerably less in areas of greatest ridge density.
- III. The ribbed moraines occur upstream from fields of streamlined subglacial landforms (drumlins/MSGs), indicating that they might be formed in the onset zone of ice streaming or in a “transition zone” between cold-based and warm-based ice.
- IV. Extensional ice flow likely resulted in large, transverse surface crevasses in the area of transition between cold-based and warm-based ice. It is proposed that the ribbed moraines are formed underneath these transverse crevasses due to variations in water pressure and lower effective stress at the glacier bed. Sediment flux towards these areas results in the accretion of subglacial till and glaciofluvial sediments and the formation of ribbed moraine ridges.
- V. The ribbed moraines superimpose or segment drumlins and MSGs in Tunguheiði, indicating that they are a secondary feature to drumlin formation and that they are potentially formed during deglaciation.
- VI. This study provides limited insight into ribbed moraine fields in the Vopnafjörður region. Further investigations of these and other ribbed moraine fields in NE-Iceland are necessary in order to test previous hypotheses of ribbed moraine formation. Increasing the knowledge of ribbed moraines could prove essential in order to fully understand and reconstruct the deglaciation dynamics of the northeastern part of the IIS.

References

- Aario, R., 1977a. Associations of flutings, drumlins, hummocks and transverse ridges. *GeoJournal*, 16: 65-72.
- Aario, R., 1977b. Classification and terminology of morainic landforms in Finland. *Boreas*, 6: 87-100.
- Aario, R., 1987. Drumlins of Kuusamo and Rogen-ridges of Ranua, northeast Finland. In: J.M.J. Rose (Editor), *Drumlin symposium*, Rotterdam: Balkema, pp. 87-101.
- Alley, R.B. and Bindschadler, R.A., 2001. The West Antarctic Ice Sheet and sea-level change. *Antarctic Research Series*, 77: 1-11.
- Alley, R.B., Blankenship, D.D., Bentley, C.R. and Rooney, S.T., 1986. Deformation of till beneath ice stream B, West Antarctica. *Nature*, 322: 57-59.
- Alley, R.B., Blankenship, D.D., Bentley, C.R. and Rooney, S.T., 1987. Till beneath ice stream B: 3. Till deformation: evidence and implications. *Journal of Geophysical Research*, 92.
- Alley, R.B., Clark, P.U., Huybrechts, P. and Joughin, I., 2005. Ice sheet and sea level changes. *Science*, 310: 456-460.
- Anandakrishnan, S. and Alley, R.B., 1997. Stagnation of ice stream C, West Antarctica by water piracy. *Geophysical Research Letters*, 24: 265-268.
- Andrews, J.T., Jónunn Hardardóttir, Gudrún Helgadóttir, Anne E. Jennings, Áslaug Geirsdóttir, Árny E. Sveinbjörnsdóttir, Stephanie Schoolfield, Gréta B. Kristjánsdóttir, L. Micaela Smith, Kjartan Thors, James P.M. Syvitski 2000. The N and W Iceland Shelf: insights into Last Glacial Maximum ice extent and deglaciation based on acoustic stratigraphy and basal radiocarbon AMS dates. *Quaternary Science Reviews*, 19: 619-631.
- Angelis, H.D. and Kleman, J., 2008. Palaeo-ice-stream onsets: examples from the north-eastern Laurentide Ice Sheet. *Earth Surface Processes and Landforms*, 33(4): 560-572.
- Aylsworth, J.M. and Shilts, W.W., 1989a. Bedforms of the Keewatin Ice Sheet, Canada. *Sedimentary Geology*, 62: 407-428.
- Aylsworth, J.M. and Shilts, W.W., 1989b. Glacial features around the Keewatin Ice Divide: Districts of MacKenzie and Keewatin. *Geological Survey of Canada Paper*, 88: 21 pp.
- Bamber, J.L., Vaughan, D.G. and Joughin, I., 2000. Widespread complex flow in the interior of the Antarctic Ice Sheet. *Science*, 287: 1248-1250.
- Beaney, C.L. and Shaw, J., 2000. The subglacial geomorphology of southeast Alberta: evidence for subglacial meltwater erosion. *Canadian Journal of Earth Sciences*, 37: 51-61.
- Benediktsson, Í.Ö., Jónsson, S. A., Schomacker, A., Johnson, M. D., Ingólfsson, Ó., Zoet, L., Iverson, N.R., Stötter, J., 2016. Progressive formation of modern drumlins at Múlajökull, Iceland: stratigraphical and morphological evidence. *Boreas*, 45: 567-583.
- Benediktsson, Í.Ö., McKenzie, M. and Principato, S., 2018. Geomorphological and sedimentological evidence for a palaeo-ice stream in Bárðardalur, North Iceland, 6th International Conference on 'Palaeo-Arctic Spatial and Temporal (PAST) Gateways. , Durham University.
- Benn, D. and Evans, D., 2004. *A Practical Guide to the Study of Glacial Sediments*. Routledge.

- Benn, D.I. and Ballantyne, C.K., 1993. The description and representation of clast shape. *Earth Surface Processes and Landforms*, 18: 665-72.
- Benn, D.I. and Evans, D.J.A., 2010. *Glaciers and Glaciation*. Hodder Education, London, UK, 802 pp. pp.
- Bennett, M.R., 2003. Ice streams as the arteries of an ice sheet: their mechanics, stability and significance. *Earth-Science Reviews*, 61: 309-339.
- Bentley, C.R. and Giovinetto, M.B., 1991. Mass balance of Antarctica and sea level change. Weller, G., Wilson, C.L., Sevberin, B.A.B. (Eds.) *International Conference on the Role of the Polar Regions in Global Change: Proceedings of a Conference Held June 11 – 15, 1990 at the University of Alaska Fairbanks*, vol. II. Geophysical Institute/Centre for Global Change and Arctic Systems Research, Fairbanks: 481-488.
- Beskow, G., 1935. Praktiska och kvartärgeologiska resultat av grusinventeringen i Norrbottens län. *Geologiska Föreningens i Stockholm Förhandlingar*, 57: 120–123.
- Bindschadler, R.A., King, M.A., Alley, R.B., Anandakrishnan, S. and Padman, L., 2003. Tidally controlled stick-slip discharge of a West Antarctic ice stream. *Science*, 301: 1087-1089.
- Blankenship, D.D., Bentley, C.R., Rooney, S.T. and Alley, R.B., 1986. Seismic measurements reveal a saturated porous layer beneath an active Antarctic ice stream. *Nature*, 322: 54-57.
- Bouchard, M.A., 1980. Late Quaternary geology of the Témiscamie area, central Québec, Canada. Dissertation, Department of Geological Sciences, McGill University.
- Bouchard, M.A., 1986. *Geologie des depots meubles de la région de Témiscamie, Territoire du Nouveau-Québec*. Ministère de l'Énergie et des Ressources du Québec, Mémoire, 83-03: 90.
- Bouchard, M.A., 1989. Subglacial landforms and deposits in central and northern Quebec, Canada, with emphasis on Rogen moraines. *Sedimentary Geology*, 62: 293–308.
- Boulton, G.S., 1976. The origin of glacially fluted surfaces - observations and theory. *Journal of Glaciology*, 17: 287-309.
- Boulton, G.S., 1987. A theory of drumlin formation by subglacial sediment deformation. *Drumlin Symposium*: 25-80.
- Bourgeois, O., Dauteuil, O. and Vliet-Lanoe, B.V., 1998. Pleistocene subglacial volcanism in Iceland: tectonic implications. *Earth and Planetary Science Letters*, 164: 165-178.
- Burgess, D.O., Shaw, J. and Eyton, J.R., 2003. Morphometric Comparisons Between Rogen Terrain and Hummocky Terrain. *Physical Geography*, 24(4): 319–336.
- Chapwanya, M., Clark, C.D. and Fowler, A.C., 2011. Numerical computations of a theoretical model of ribbed moraine formation. *Earth Surface Processes and Landforms*, 36: 1105-1112.
- Clark C.D., T.S.M., Stokes C.R., Canals M. , 2003. A groove- ploughing theory for the production of mega-scale glacial lineations, and implications for ice-stream mechanics. *Journal of Glaciology*, 49: 240-256.
- Clark, C.D., 1993. Mega-scale glacial lineations and cross-cutting ice-flow landforms. *Earth Surface Processes and Landforms*, 18: 1-28.
- Clark, C.D. and Meehan, R.T., 2001. Subglacial bedform geomorphology of the Irish Ice Sheet reveals major configuration changes during growth and decay. *Journal of Quaternary Science*, 16: 483-496.

- Clark, P.U. and Walder, J.S., 1994. Subglacial drainage, eskers, and deforming beds beneath the Laurentide and Eurasian ice sheets. *Geological Society of America Bulletin*, 106: 304-314.
- Cowan, W.R., 1968. Ribbed moraine: Till-fabric analysis and origin. *Canadian Journal of Earth Sciences*, 5: 1145-1159.
- Craig, B.G., 1965. Glacial Lake McConnell, and the surficial geology of parts of Slave River and Redstone River map-areas, District of Mackenzie. *Geological Survey of Canada Bulletin*, 122: 33.
- Dowling, T.P.F., Spagnolo, M., Möller, P., 2015. Morphometry and core type of streamlined bedforms in southern Sweden from high resolution LiDAR. *Geomorphology*, 236: 54-63.
- Dredge, L.A., Nixon, F.M. and Richardson, R.J., 1986. Quaternary geology and geomorphology of northwestern Manitoba. *Geological Survey of Canada Memoir*, 418: 38 pp.
- Dunlop, P. and Clark, C.D., 2006. The morphological characteristics of ribbed moraine. *Quaternary Science Reviews*, 25: 1668-1691.
- Dunlop, P., Clark, C.D. and Hindmarsh, R.C.A., 2008. Bed Ribbing Instability Explanation: Testing a numerical model of ribbed moraine formation arising from coupled flow of ice and subglacial sediment. *Journal of Geophysical Research*, 113.
- Dyke, A.S., 1993. Landscapes of cold-centered late Wisconsinan ice caps, Arctic Canada. *Progress in Physical Geography*, 17: 223-247.
- Dyke, A.S., Morris, T.F., Green, D.E.C. and England, J., 1992. Quaternary geology of Prince of Wales Island, Arctic Canada. *Geological Survey of Canada Memoir*, 433: 142pp.
- Ely, J.C., Clark, C.D., Spagnolo, M., Stokes, C.R., Greenwood, S.L., Hughes, A.L.C., Dunlop, P. and Hess, D., 2016. Do subglacial bedforms comprise a size and shape continuum? *Geomorphology*, 257.
- Evans, D.J.A., Phillips, E.R., Hiemstra, J.F. and Auton, C.A., 2006. Subglacial till: Formation, sedimentary characteristics and classification. *Earth-Science Reviews*, 78: 115-176.
- Eyles, N., Putkinen, N., Sookhan, S., Arbelaez-Moreno, L. , 2016. Erosional origin of drumlins and megaridges. *Sedimentary Geology*, 338: 2-23.
- Finlayson, A.G. and Bradwell, T., 2008. Morphological characteristics, formation and glaciological significance of Rogen moraine in northern Scotland. *Geomorphology*, 101(4): 607-617.
- Fisher, T.G. and Shaw, J., 1992. A depositional model for Rogen moraine, with examples from the Avalon Peninsula, Newfoundland. *Canadian Journal of Earth Sciences*, 29: 669-686.
- Fowler, A.C., 2010. The formation of subglacial streams and mega-scale glacial lineations. *Proceedings of the Royal Society A*, 466: 3181-3201.
- Frödin, G., 1913. Bidrag till västra Jämtlands senglaciala geologi. *Sveriges Geologiska undersökning C*, 246: 236.
- Frödin, G., 1925. Studien über die Eissheide in Zentralskandinavien. *Bulletin of the Geological Institutions at the oniversity of opsala*, 19: 214.
- Frödin, G., 1954. De sista skedena av Centraljämtlands glaciala historia. *Geographica*, 24: 1-251.
- Fromm, E., 1965. Beskrivning till jordartskartan över Norrbottens län nedanför Lappmarksgränsen. *Sveriges Geologiska undersökning Ca*, 39: 236.

- Geirsdóttir, Á., Miller, G.H., Axford, Y. and Ólafsdóttir, S., 2009. Holocene and latest Pleistocene climate and glacier fluctuations in Iceland. *Quaternary Science Reviews*, 28: 2107-2118.
- Graham, A.G.C., Later, R.D., Gohl, K., Hillenbrand, C.-D., Smith, J.A. and Kuhn, G., 2009. Bedform signature of a West Antarctic ice stream reveals a multi-temporal record of flow and substrate control. *Quaternary Science Reviews*, 28: 2774–2793.
- Graham, D.J. and Midgley, N.G., 2000. Graphical representation of particle shape using triangular diagrams: an Excel spreadsheet method. *Earth Surface Processes and Landforms*, 25: 1473-1477.
- Granlund, E., 1943. Beskrivning till jordartskarta över Västerbottens län nedanför odlingsgränsen. *Sveriges Geologiska undersökning Ca*, 26: 185.
- Hambrey, M.J. and Ehrmann, W., 2004. Modification of sediment characteristics during glacial transport in high- alpine catchments: Mount Cook area, New Zealand. *Boreas*, 33: 300-318.
- Hanna, E., Navarro, F.J., Pattyn, F., Domingues, C.M., Fettweis, X., Ivins, E.R., Nicholls, R.J., Ritz, C., Smith, B., Tulaczyk, S., Whitehouse, P.L., Zwally, H.J., 2013. Ice sheet mass balance and climate change. *Nature*, 498: 51-59.
- Hättestrand, C., 1997. Ribbed moraines in Sweden - distribution pattern and palaeoglaciological implications. *Sedimentary Geology*, 111: 41-56.
- Hättestrand, C. and Kleman, J., 1999. Ribbed moraine formation. *Quaternary Science Reviews*, 18: 43-61.
- Heine, J.T. and McTigue, D.E., 1996. A case for cold-based continental ice sheets - a transient thermal model. *Journal of Glaciology*, 42: 3742.
- Henderson, E.P., 1959. A glacial study of Central Quebec-Labrador. *Geological Survey of Canada Bulletin*, 50: 94.
- Hess, D.P., Briner, J. P., 2009. Geospatial analysis of controls on subglacial bedform morphometry in the New York Drumlin Field – implications for Laurentide Ice Sheet dynamics. *Earth Surface Processes and Landforms*, 34: 1126-1135.
- Högbom, A.G., 1885. Glaciala och petrografiska lakttagelser i Jemtlands län. *Sveriges Geologiska undersökning C*, 70: 39.
- Högbom, A.G., 1894. Geologisk beskrifning över Jemtlandslän. *Sveriges Geologiska undersökning C*, 140: 107.
- Högbom, A.G., 1920. Geologisk beskrivning över Jämtlandslän 2nd edn. *Sveriges Geologiska undersökning C*, 140: 139.
- Hooke, R.L., 1977. Basal temperatures in polar ice sheets: A qualitative review. *Quaternary Research*, 7: 1-13.
- Hoppe, G., 1948. Isrecessionen från Norrbottens kustland. *Geographica*, 20: 1-112.
- Hoppe, G., 1968. Tärnasjö-områdets geomorfologi - En översiktlig orientering med särskild hänsyn till de glaciala och postglaciala formelementen. University of Stockholm, Department of Physical Geography, Research Report, 8: 17.
- Hubbard, A., 2006. The validation and sensitivity of a model of the Icelandic ice sheet. *Quaternary Science Reviews*, 25: 2297–2313.
- Hubbard, A., Sugden, J., Dugmore, A., Norðdahl, H. and Pétursson, H.G., 2006. A modelling insight into the Icelandic Late Glacial Maximum ice sheet. *Quaternary Science Reviews*, 25: 2283-2296.
- Hughes, O.L., 1964a. Surficial geology, Nichicun-Kaniapiskau map- area, Quebec. *Geological Survey of Canada Bulletin*, 106: 18.

- Hughes, O.L., 1964b. Surficial geology, Nichicun-Kaniapiskau map-area, Quebec. Geological Survey of Canada Bulletin, 106: 18.
- Hughes, T., 1973a. Glacial permafrost and Pleistocene ice ages. Permafrost, 2nd International Conference: 213-223.
- Hughes, T., 1973b. Is the West Antarctic Ice Sheet disintegrating? Journal of Geophysical Research, 78: 7884-7910.
- Huybrechts, P. and T'siobbel, S., 1995. Thermomechanical modelling of northern hemisphere ice sheets with a two-level mass-balance parametrization. Annals of Glaciology, 21: 111-116.
- Ingólfsson, Ó., 1991. A Review of the Late Weichselian and Early Holocene Glacial and Environmental History of Iceland. In: J. Maizels, C. Caseldine (eds.), Environmental Change in Iceland: Past and Present, Kluwer Academic Publishers, Dordrecht: 13-29.
- Ingólfsson, O. and Norðdahl, H., 2001. High Relative Sea Level during the Bölling Interstadial in Western Iceland: A Reflection of Ice-sheet Collapse and Extremely Rapid Glacial Unloading. Arctic, Antarctic and Alpine Research, 33: 231-243.
- Ives, J.D., 1956. Till patterns in Central Labrador. Canadian Geographic, 8: 25-33.
- Jennings, A.E., Syvitski, J.P.M., Gerson, L., Grönvold, K., Geirsdóttir, Á., Harðardóttir, J., Andrews, J.T., Hagen, S., 2000. Chronology and paleoenvironments during the late Weichselian deglaciation of the south-west Iceland shelf. Boreas, 29: 167-183.
- Jóhannesson, H. and Sæmundsson, K., 2014. Geological Map of Iceland, Bedrock Geology. Icelandic Institute of Natural History.
- Jóhannesson, H., Sæmundsson, K., Sveinbjörnsdóttir, Á. E., Símonarson, L. A., 1997. Nýjar aldursgreiningar á skeljum á Reykjanesskaganum. , Geological Society Iceland Spring Meeting, pp. 29-30.
- Johnson, M.D., Schomacker, A., Benediktsson, Í.Ö., Geiger, A.J., Ferguson, A., Ingólfsson, Ó., 2010. Active drumlin field revealed at the margin of Múlajökull, Iceland: A surge-type glacier. Geology, 38: 943-946.
- Joughin, I., MacAyeal, D.R. and Tulaczyk, S., 2004. Basal shear stress of the Ross ice streams from control method inversions. Journal of Geophysical Research, 109: B09405.
- Joughin, I.R., Smith, B.E., Medley, B., 2014. Marine ice sheet collapse potentially under way for the Thwaites Glacier Basin, West Antarctica. Science, 344: 735-738.
- Kamb, B., 2001. Basal zone of the West Antarctic ice streams and its role in lubrication of their rapid motion. In: West Antarctic Ice Sheet: Behavior and Environment. Antarctic Research Series, 77: 157-199.
- Kleman, J. and Borgström, I., 1994. Glacial landforms indicative of a partly frozen bed. Journal of Glaciology, 49: 255-264.
- Knight, J., 2011. Subglacial processes and drumlin formation in a confined bedrock valley, northwest Ireland. Boreas, 40: 289-302.
- Knight, J., 2016. Subglacial processes from drumlins in Clew Bay, western Ireland. Earth Surface Processes and Landforms, 41: 277-288.
- Knight, J. and McCabe, A.M., 1997. Identification and significance of ice-flow-transverse subglacial ridges (Rogen moraines) in northern central Ireland. Journal of Quaternary Science, 12: 519-524.
- Krüger, J. and Kjær, K.H., 1999. A data chart for field description and genetic interpretation of glacial diamicts and associated sediments - with examples from Greenland, Iceland, and Denmark. Boreas, 28: 386-402.

- Kurimo, H., 1980. Depositional deglaciation forms as indicators of different glacial and glaciomarginal environments. *Boreas*, 9: 179-191.
- Lamsters, K., Zelcs, V., 2015. Subglacial bedforms of the Zemgale Ice Lobe, south-eastern Baltic. *Quaternary International*, 386: 42-54.
- Lee, H.A., 1959. Surficial geology of the southern district of Keewatin and the Keewatin Ice Divide, Northwest Territories, Canada. *Geological Survey of Canada Bulletin*, 51: 42.
- Lindén, M., Möller, P. and Adrielsson, L., 2008. Ribbed moraine formed by subglacial folding, thrust stacking and lee-side cavity infill. *Boreas*, 37: 102-131.
- Lindqvist, A. and Svensson, S., 1957. Glacialmorfologiska studier i Gysenomras det i nordvästra Jämtland. *Geographica*, 31: 206-222.
- Livingstone, S.J., Cofaigh, C.O., Stokes, C.R., Hillenbrand, C.-D., Vieli, A. and Jamieson, S.S.R., 2012. Antarctic palaeo-ice streams. *Earth-Science Reviews*, 111: 90-128.
- LMÍ, 2016. IcelandDEM. Landmælingar Íslands, pp. 10 m resolution.
- Loftmyndir, 2000, 2016. Loftmyndir ehf.
- Loftmyndir, 2016, 2000. Jarðfræðikort af Íslandi. Berggrunnur. 1. útg. Jarðfræði Íslands. Náttúrufræðistofnun Íslands, <http://jardfraedikort.ni.is>
- Lukas, S., Benn, D.I., Boston, C.M., Brook, M., Coray, S., Evans, D.J.A, Graf, A., Kellerer-Pirklbauer, A., Kirkbride, M.P., Krabbendam, M., Lovell, H., Machiedo, M., Mills, S.C., Nye, K., Reinardy, B.T.I., Ross, F.H., Signer, M., 2013. Clast shape analysis and clast transport paths in glacial environments: A critical review of methods and the role of lithology. *Earth-Science Reviews*, 121: 96-116.
- Lundqvist, G., 1935. Isavsmältningen i Bergslagen. *Geologiska Föreningens i Stockholm Förhandlingar*, 57: 287-301.
- Lundqvist, G., 1937. Sjösediment från Rogenområdet i Härjedalen. *Sveriges Geologiska undersökning C*, 408: 80.
- Lundqvist, G., 1943. Norrlands jordarter. *Sveriges Geologiska undersökning C*, 457: 166.
- Lundqvist, G., 1951. Beskrivning till jordartskarta över Kopparbergs län. *Sveriges Geologiska undersökning Ca*, 21: 213.
- Lundqvist, J., 1958. Beskrivning till jordartskarta över Värmlands län. *Sveriges Geologiska undersökning C*, 38: 229.
- Lundqvist, J., 1969a. Problems of the so-called Rogen moraine. *Sveriges Geologiska undersökning C*, 648: 32.
- Lundqvist, J., 1989. Rogen (ribbed) moraine - Identification and possible origin. *Sedimentary Geology*, 62: 281-292.
- Lundqvist, J., 1997. Rogen moraine - an example of two-step formation of glacial landscapes. *Sedimentary Geology*, 111: 27-40.
- MacAyeal, D.R., 1989. Large-scale ice flow over a viscous basal sediment: theory and application to ice stream B, Antarctica. *Journal of Geophysical Research, Solid Earth* 94: 4071-4087.
- MacAyeal, D.R., 1992. The basal stress distribution of Ice Stream E, Antarctica, inferred by control methods. *Journal of Geophysical Research*, 97: 9101-9109.
- MacAyeal, D.R., Bindshadler, R.A. and T.A., S., 1995. Basal friction of Ice Stream E, west Antarctica. *Journal of Glaciology*, 5: 661-603.
- MacLachlan, J.C., Eyles, C. H., 2013. Quantitative geomorphological analysis of drumlins in the Peterborough Drumlin Field, Ontario, Canada. *Geografiska Annaler*, 95: 125-144.
- Mannerfelt, C., 1942. Några norrländska kartanalyser. *Globen*, 3: 17-20.

- Mannerfelt, C., 1945. Några glacialgeologiska formelement och deras vittnesbörd om inlandsisens avsmättningsmekanik i svensk och norsk fjällterräng. *Geografiska Annaler*, 27A: 1-239.
- Margold, M., Stokes, C.R. and Clark, C.D., 2015. Ice streams in the Laurentide Ice Sheet: Identification, characteristics and comparison to modern ice sheets. *Earth-Science Reviews*, 143: 117-146.
- McKenzie, M.A., Principato, S.M. and Benediktsson, Í.Ö., 2017. Geomorphic evidence for a palaeo-ice stream near Bárðardalur, north Iceland, GSA Annual Meeting, Seattle, WA, USA.
- Menzies, J., 1979. A review of the literature on the formation and location of drumlins. *Earth-Science Reviews*, 14: 314-359.
- Mercer, J.H., 1978. West Antarctic ice sheet and CO₂ greenhouse effect: a threat of disaster. *Nature*, 271: 321-325.
- Miall, A.D., 1977. A review of the braided-river depositional environment. *Earth-Science Reviews*, 13: 1-62.
- Miall, A.D., 1985. Architectural-Element Analysis: A New Method of Facies Analysis Applied to Fluvial Deposits. *Earth-Science Reviews*, 22: 261-308.
- Minell, H., 1977. Transverse moraine ridges of basal origin in Härjedalen. *Geol. Fören. Stockholm Förh.*, 99: 271-277.
- Minell, H., 1980. The distribution of local bedrock material in some moraine forms from the inner part of northern Sweden. *Boreas*, 9: 275-281.
- Möller, P., 2006. Rogen moraine: an example of glacial reshaping of pre-existing landforms. *Quaternary Science Reviews*, 25: 362-389.
- Norðdahl, H., 1983. Late Quaternary stratigraphy of Fnjoskadalur Central North Iceland, a study of sediments, ice-lake strandlines, glacial isostasy and ice-free areas. *Lundqua Thesis* 12: 1-78.
- Norðdahl, H., 1991. Late Weichselian and Early Holocene deglaciation history of Iceland. *Jökull*, 40.
- Norðdahl, H. and Ingólfsson, Ó., 2015. Collapse of the Icelandic ice sheet controlled by sea-level rise? *Arktos: The Journal of Arctic Geosciences*, 1: 1-18.
- Norðdahl, H., Ingólfsson, Ó., Vogler, E.D., Steingrímsson, B.Ó. and Hjartarson, Á., 2019. Glacio-isostatic age modelling and Late Weichselian deglaciation of the Logurinn basin, East Iceland. *Boreas*.
- Norðdahl, H., Ingólfsson, Ó., 1994. A review of the environmental history of Iceland, 13000-9000 yr BP. *Journal of Quaternary Science*, 9(2): 147-150.
- Norðdahl, H., Ingólfsson, Ó., Pétursson, H.G., 2012. Ísaldarlok á Íslandi. *Náttúrufræðingurinn*, 82 (1-4): 73-86.
- Norðdahl, H., Ingólfsson, Ó., Pétursson, H.G., Hallsdóttir, M., 2008. Late Weichselian and Holocene environmental history of Iceland. *Jökull*, 58: 343-364.
- Norðdahl, H., Pétursson, H.G., 2005. Relative Sea-Level Changes in Iceland: new Aspects of the Weichselian Deglaciation of Iceland. In: Caseldine, C., Russel, A., Hardardóttir, J. & Knudsen, O. (Eds.), *Iceland - Modern Processes and Past Environments*, Elsevier, Amsterdam.: pp. 25-78.
- Nye, J.F., 1952. The mechanics of glacier flow. *Journal of Glaciology*, 2: 82-93.
- Patton, H., Hubbard, A., Bradwell, T. and Schomacker, A., 2017. The configuration, sensitivity and rapid retreat of the Late Weichselian Icelandic ice sheet. *Earth-Science Reviews*, 166: 223-245.

- Pétursson, H.G., Norðdahl, H. and Ingólfsson, Ó., 2015. Late Weichselian history of relative sea level changes in Iceland during a collapse and subsequent retreat of marine based ice sheet. *Cuadernos de Investigaci on Geografica* 41: 241-277.
- Porter, C., Morin, P., Howat, I., Noh, M., Bates, B., Peterman, K., Keesey, S., Schlenk, M., Gardiner, J., Tomko, K., Willis, M., Kelleher, C., Cloutier, M., Husby, E., Foga, S., Nakamura, H., Platson, M., Wethington, M., Williamson, C., Bauer, G., Enos, J., Arnold, G., Kramer, W., Becker, P., Doshi, A., D'Souza, C., Cummins, P., Laurier, F., Bojesen, M., 2018. ArcticDEM. Harvard Dataverse V1.
- Powers, M.C., 1953. A new roundness scale for sedimentary particles. *Journal of Sedimentary Petrology*, 23: 117-119.
- Price, S.F., Bindschadler, R.A., Hulbe, C.L., Blankenship, D.D., 2002. Force balance along an inland tributary and onset to Ice Stream D, West Antarctica. *Journal of Glaciology*, 48: 20-30.
- Principato, S.M., Moyer, A.N., Hampsch, A.G. and Ipsen, H.A., 2016. Using GIS and streamlined landforms to interpret palaeo-ice flow in northern Iceland. *Boreas*, 45: 470-482.
- Rasmusson, G., Tarras-Wahlberg, N., 1951. Terriingformerna vid Saxvattnet. *Sven. Geogr. Årsbok*: 173-176.
- Raunholm, S., Serjup, H.P. and Larsen, E., 2003. Lateglacial landform associations at Jæren (SW Norway) and their glaci-dynamic implications. *Boreas*, 32: 462-475.
- Raymond, C.F., Echelmeyer, K.A., Whillans, I.M. and Doake, C.S.M., 2001. Ice stream shear margins. In: *The West Antarctic Ice Sheet: Behavior and Environment*. Antarctic Research Series, 77: 137-155.
- Rijsdijk, K.F., Owen, G., Warren, W.P., McCarroll, D. and van der Meer, J.J.M., 1999. Clastic dykes in over-consolidated tills: evidence for subglacial hydrofracturing at Killiney Bay, eastern Ireland. *Sedimentary Geology*, 129: 111-26.
- Sæmundsson, T., 1995. Deglaciation and shoreline displacement in Vopnafjörður, North-eastern Iceland. *Lundqua Thesis* 33: 1-106.
- Sarala, P., 2006. Ribbed moraine stratigraphy and formation in southern Finnish Lapland. *Journal of Quaternary Science*, 21(4): 387-398.
- Schytt, V., 1974. Inland ice sheets - recent and Pleistocene. *Geol. Fören. Stockholm Fören.*, 96: 299-309.
- Sergienko, O.V. and Hindmarsh, R.C.A., 2013. Regular patterns in frictional resistance of ice-stream beds seen by surface data inversion. *Science*, 342: 1086-1089.
- Shaw, J., 1979. Genesis of the Sveg tills and Rogen moraines of central Sweden: a model of basal melt-out. *Boreas*, 8: 409-426.
- Shaw, J., 2002. The meltwater hypothesis for subglacial bedforms. *Quaternary International*, 90: 5-22.
- Shepherd, A., Ivins, E.R., Gerou, A., Barletta, V.R., Bentley, M.J., Bettadpur, S., Briggs, K.H., Bromwich, D.H., Forsberg, R., Galin, N., Horwath, M., Jacobs, S., Joughin, I., King, M.A., Lenaerts, J.T.M., Li, J., Ligtenberg, S.R.M., Luckman, A., Luthcke, S.B., McMillan, M., Meister, R., Milne, G., Mouginot, J., Muir, A., Nicolas, J.P., Paden, J., Payne, A.J., Pritchard, H., Rignot, E., Rott, H., Sorensen, L.S., Scambos, T.A., Scheuchl, B., Schrama, E.J.O., Smith, B., Sundal, A.V., van Angelen, J.H., van de Berg, W.J., van den Broeke, M.R., Vaughan, D.G., Velicogna, I., Wahr, J., Whitehouse, P.L., Wingham, D.J., Yi, D., Young, D., Zwally, H.J., 2012. A reconciled estimate of ice sheet mass balance. *Science*, 338: 1183-1189.

- Sigbjarnarson, G., 1983. The Quaternary Alpine glaciation and marine erosion in Iceland. *Jökull*, 33: 87-98.
- Sneed, E.D. and Folk, R.L., 1958. Pebbles in the Lower Colorado River, Texas - A study in particle morphogenesis. University of Chicago: 114-150.
- Sollid, J.L. and Sorbel, L., 1984. Distribution and genesis of moraines in Central Norway. L.-K. Ktnigsson (Editor), *Ten Years of Nordic Till Research. Striae*, 20: 63-67.
- Spagnolo, M. and Clark, C.D., 2009. A geomorphological overview of glacial landforms on the Icelandic continental shelf. *J. Maps*.
- Stokes, C.R., 2018. Geomorphology under ice streams: Moving from form to process. *Earth Surface Processes and Landforms*, 43: 85-123.
- Stokes, C.R., Clark C.D., 2002. Are long subglacial bedforms indicative of fast ice flow? *Boreas*, 31.
- Stokes, C.R., Clark C.D., Lian O.B., Tulaczyk, S., 2006. Geomorphological Map of Ribbed Moraines on the Dubawnt Lake Palaeo-Ice Stream Bed: A Signature of Ice Stream Shut-down? *Journal of Maps*, 2:1: 1-9.
- Stokes, C.R. and Clark, C.D., 1999. Geomorphological criteria for identifying Pleistocene ice streams. *Annals of Glaciology*, 28: 67-74.
- Stokes, C.R. and Clark, C.D., 2001. Palaeo-ice streams. *Quaternary Science Reviews*, 20: 1437-1457.
- Stokes, C.R., Fowler, A. C., Clark, C. D., Hindmarsh, R. C. A., Spagnolo, M., 2013b. The instability theory of drumlin formation and its explanation of their varied composition and internal structure. *Quaternary Science Reviews*, 62: 77-96.
- Stokes, C.R., Lian O.B., Tulaczyk S., Clark C.D., 2008. Superimposition of ribbed moraines on a palaeo-ice-stream bed: implications for ice stream dynamics and shutdown. *Earth Surface Processes and Landforms*, 33: 593-609.
- Stokes, C.R., Margold, M. and Creyts, T.T., 2016. Ribbed bedforms on palaeo-ice stream beds resemble regular patterns of basal shear stress ('traction ribs') inferred from modern ice streams. *Journal of Glaciology*: 1-18.
- Stokes, C.R., Spagnolo, M., Clark, C. D., O Cofaigh, C., Lian, O. B. & Dunstone, R. B. , 2013a. Formation of mega-scale glacial lineations on the Dubawnt Lake Ice Stream bed: 1. size, shape and spacing from a large remote sensing dataset. *Quaternary Science Reviews*, 77: 190-209.
- Syvitski, J.P.M., Jennings, A.E. and Andrews, J.T., 1999. High-resolution seismic evidence for multiple glaciation across the southwest Iceland Shelf. *Arctic, Antarctic and Alpine Research*, 31: 50-57.
- Tulaczyk, S., Kamb, W.B. and Engelhardt, H.F., 2000. Basal mechanics of Ice Stream B, West Antarctica: 2. Undrained plastic bed model. *Journal of Geophysical Research, Solid Earth* 105: 483-494.
- Tulaczyk, S.M., Scherer, R.P., Clark, C.D., 2001. A ploughing model for the origin of weak tills beneath ice streams: a qualitative treatment. *Quaternary International*, 86: 59-70.
- van den Broeke, M., Bamber, J., Ettema, J., Rignot, E., Schrama, E., van de Berg, W.J., van Meijgaard, E., Velicogna, I. and Wouters, B., 2009. Partitioning recent Greenland mass loss. *Science*, 326: 984-986.
- van der Meer, J.J.M., Kjær, K.H., Krüger, J., Rabassa, J. and Kilfeather, A.A., 2009. Under pressure: clastic dykes in glacial settings. *Quaternary Science Reviews*, 28: 708-720.

- van der Meer, J.J.M., Menzies, J. and Rose, J., 2003. Subglacial till: the deforming glacier bed. *Quaternary Science Reviews*, 22: 1659-1685.
- Warren, W.P. and Ashley, G.M., 1994. Origins of the Ice-contact Stratified Ridges (Eskers) of Ireland. *Journal of Sedimentary Research*, 64A: 433-449.
- Wastenson, L., 1983. Geomorphological Map 17C Funäsdalen - Description and Assessment of Areas of Geomorphological Importance. Statens Naturvårdsverk, PM 1709, Stockholm: 25-31.
- Weertman, J., 1974. Stability of the junction of an ice sheet and an ice shelf. *Journal of Glaciology*, 13: 3-11.
- Winberry, J.P., Anandakrishnan, S., Alley, R.B., Wiens, D.A. and Pratt, M.J., 2014. Tidal pacing, skipped slips and the slowdown of Whillans Ice Stream, Antarctica. *Journal of Glaciology*, 60: 795-807.